ASSESSMENT OF THE NEW GLOBAL PRECIPITATION MEASUREMENT MISSION

HOSSEIN MAROFI
February 2015

SUPERVISORS:
Dr. B.H.P Maathuis
Prof. Dr. Ing. W. Verhoef

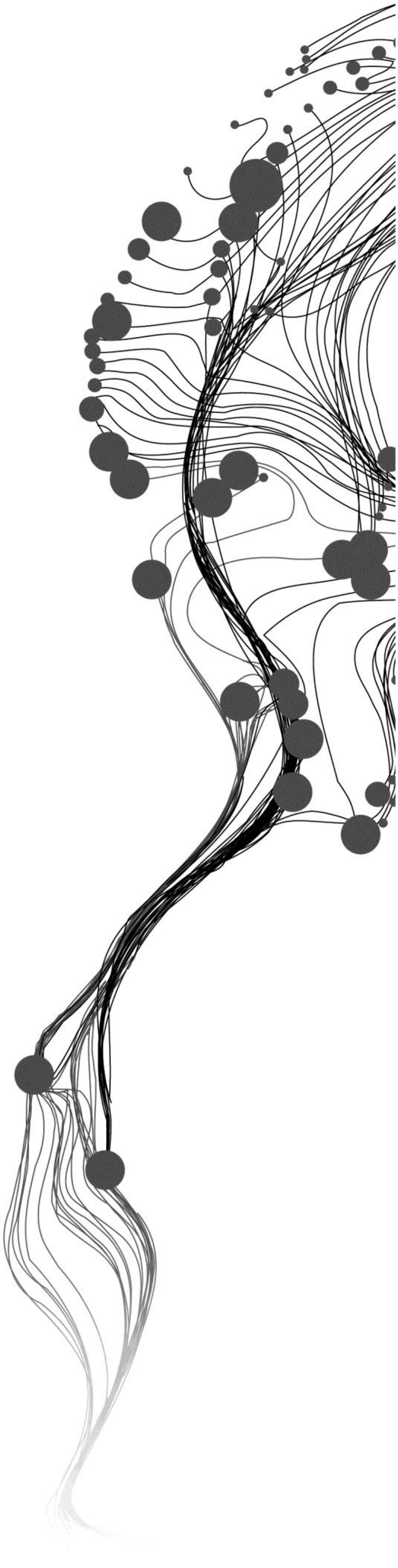

ASSESSMENT OF THE NEW GLOBAL PRECIPITATION MEASUREMENT MISSION

HOSSEIN MAROFI
Enschede, The Netherlands, February 2015

Thesis submitted to the Faculty of Geo-Information Science and Earth Observation of the University of Twente in partial fulfilment of the requirements for the degree of Master of Science in Geo-information Science and Earth Observation.
Specialization: Water Resources and Environmental Management

THESIS ASSESSMENT BOARD:
Prof. Dr. Z. Bob Su (Chairman)
Dr. R. Sluiter (External Examiner, Royal Netherlands Meteorological Institute)
Dr. B.H.P. Maathuis (First Supervisor)
Prof. Dr. Ing. W.Verhoef (Second Supervisor)

ABSTRACT

Precipitation is a major component of the water cycle, and is responsible for depositing most of the fresh water on the planet. One important aspect of hydrologic modelling is the estimation of precipitation and its distribution within a watershed. Precipitation, as generating flow, is the most crucial hydrological parameter. Rainfall estimation is very important too, in terms of its effects on human life, water resources, and water usage areas.

Precipitation affected by the meteorological processes, the geographical and regional variations and features is very difficult to be estimated. On the other hand, local precipitation measurement is very limited because of economical issues, in the most regions, especially in the developing countries. Accurate estimation of precipitation has also an important role in management of water crisis that is a natural disaster and affected the dry countries.

This study is conducted to make an assessment on the new GPM mission which is the latest satellite mission released by NASA and JAXA. Several comparison methods are involved in this study in order to obtain to most accurate and reliable results at the end. In this study statistical comparisons are divided in two parts, first point to raster analysis which consists of comparing value obtained in the rain gauge stations of The Netherlands and north of Belgium. Statistics which are used in this part are R-squared, root mean square of error, mean bias of error and mean absolute error. The results of comparison demonstrate that GPM has good correlation with gauge station in The Netherlands and north of Belgium, specially in south on Netherlands and north of Belgium.

The other comparison consists of raster to raster analysis. In this part raster maps of GPM are compared with TRMM and MPE in order to quantify the correlation between them. The results shows that GPM rainfall maps have a good correlation with TRMM map in the tropics and sub-tropics, however the number of pixel detected by TRMM is higher than that of GPM.

ACKNOWLEDGMENT

It is my pleasure to use this opportunity to express my special gratitude to my supervisors Dr. Ben Maathuis and Professor Wouter Verhoef for their useful comments, remarks and engagement through the learning process and span of this master thesis. Their valuable advice on developing my ability in research as well as making my career is highly appreciated. Furthermore, I would also like to thank Professor Z. Bob Su and Mr. Arno van Lieshout for their valuable helps and supports.

Also, I like to thank the participants in my survey, who have willingly shared their precious time during the process of interviewing. I would like to thank my dear friends who have supported me throughout entire process as well as difficult times.
Last but not least, I am truly grateful of SALAM Society for their financial support to finish my MSc program.

Table OF Contents

LIST OF FIGURES

LIST OF TABLES

1. INTRODUCTION

1.1. Background

Not just due to its principal impacts on the accessibility of water for drinking and farming, additionally on account of its fundamental effects on the ecosystem and the nature, precipitation is perceived as one of the most important variables in the water cycle.

Incessant and overwhelming rains and flooding as well as drought influence almost every living body on the planet. In order to pick up a finer understanding of the circulation of water around the globe, researchers should do precipitation estimations with the best quality and accuracy. For this purpose observe moisture and precipitation in the atmosphere in order to better understand the connections and impacts of precipitation with other variables of the water cycle.

However, most studies have been conducted in order to estimate precipitation from direct measurement on the earth meteorological stations, but it is necessary to use a rapid, accurate and modern method. Satellite observations are an essential input to numerical weather prediction systems and also assist the human forecaster in the diagnosis of potentially hazardous weather developments. Of growing importance is the capacity of weather satellites to gather long-term measurements from space in support of climate change studies.

The advantages of using such instrument, enables us to estimate evaporation, precipitation, runoff, wind speed and the other related parameters. Having accurate precipitation data, it is thus possible to predict many hydro-climatologic events such as extreme flood and drought, water shortage as well as climate change that are highly occurred in many parts of the world.

1.2. Relevance of the research

In order to obtain valid results in meteorological, hydrological, and environmental applications such as numerical weather prediction (NWP), flash flood warning, tropical precipitation potential, water resources monitoring, recharge estimation and water modelling as well as ameliorating weather forecasting and climate change studies, precise precipitation estimation is fundamental (Levizzani, Bauer, & Turk, 2007).

Nowadays, various kind of remote sensing and in situ methods are developed in order to estimate precipitation. These methods can be classified regarding their platforms that can be ground-based or space-borne. Instruments used for the estimation are rain gauges, rain radars, and microwave, visible or infrared sensors. Each instrument has its own advantages and disadvantages with respect to spatial sampling, spectral resolution, spatial coverage, temporal coverage, cost of purchase and operation, calibration, accuracy, and consistency of the retrievals (Sene, 2013). For example, the only device by which we can directly measure the accumulated rainfall is the rain gauge. But they cannot represent regional purpose because they are point measurements. Furthermore, in order to retrieve representative results, rain gauges should be well distributed in the area having financial impacts. Finally, rain gauge recording is not covering oceans and uninhabited zones.

In order to ameliorate our knowledge about Earth's energy and water cycles, and to help answer important questions about climate change, global warming and its consequences on the Earth, changes in precipitation intensities and patterns over last decades and its effect on human society, the National Aeronautics and Space Administration (NASA) and Japan Aerospace Exploration Agency (JAXA) started a new generation of global precipitation measurement named GPM (Harris, 2014). This international cooperation mission consists of a network of satellites that together will generate global observations of precipitation from space. Expanded on the achievement of the Tropical Rainfall Measuring Mission (TRMM), another joint program of NASA and JAXA which estimate rainfall only in the tropical area, the GPM program estimates the rainfall between approximately 65° north latitude and 65° south latitude.

The combination of measurements done by the satellites in the constellation, will supply global precipitation observations every three hours (Hanson & Bensusen, 2013). The core GPM satellite platform is composed of combination of passive and active sensors, the dual-frequency precipitation radar (DPR) as active and the GPM microwave imager (GMI) as passive sensor that together obtain rain information (Islam, Rico-Ramirez, Han, Srivastava, & Ishak, 2012). *"The GMI has the capability to measure the amount, size, intensity and type of precipitation. The DPR will return three-dimensional profiles and intensities of liquid and solid precipitation"* (Hanson & Bensusen, 2013). The TRMM Microwave Imager (TMI) uses 9 channels, from 10 to 85.5 GHz, to measure the intensity of microwave radiation emitted from Earth's surface and atmosphere, the GMI uses a wider range of frequencies, 13 channels from 10 to 183 GHz, which leads to measuring heavy-to-light precipitation (Hanson & Bensusen, 2013).

As an example of GPM algorithms, 3CMB "Combined precipitation", is an algorithm of combined rainfall data retrieved from GMI and DPR, generates outputs at 5° x 5° latitude/longitude and 0.25° x 0.25° latitude/longitude. This algorithm generates gridded products with geographic coverage of 70°N to 70°S. The data are provided in monthly and daily timescale (Goddard Space Flight Center, 2014)

Scientists believe that monitoring precipitation over the globe with high spatial and temporal resolution will provide us a clearer idea of how different earth systems interact and help us to arrive at the edge of the world's knowledge in the field of meteorology and climatology. An important benefit of GPM mission is in continuation of the 15 years rainfall data record done by TRMM (Harris, 2014). On the other hand, NASA expect that the output provided by GPM will have various social benefits like improving our knowledge about natural disasters and droughts, fresh water accessibility, water resources management and monitoring, forecasting extreme rainfall events and storms (Maxwell, 2014).

This study is conducted to make an assessment of the new precipitation data released by GPM and compare them with other independent data resources.

The following picture clarifies the status of 9 satellites of GPM constellation.

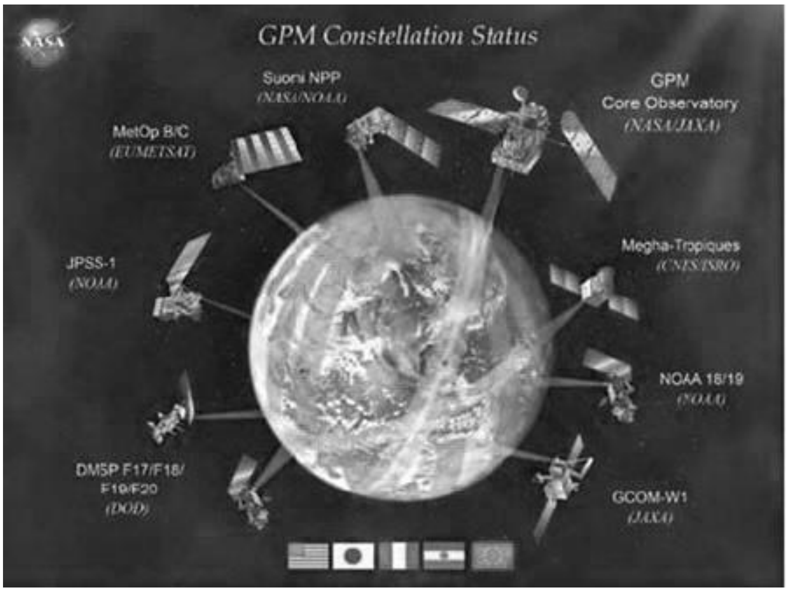

Figure (1): GPM Constellation Status (Source: NASA)

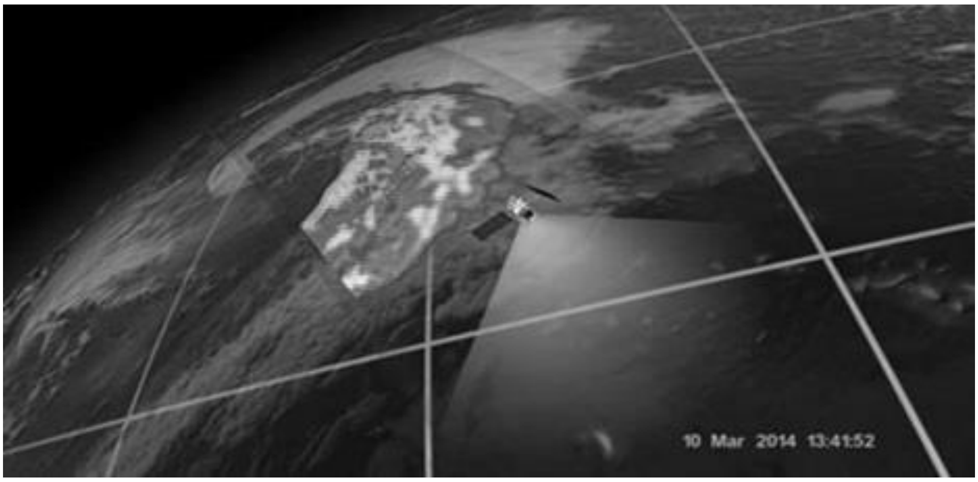

Figure (2): An image provided from GPM Microwave Imager. A cyclone is observed in the coastal area of Japan on March 10, 2014 (Maxwell, 2014).

1.3. Research Objectives

The main objective of this research is to assess the quality of the new rainfall product of the GPM mission. In order to fulfill the main objective, the following specific objectives are defined:

- To compare the data retrieved from the new GPM with those from TRMM.
- To ground validate the data retrieved from the GPM by gauge estimates as a “ground truth”.
- To compare the data retrieved from the new GPM with those from the near real time EUMETSAT MPE in two different areas with different types of precipitations.

1.4. Research Questions

In order to achieve the objectives mentioned above, the following main research questions are formulated:

- Is there a statistically significant difference between the data retrieved from GPM and the TRMM data in overlapped area?
- If there is statistically significant difference, how much is it?
- What is the accuracy of the data retrieved from GPM compared with combined gauge data?
- How much is the difference between the GPM data and the data of the near real time EUMETSAT MPE regarding rainfall intensity?
- How good is GPM in detecting frontal rainfall intensities?

1.5. Hypothesis

- For this case, a combined gauge data is the most convenient choice as “ground truth” in order to do the validation.
- EUMETSAT MPE product is suitable for convective rainfall, as it is based on cloud top temperature.

1.6. Logical sequence of research approach / methodology

In the following flowchart all processes of this research study is described

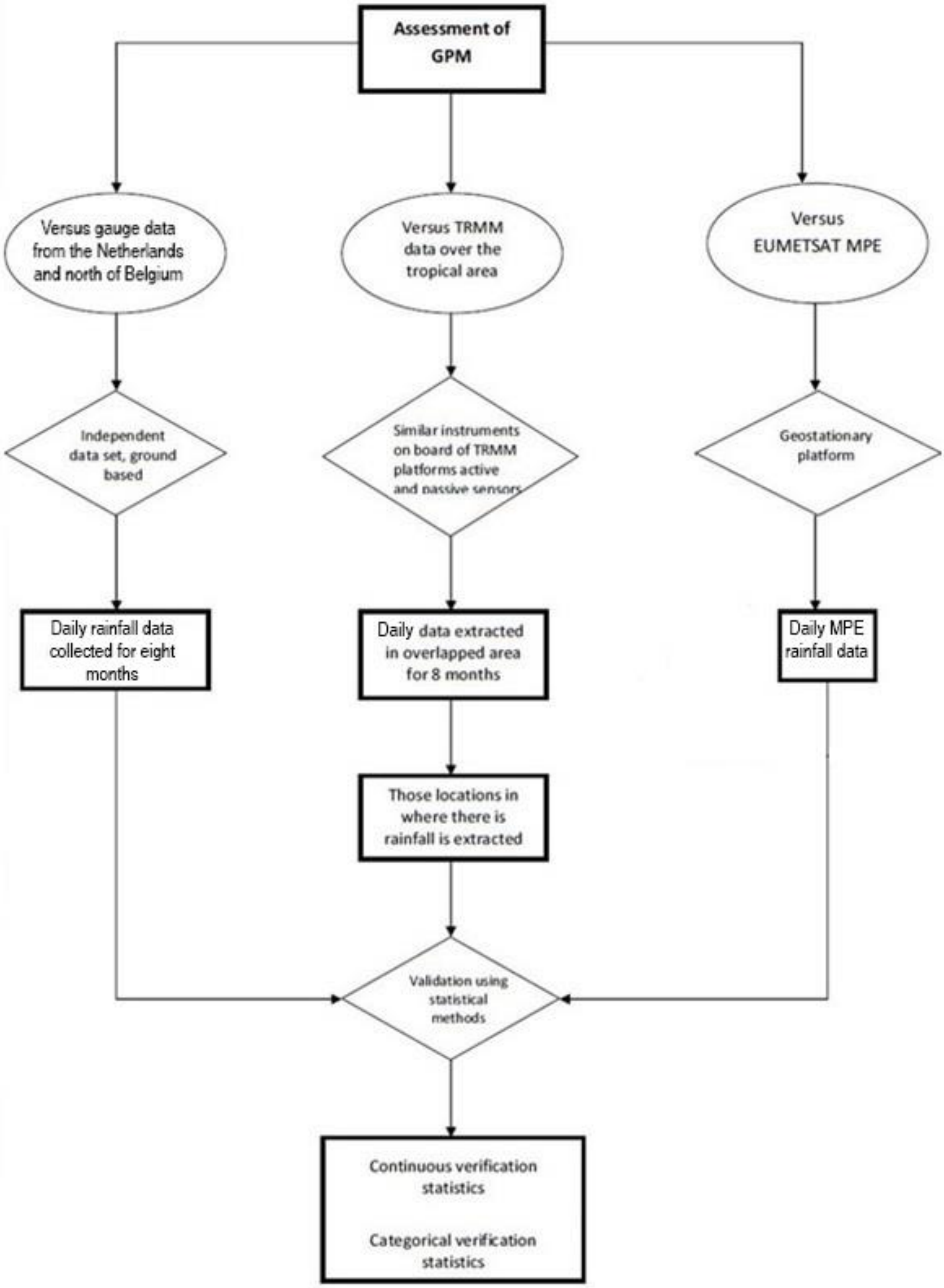
Assessment of GPM
Versus gauge data from the Netherlands and north of Belgium
Versus TRMM data over the tropical area
Versus EUMETSAT MPE
Independent data set, ground based
Similar instruments on board of TRMM platforms active and passive sensors
Geostationary platform
Daily rainfall data collected for eight months
Daily data extracted in overlapped area for 8 months
Daily MPE rainfall data
Those locations in where there is rainfall is extracted
Validation using statistical methods
Continuous verification statistics
Categorical verification statistics

2. LITERATURE REVIEW

2.1. Background

Novella and Thiaw (2009) conducted a study in validation of high-resolution precipitation products (HRPP) in West Africa during the summer season of 2008. In their study rain gauge data was considered as "ground truth". So, they collected the data of 133 rain gauge station in Mali, Senegal and Burkina Faso. To do the validation, the author divided this part in three different categories: dichotomous, continuous, and precision. Dichotomous validation is used in order to verify the ability of HRPP to detect daily rainfall. For this goal the author considered thresholds. Rainfall events are specified by rain (>= 1.0 mm) and no rain (<1.0 mm). In order to determine the number of misses, hits, false alarms and correct negatives, the number of rain and no rain events are accumulated in a 2x2 contingency table. To verify how the data of HRPP differs from the data retrieved from gauge station, a number of continuous methods like sample Pearson correlation coefficient (r), bias and root mean square error are used.

In another study done by Gómez (2007), rainfall gauge data is compared with TRMM 3B42 V.6 data. For that study eight years observation from TRMM 3B42 V.6 for monthly maximum precipitation in 24 hours and monthly accumulated rainfall is compared versus rainfall gauge data in Oruro in western sector of Bolivia. All the gaps and missing values in gauge stations are filled by Correlation Coefficient Weighting Method (CCWM). This method is relying on "existence" of Pearson correlation coefficient between two data sets retrieved in two different areas. Because correlation coefficient is a technic for calculating spatial correlation, it is accepted to substitute the weighting factor by correlation coefficient (Aly, 2008).
According to CCWM equation:

$$\theta_b = \frac{\sum_{i=1}^{n} \theta_i E_{bi}}{\sum_{i=1}^{n} E_{bi}}$$

eq 1.

Where θ_b and θ_i are the rainfall at station "b" and "i" respectively, E_{bi} is the ratio of covariance of data sets of stations "b" and "i" to the product of standard deviations of data sets. After completing the gauge datasets, visual comparison, statistical analysis and descriptive statistics are used by (Gómez, 2007) in order to do the validation. Statistical methods used by the author are including mean error (ME), mean absolute error (MAE), root mean square error (RMSE), and correlation coefficient. Descriptive statistics consisted on determining the number of misses, hits, false alarms and correct negatives by a 2x2 contingency table, which in turn, leads to determining the accuracy, frequency bias, false alarm ratio (FAR), critical success index (CSI), probability of detection (POD) and probability of false detection (POFD).

In a study done by (Worqlul et al., 2014), precipitation estimates of 3 satellite is compared versus ground-based precipitation measurement in order to obtain enhanced spatial measurement of precipitation. The area of study is the Lake Tana basin in Ethiopia which is 15 000 km2. In this catchment 38 rain gauge stations are recording daily precipitation measurements. These observations are considered as "ground

truth" and the estimation of TRMM 3B42, Multi-Sensor Precipitation Estimate–Geostationary (MPEG) and the Climate Forecast System Reanalysis (CFSR) are compared to "ground truth" to compute the accuracy of these 3 satellite products. This task is done in 2 methods. First, by Point-to-grid comparison in which the daily satellite estimates at the exact location of gauge stations are found out and summed to generate monthly products. These data are compared to monthly gauge data by three statistical techniques which are coefficient of determination (R2), multiplicative bias (bias) and root mean square error (RMSE). The other comparison method is areal comparison. Since the gauge stations are irregularly distributed in the area of study, an interpolation is done by using Thiessen polygon method on the stations likely affected by convective rainfall and then the comparison is carried out by the three statistical techniques mentioned before.
According to the results of this study MPEG and CFSR satellites produce the most precise precipitation estimates.

2.2. Satellite-based rainfall estimation

2.2.1. Introduction

However its spatial and temporal resolutions are tremendous, precipitation plays the most important role in the hydrologic cycle. In order to enhance our knowledge on weather and climate predictions, a precise worldwide coverage of precipitation records is fundamental. Since rain gauge records are mostly accessible on land and principally in highly populated areas, an all-around observation of rainfall is not possible (Geerts, 2010)

Remotely estimated rainfall by ground-based weather radars is performed to carry out high spatial and temporal resolution estimations. The function of weather radars is based on active sensors sending radiation around 1 to 10 cm of wavelengths and receiving the reverberation from meteorological targets like raindrops. Just like other rainfall observation devices, radar has its own advantages and disadvantages. The coverage of radars is very limited. They cannot estimate rainfall events far away from 300 km. furthermore establishing a ground-based weather radars stations is very expensive (Geerts, 2010).

Based on their orbiting patterns, satellites are classified in three groups (COMET, 2011):

- Geostationary Satellites which orbits at the same speed as the earth over the equator (35800 km above). Due to their high temporal resolution and hemispheric view on earth, geostationary satellites are the most effective satellites to extract meteorological events.
- Polar Orbiting Satellites which circle the earth around the poles, carry out a better spatial resolution over a limited field of view (850 km above).
- Skewed Orbit satellites that circle the earth among particular latitudes (few hundreds of kilometers above).

2.2.2. SSM/I

Since 1978 passive microwave sensors have been placed on polar orbiting satellites to get accurate rainfall estimation. The frequency they use to detect and quantify rainfall over the water and land is different. They use low-frequency channels (<20 GHz) over water and high frequencies (>35GHz) over the land (Kidd & Levizzani, 2011).
One of these passive microwave sensors is Special Sensor Microwave/Imager (SSM/I) on board of the Defense Meteorological Satellite Program (DMSP) (Geerts, 2010).

Generally speaking, in a global scale the majority of rainfall events are caused by cold clouds like clouds containing ice. One of the most significant functions of SSM/I is estimating rainfall over the oceans, because in comparison to water, ice particles have much higher microwave emissivity. *"Over land, the surface has a much higher background emissivity and consequently emissions from hydrometeors cannot be reliably measured. Here, scattering caused by ice particles, resulting in a decrease in received radiation at high frequencies must be utilized"* (Kidd & Levizzani, 2011).
On of disadvantages of infrared technics is that we have problem in recognizing precipitating clouds from and non-precipitating clouds (COMET, 2011).
An advantage of SSM/I over infrared methods is that SSM/I estimate rainfall in clouds directly.

2.2.3. TRMM

Launched in 1997, TRMM is a joint program designed by NASA and JAXA, the Japan Aerospace Exploration Agency, estimates rainfall in tropical and subtropical regions in order to improve our knowledge of rainfall pattern and intensity in these areas. TRMM uses three different instruments in order to measure the rainfall. First, by using the Precipitation Radar (PR), it can observe through the precipitation section and provides three dimensional precipitation retrievals, which leads to giving new bits of knowledge about storm formation (Masika, 2007). The other instrument is the TRMM Microwave Imager (TMI) by which it quantifies the microwave radiation emitted from the atmosphere in order to measure the rainfall intensity, water vapor and cloud water in the atmosphere. The last instrument is Visible and Infrared Scanner (VIRS) which is used as an indirect indicator of precipitation. By observing radiation emitted from the Earth from, VIRS is used to quantify the brightness of temperature of the source (Masika, 2007)

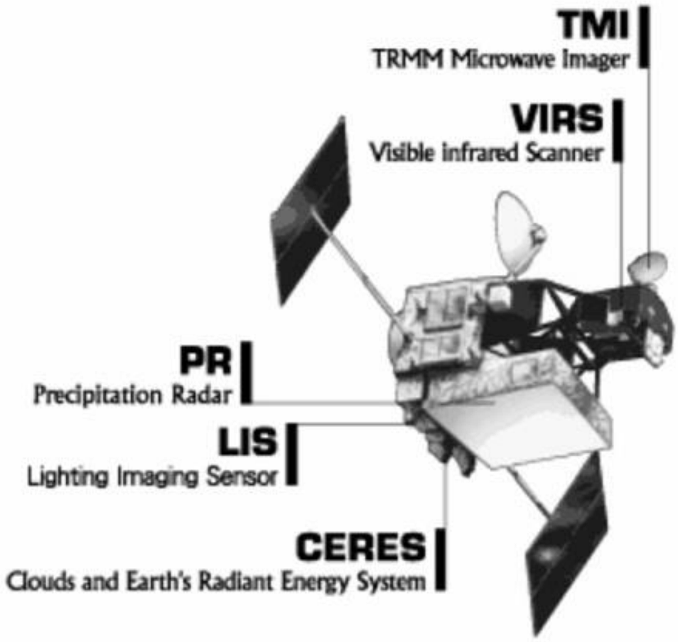

Figure (3): TRMM satellite and instruments (NASA, 2014)

2.2.4. EUMETSAT Multi-sensor Precipitation Estimate (MPE)

The EUMETSAT Multi-sensor Precipitation Estimate (MPE) is created with a specific end goal which is to measure near real time precipitation intensities from MSG.

The technique is focused on the mixing of brightness temperatures of the MSG infrared bands with precipitation intensities retrieved from SSM/I, the Special Sensor Microwave/Imager on the DMSP satellites. the MPE technique is based on cloud temperature (Masika, 2007). The hotter clouds are more averse to create precipitation than colder clouds. According to the research done by Heinemann (2007), the correlation between the cloud top temperature and surface precipitation intensity depends emphatically on the current weather status and that is non-linear. This technique is developed to accurately measure the spatial distribution on convective precipitation over large scale tropical convection as well as small scale convective systems and cold fronts. it is therefore not convenient for measuring rainfall from warm fronts as well as orographic rainfall which is generally detected but misplaced to huge distances (Heinemann, 2007).

According to the algorithm developed by Turk et al. (1999), the precipitation intensities retrieved from passive microwave data and infrared brightness temperatures (BBT) are co-located in time and space. Some look-up tables are obtained due to statistical matching done between BBT and precipitation intensities (Heinemann, Lattanzio, & Roveda, 2007). A data base is demonstrated by these look-up tables in order to obtain precipitation rates from infrared brightness temperature in the spatial and temporal resolution of METEOSAT (Heinemann et al., 2007). The calibration of BBT against SSM/I retrievals is done in particular temporal and spatial windows. These windows must be considered big enough in order to retrieve enough data for statistical matching and at the same time it should be short enough to be assumed as the actual weather condition (Heinemann et al., 2007).

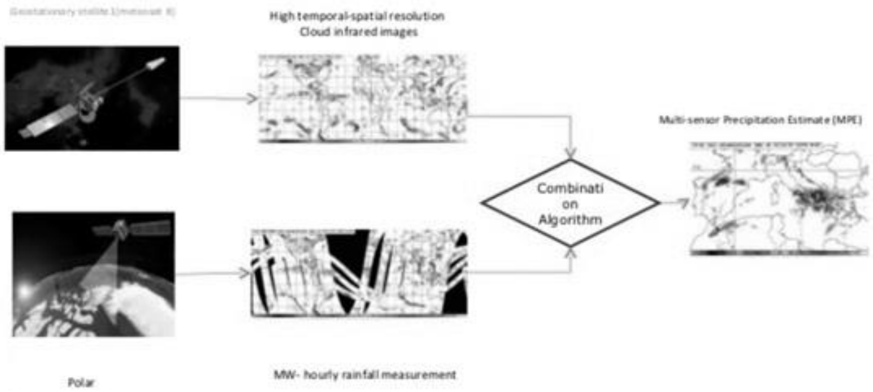

Figure (4): MPE formation (Seyyedi, 2010)

2.2.5. The GPM mission

Only 3 percent of water on Earth resides as fresh water and only a tiny fraction of that is accessible for us on the surface. 7 billions of humans live in this planet; we all have to drink water to live. GPM is an international satellite cooperation providing a new generation of observation of rain and snow in all parts of world every 3 hours. There is about one major flood a day some place on the world, so it’s not considered as a rare event. Understanding how much snow is falling is important for transportation, safety, how much fresh water falls and is stored in snow packs. We need to focus in all faces of precipitation, so we know the global picture of where fresh water exists in the earth system.

The global precipitation core observatory is an international mission led by NASA and JAXA. The launch of GPM core observatory is assuring a new era of climate science and global weather observation. By linking together data from a constellation of satellites, the core observatory will produce a global measurement of rain and snowfall from space. Expanded from TRMM which is a successful collaboration of NASA and JAXA in the 1990s, the GPM is a space based precipitation measurement (Hanson & Bensusen, 2013).

Rain is affecting our daily life in many ways. The distribution of precipitation in space directly affects the availability of fresh water for sustaining life. Extreme precipitation events like hurricanes, blizzards, floods have different socioeconomic impacts on our society. Precipitation also plays a key role in coupling the earth water energy and biogeochemical cycles and its influence by changing the climate. Since rainfall and snowfall vary greatly from place to place and in space and time a more uniform global observations compared to ground instruments(Goddard Space Flight Center, 2014).

The GPM through its core observatory in constellation of satellites will dramatically improve our knowledge on global precipitation and our ability to forecast it and its consequences. GPM makes part of NASA earth science missions. 16 missions are currently in orbit. They are devoted to study the earth as an integrated system in 6 science focus areas ranging from atmosphere composition to the earth surface and interior. GPM will support the water-energy cycle, the weather and the climate science focus areas. GPM follows the highly successful NASA-JAXA Tropical Rainfall Measuring Mission (TRMM) which was launched in 1997. Although it focus has been only on tropics and sub-tropics, TRMM has pioneered the measurement of precipitation from space areas(Goddard Space Flight Center, 2014).

GPM will improve on TRMM rain fall measurements by extending precipitation observations to higher latitudes, the Arctic and Antarctic. The GPM is a cooperation mission by NASA and JAXA and consisted of an international network or constellation of at least eleven satellites that together will generate rainfall observation. NASA and JAXA will contribute satellites to this constellation as well as The French Space Agency, The Indian Space Research Organization, the European Organization for the Exploitation of Meteorological Satellites, The US National ocean Organization Atmospheric Administration and The US Department of Defence (Hanson & Bensusen, 2013).

The GPM core observatory which is a precipitation science observatory provided by NASA and JAXA, is also the primary satellite in the constellation and will calibrate and unify precipitation data from other constellation satellites every three hours. The NASA built spacecraft carries two instruments, the GPM Microwave Imager supplied by NASA known as GMI and the Dual Frequency Precipitation Radar provided by JAXA also known as DPR. These instruments will allow us to see inside clouds. The GMI will send the total precipitation including for the first time light rain and snowfall. The DPR will make detailed 3 dimensional measurements of precipitation structures as well as drop size (Hanson & Bensusen, 2013).
GPM core observatory is the largest observatory ever designed, built and tested at NASA Goddard Space Flight Center. It weighs 3850 kilogram.

GPM microwave imager is one of the most sophisticated passive radiometers to be flown with 1.2 meter diameter and a reflector rotating at 32 rpm. It has 13 channels covering the frequencies of 10 to 183 gigahertz including the 2 newest high frequency channels for detecting falling snow and ice (Goddard Space Flight Center, 2014).

JAXA's most important contribution to GPM mission is development of DPR. DRP is the only one space born dual frequency precipitation radar in the world. It is based on the heritage of the precipitation radar on TRMM satellite. DPR will provide global 3 dimensional precipitation measurement with high accuracy. TRMM observes tropical and sub-tropical regions only, while GPM observes most of the whole worlds. Therefore DPR needs to observe heavy rainfall in the tropical regions and also weak rainfall and snowfall in high latitude regions. DPR contains Ku-band radar designed to measure heavy rainfall and also Ka-band radar designed to measure weak rainfall and snowfall. Both Ku- band and Ka-band produce electrical beam scanning perpendicular to the spacecraft moving direction. DRP provides very accurate precipitation profile information and it plays a key role to improve the precipitation estimation accuracy (Hanson & Bensusen, 2013).
The constellation include a core satellite with dual-frequency precipitation radar (DPR) as active sensor and GPM microwave imager (GMI) as passive sensor and a network of polar-orbiting satellites whose estimations are calibrated by those of the core satellite. Contrary to TRMM mission that only measure rainfall in tropics, GPM has full globe coverage of rainfall estimation. "The GMI has the capability to measure the amount, size, intensity and type of precipitation. The DPR will return three-dimensional profiles and intensities of liquid and solid precipitation" (Hanson & Bensusen, 2013).

2.2.5.1. The GPM microwave imager

The GPM microwave imager on board of the core satellite uses 13 channels from 10 to 183 GHz to detect the rainfall, which leads to measuring heavy-to-light precipitation (Hanson & Bensusen, 2013). The GMI not only carry microwave channel of Tropical Rainfall Measuring Mission (TRMM) Microwave Imager (TMI), but also utilize four high frequency channels approximately 166 GHz and 183 GHz. the-earth-incidence angle of GMI is as same as that of TRMM (NASA, 2014).

2.2.5.2. The Dual-frequency Precipitation Radar (DPR)

The Dual-frequency Precipitation Radar (DPR) on board of the core satellite include of two radar, which are Ku-band (13.6 GHz) precipitation radar (KuPR) for measuring heavy rainfall events and Ka-band (35.55 GHz) precipitation radar (KaPR) for measuring snow and light rainfall events. The function of Dual-frequency Precipitation Radar (DPR) is to demonstrate the structure of precipitations in three-dimension and to enhance the sensibility and precision of precipitation observation (Miura, 2010).

Table (1): The Dual-frequency Precipitation Radar properties

	KuPR	KaPR
Frequency	13.597 and 13.603 GHz	35.547 and 35.553 GHz
Range Resolution	250 m	250 m / 500 m
Spatial Resolution	5 km (at nadir)	5 km (at nadir)
Minimum Detectable Rainfall Rate	0.5 mm/hr	0.5 mm/hr

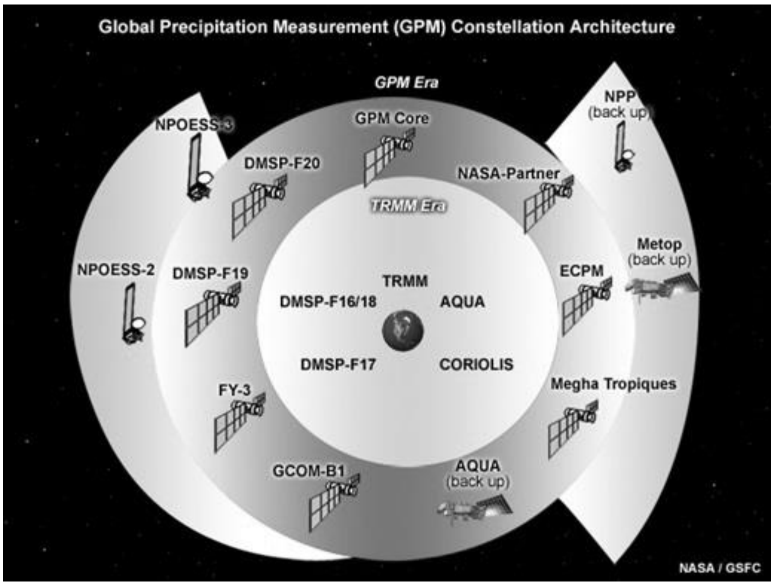

Figure (5): GPM constellation architecture

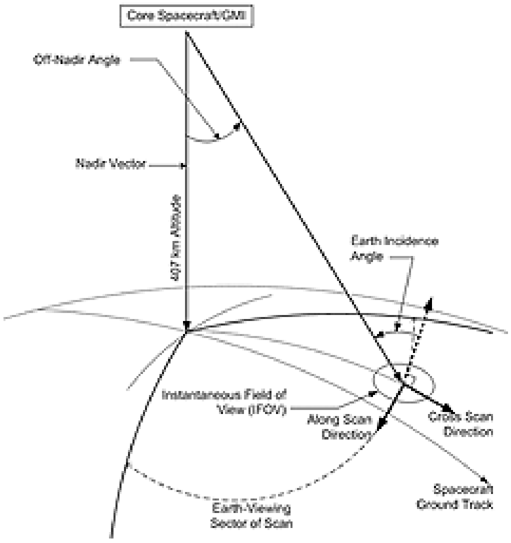

Figure (6): The GMI scan geometry (NASA, 2014)

2.3. Precipitation type

Convective rainfall occurs when moist air parcels rise due to augmentation of surface temperature, and as much as they rise, they cool. At a special level, named condensation level, the water vapor condenses and forms cumulonimbus clouds and then the convective rainfall happens accompanied by thunder and lightning which occurs in many areas through the world mostly in the tropics where there is a water source and intense heating ("Convectional Rainfall," 2006).

Frontal rainfall happens when a warm air mass and one a cold air mass meet (Barcelona Field Studies Centre, 2013). The counter-clockwise circulation around the low-pressure area causes parcels of less dense warm air to go up and parcels of denser drier cold air (heavier) go underneath which in turn causes the warm air to become cool and start to condense. By persisting in condensation, the size of water droplets increase and when they are heavy enough the rain is produced. A cold front happens since the heavier cold air mass advances and pushes under the warm air mass replace it (Catto et al., 2012). Normally, the air mass ahead of a cold front is warmer and moister than the air mass behind a cold front which is dry and cold (National Weather Service, 2010). A warm front which is generated when a warm air mass rises over a cold air mass, moves slower than a cold front. “These differences in speed mean differences in precipitation type and intensity” (Catto et al., 2012). This type of rainfall is very common in Atlantic Canada and Europe.

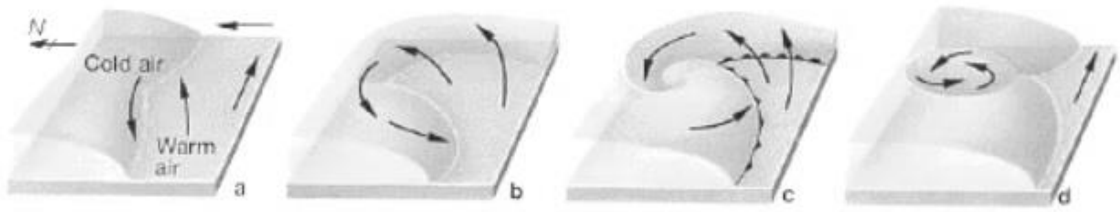

Figure (7): Formation of a frontal rainfall is illustrated (Barcelona Field Studies Centre, 2013).

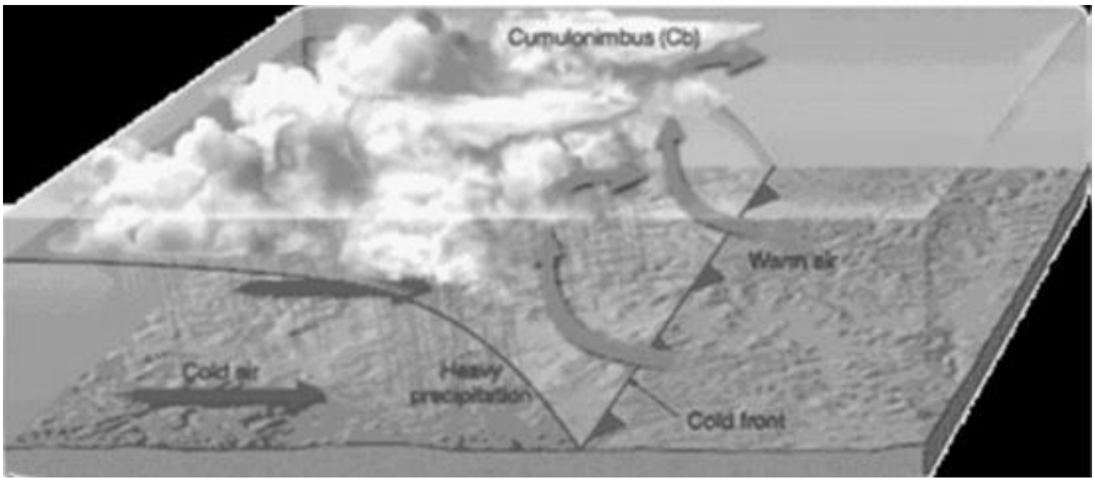

Figure (8): A cold front (Dimitris, 2014)

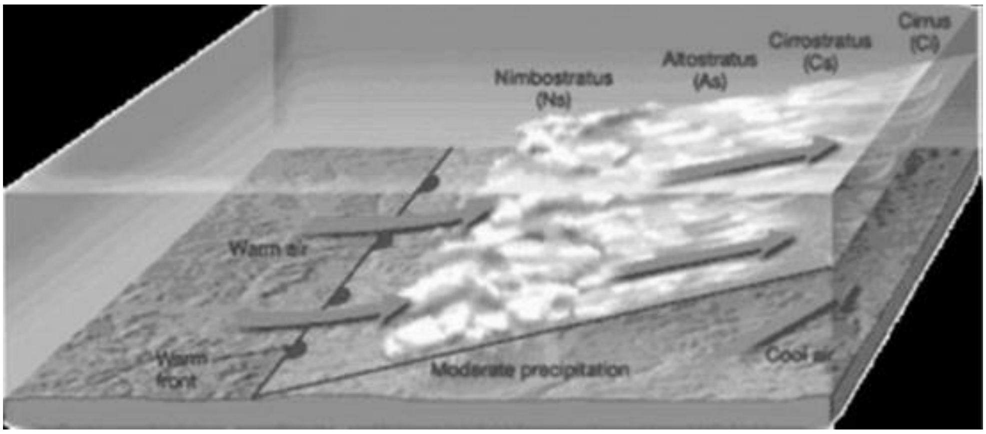

Figure (9): A warm front (Dimitris, 2014)

2.4. Statistical validation

The benefits of the standard statistics verifications are mentioned in the following:

- They are recognizable and understandable for the majority of people
- They are also easy to calculate by simple equations, and
- They are effective for comparing the efficiency and accuracy of different algorithms.

Since 80 percent of overlapped areas between TRMM, MPE and GPM are not affected by rainfall, we will have a large number of "Nulls" or "correct negatives" in our validation, which in turn, will give us a very good output in statistical verifications with high percentage of accuracy which is not a good assessment. So in this study, a threshold is implied on spreadsheet of data in which ground observations, GPM and TRMM estimations are gathered. According to this, all the rainfall events lower than 2 mm per day are removed from the spreadsheet.

2.4.1. Statistical verification methods

The accuracy of a continuous parameter, like precipitation intensity, can be measured by these statistics. "These are the most commonly used statistics in the validation of satellite estimates" (Ebert, 1997).

2.4.1.1. Mean errors or Bias:

It calculates the mean difference among observed data and estimated data (Ebert, 1997). According to the definition of bias, bias is a rating that demonstrate how the average satellite magnitude fits to the ground precipitation observations (Maathuis, 2014)

2.4.1.2. Root mean square error:

As the same as mean absolute error, It calculates the differences between the distributions of two datasets. It measures the magnitude of errors but consider higher weight to greater errors (Ebert, 1997). According to Murphy (1995) when large errors are objectionable, the root mean square error is more convenient.

2.4.1.3. Coefficient of determination:

The coefficient of determination calculates how well the regression line corresponds to the real data points. In this study R2 is used to determine how well satellites rainfall estimates fit to ground observations (Maathuis, 2014).

$$\text{Bias} = \frac{\sum S_i}{\sum G_i},$$

eq 2. Mean error or Bias

$$\text{RMSE} = \sqrt{\frac{\sum (G_i - S_i)^2}{n}},$$

eq 3. Root mean square of error

$$R^2 = \left(\frac{n \sum (G_i S_i) - (\sum G_i)(\sum S_i)}{\sqrt{\left(n \left(\sum G_i^2\right) - (\sum G_i)^2\right)\left(n \left(\sum S_i^2\right) - (\sum S_i)^2\right)}} \right)^2.$$

eq 4. Coefficient of determination

3. MATERIALS AND METHODS

3.1. Study Area:

To accomplish the primary objective of the assessment of the new GPM mission, which is comparing the data retrieved from GPM with those from TRMM, the entire overlapped region between GPM and TRMM estimations are considered as the study area. These areas consist of between approximately 35° north latitude and 35° south latitude. To carry out the second objective, that is ground validating the data retrieved from GPM by gauge estimates as a “ground truth” the entire territory of the Netherlands and north of Belgium is considered as the study area. Finally, for the last objective, that consists of comparing EUMETSAT MPE daily products with GPM, TRMM and gauge stations, the Netherlands and north of Belgium and the full earth disc MSG image are assumed as the study area. This area was selected because in these areas, we have mainly frontal rainfall event which occurs mostly during summer and autumn, but EUMETSAT MPE product is suitable for convective rainfall, as it is based on cloud top temperature.

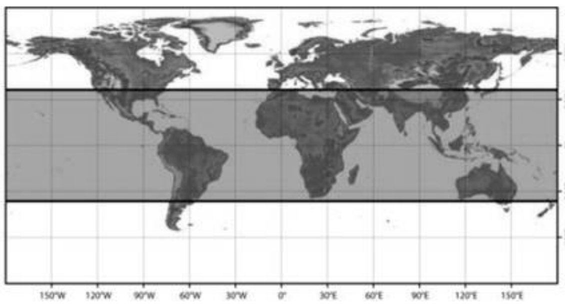

Figure (10): the overlapped areas between GPM and TRMM estimations

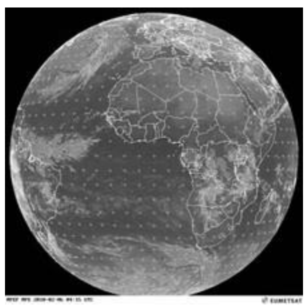

Figure (11): The view of MSG

3.2. Data sets

The main goal of this research is to compare the retrievals of GPM with the other estimations which are gauge data, TRMM data and MPE data in order to accomplish an assessment on GPM data. All the data used in this study are the time series measured from beginning of March 2014, until end of October 2014.
In order to compare the GPM data with the TRMM data we need time series of measured rainfall from both of these satellites in all of the tropical area. The GPM 3GPROF data which are the selected GPM dataset for this study were released in mid-September 2014. The format of these data is HDF5. These data are available for download in the NASA GPM Mission website (http://pmm.nasa.gov/data-

access/downloads/gpm). The TRMM data set which will be used for this study is TRMM 3B42 (V.7) which can be downloaded in NASA website (http://gdata1.sci.gsfc.nasa.gov/daac-bin/G3/gui.cgi?instance_id=TRMM_3-Hourly). These data can be downloaded either in HDF or ASCII format.
The GMP and TRMM data have an area averaged over 0.25°x0.25° latitude/longitude grid boxes and are released every 3 hours (UTC 00, 03, 06, 09, 12, 15, 18 and 21).
Figure (3) which is taken from NASA website demonstrates the spatial and temporal resolution of 3GPROF which is the selected GPM algorithm for this study.

Table (2): The 3GPROF algorithm properties

Resolution	Regions - Dates	Latency	Format
0.25°, daily	Gridded, 90°N-90° S, March 2014 to present	daily (Prod)	HDF5

For the second objective, we need time series of rainfall measured by gauge stations of the Netherlands and north of Belgium. These data products are retrieved in the GSOD station data from the ISOD Toolbox of ILWIS. The rain gauge data set is consisted of 35 rain gauge stations which measure 24 hour accumulated precipitation.

Figure (12): Black dots are rain gauge stations of the Netherlands and north of Belgium

For the last objective, we need processed MPE data. We can have access to them in ITC file server which is (\\itcnt31.itc.nl\mpe_processed). The data are released in 15 minutes timescale and in 24 hour accumulated in ILWIS format.

3.3. GPM data pre-processing

In order to prepare GPM data for validations, some pre-processing operations should be accomplished. These operations are presented as 7 steps in the following:

1. Downloading the 3GPROF GPM data from NASA website.

2. Each pictures contains several information like cloud water (in gram per cubic meter), latent heat, surface precipitation, etc.

3. The data was presented in HDF5 format, so they have to be converted to ILWIS format (MPR) using GDAL commands. The following command line is used for this conversion:

>gdal_translate "input file name.HDF5" -sds "output file address\output file name.tif"

And then we convert the "tif" format to "mpr" in ILWIS command GDAL.

4. To get the appropriate projection, all GPM maps need to be rotated 90 degree. This task can be done in mirror/rotate command in IlWIS.

5. The projection of new rotated GPM map can be verified by using other global rainfall maps. For example Figure (5) correspond to a CMORPH rainfall map at 15/05/2014. Some prominent rainfall events are specified in this map. In a visual comparison, if these rainfall events are recognized at the same location in the GPM map it means that our maps is well projected and we can pass to the next step.

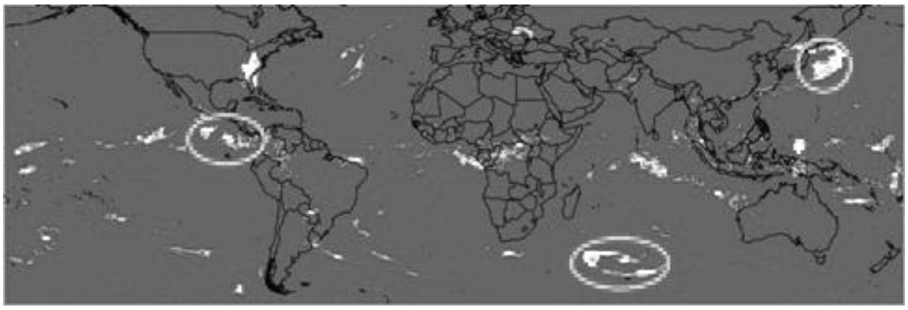

Figure (13): CMORPH rainfall map of 15/05/2014

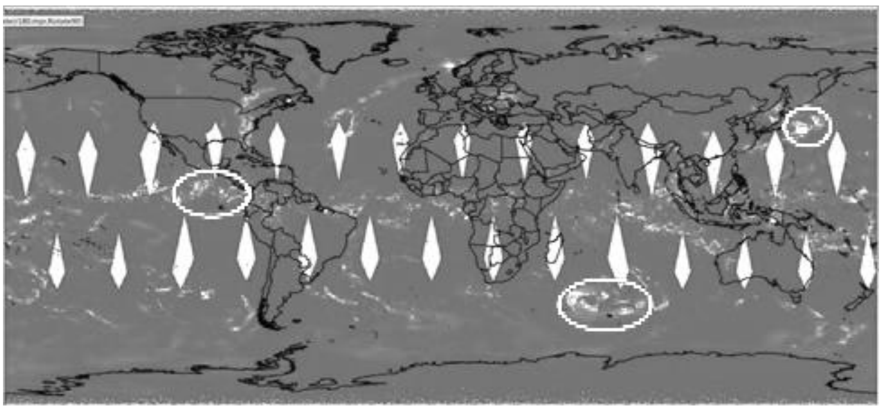

Figure (14): GPM rainfall map of 15/05/2014 rotated 90 degree

6. Since gridded data in GPM observations are defined in tables with 720 columns and 1440 rows, an appropriate georeference that defines the relation between these rows and columns and XY-coordinates must be added to GPM maps. This georeference should also define the most convenient coordinate system that may contain the projection information. For this case the LatlonWGS84 coordinate system is considered.

7. Since GPM maps demonstrate the average rainfall rate in 24 hours, each raster map should be multiplied to 24 to obtain the average of precipitation in mm per day.

3.4. Pre-processing of MPE images

Since MPE data are providing images of the full earth disc, a conversion on projection of these images is required as pre-processing step. By using nearest neighbour resampling method in ILWIS, all the MPE maps are resampled with GPM georeference.

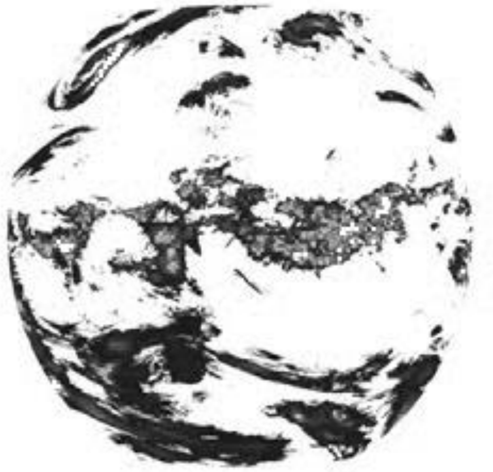

Figure (15): MPE rainfall map of 15/05/2014

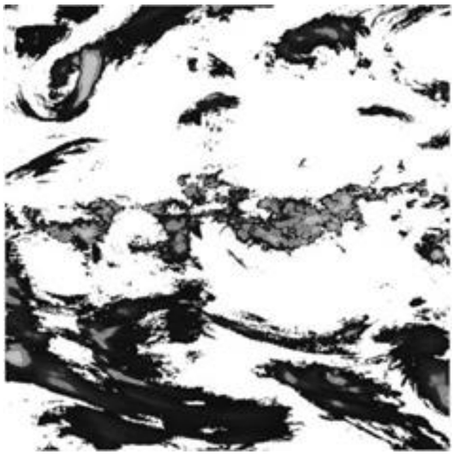

Figure (16): MPE rainfall map of 15/05/2014 after resampled with GPM georeferenced

3.5. Comparison method:

35 rain gauge stations distributed in the Netherlands and north of Belgium comprise the ground observation. These areas are affected by frontal rainfall rather than convective or orographic rainfall that

happen mostly in mountainous regions. The comparisons between GPM estimation and other satellite estimations and rain gauge observations can be done in 2 different methods:

Point to raster comparison

In this method a map list of GPM and MPE rainfall pictures are generated for each month. These map lists are added to station maps of rain gauges in ILWIS as extra layers. By clicking on location of each station, the precipitation estimated by GPM and MPE for that particular area is demonstrated in the pixel information window. By transferring these satellite rainfall estimations as well as rainfall observations from GSOD to a spreadsheet, statistical validation will be possible.

3.5.1. Raster to raster comparison:

In this method, pixels in the same location of two satellite estimations are compared. In cross operation, the output map is composed from raster values of first input map and that of the second input map. It is mandatory that both input maps have the same georeference, so before starting this operation TRMM rainfall map should be resampled by the GPM georeference. Since most of the overlapped areas in two maps are not affected by rainfall, this will cause a high correlation in our comparison. So before starting crossing a threshold of 2 mm is affected in all maps. As the next step, all the maps of a month are summed and new maps which represent rainfall of a month are generated. The cross mapping will be done between 2 monthly maps of a same month but obtained with different satellite. Figure (9) which is taken from help instruction of ILWIS demonstrate an example of cross mapping.

Example:

Input map 1:

B	B	C	D
A	A	C	D
A	A	C	C
B	C	D	A

Input map 2:

S	S	S	S
R	R	S	S
T	R	S	T
T	R	T	T

Output cross map:

BS	BS	CS	DS
AR	AR	CS	DS
AT	AR	CS	CT
BT	CR	DT	AT

Output cross table:

Domain	Map1	Map2	NPix	Area
A * R	A	R	3	.....
A * T	A	T	2	.....
B * S	B	S	2	.....
B * T	B	T	1	.....
C * R	C	R	1	.....
C * S	C	S	3	.....
C * T	C	T	1	.....
D * S	D	S	2	.....
D * T	D	T	1	.....

Figure (17): An example of cross mapping (Source: ILWIS help)

4. VALIDATION AND RESULTS

The main goal of this study is to accomplish an assessment of the new GPM mission and clarify the statistical significant difference between GPM estimates and other observation done by other satellites and gauge stations. Due to data availability reasons this study is limited to daily estimation. In order to perform a valuable comparison and obtain reliable assessment, it is essential to accomplish different statistics, because each statistic provides limited information about the error and correctness.

In this research the verification is done by two methods. First by point to raster comparison. In this method, the precipitation information of 35 rain gauge stations in The Netherlands and north of Belgium is extracted and considered as "ground truth". This data consist of daily measurement of rainfall through 8 months from the beginning of March 2014 until the end of October 2014.
In this method, point to raster comparison is done by using standard statistics and results are demonstrated in the following.

4.1. Point to raster comparison

In this method, the exact amount of daily precipitation for each station point is extracted from GPM and MPE rainfall map and collected to a specific spread sheet together with the rain gauge data. For each station the amount of accumulated rainfall for each month is calculated and transferred to another spread sheet. In this sheet each cell represents the whole amount of rainfall for each month for each station. In order to have a better understanding of the distribution of rainfall for each station in The Netherlands and north of Belgium, column bar graph for all 35 comparison points in our study area are generated. The sum of precipitation in each month retrieved by GPM, rain gauges and MPE are compared. Figure (18) represents sum of all measurement done by gauge stations, GPM and MPE for each month. Other column bars which compare measurements done for each station during the eights month is presented in Appendix A. In Appendix B the rainfall measurement for each month is presented in separate column bar graphs. These column bar graphs contain observation of all 35 stations in a month. In Appendix C the error bar graphs that demonstrate the difference between GPM observation and gauge measurement are presented for all stations in each month. In Appendix D scatterplots based on measurement done for each station during the time series is generated. Table (2) and Table (3) present the statistics done in order to get the comparison between rain gauge data, MPE and GMP. In these tables all the stations all categorized by their spatial distribution. Figure (19) is an example of scatterplot for station Vlissingen. As you can see in that picture, the majority of plots have a good correlation, but the point indicated by green circle has significantly decreased the R^2 value. After verifying the comparison computing procedure and become sure that this error is not related to our calculation, this point is removed and the new result demonstrates a far better correlation between observations. This procedure is done for all comparisons and the results is represented in two table, first without correction and then with correction.

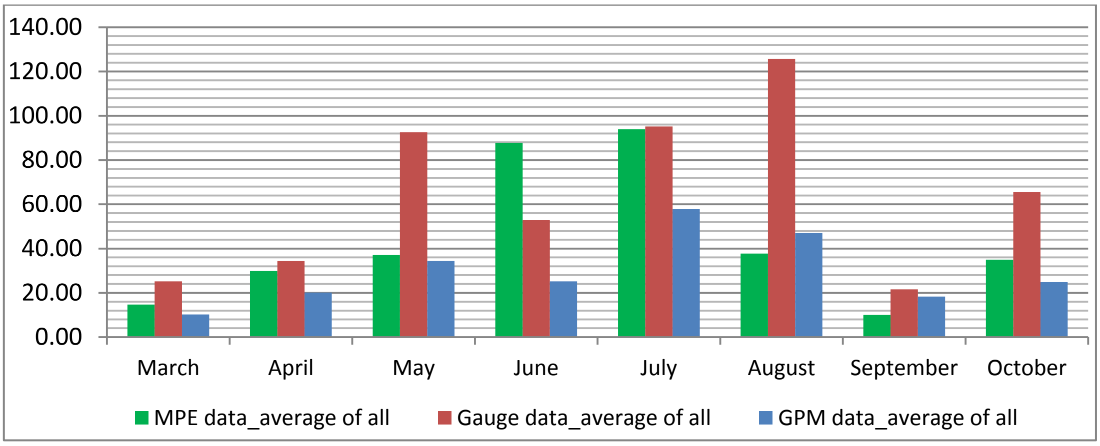

Figure (18): The sum of all measurement done by gauge stations, GPM and MPE for each month

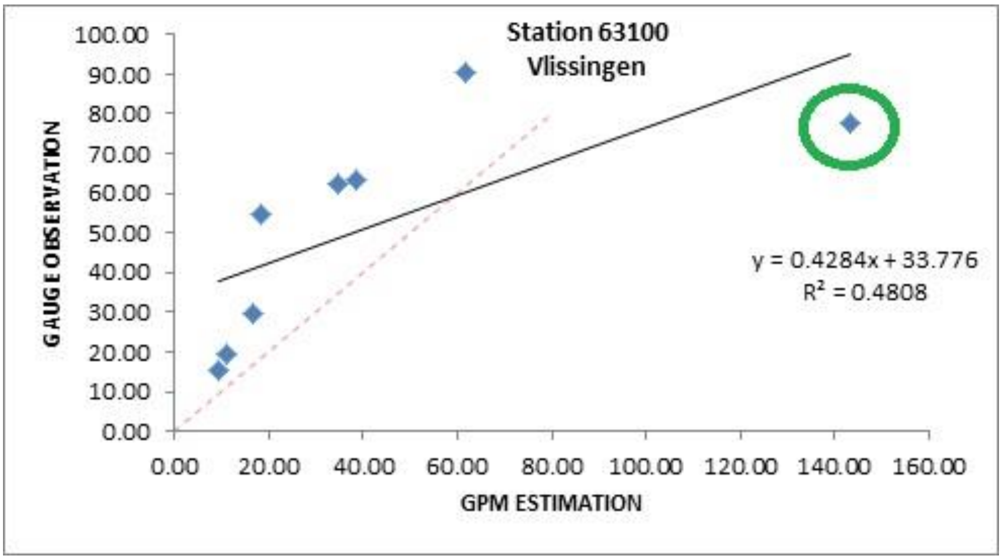

Figure (19): Scatterplot of station Vlissingen without applying correction

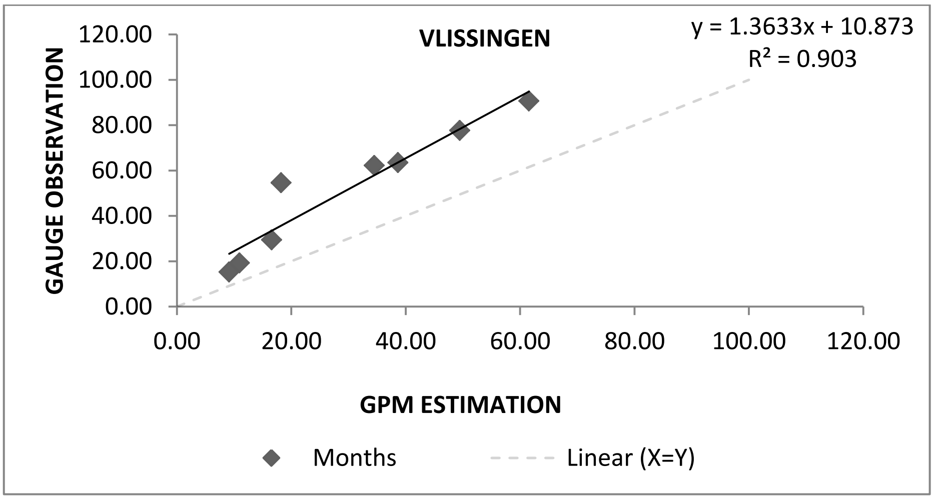

Figure (20): Scatterplot of station Vlissingen without applying correction

The following plot maps compare the R^2 value and RMSE value of all stations together and demonstrate in which station we have the better observation in GPM and MPE and finally show that which satellite has the best observation in overall.

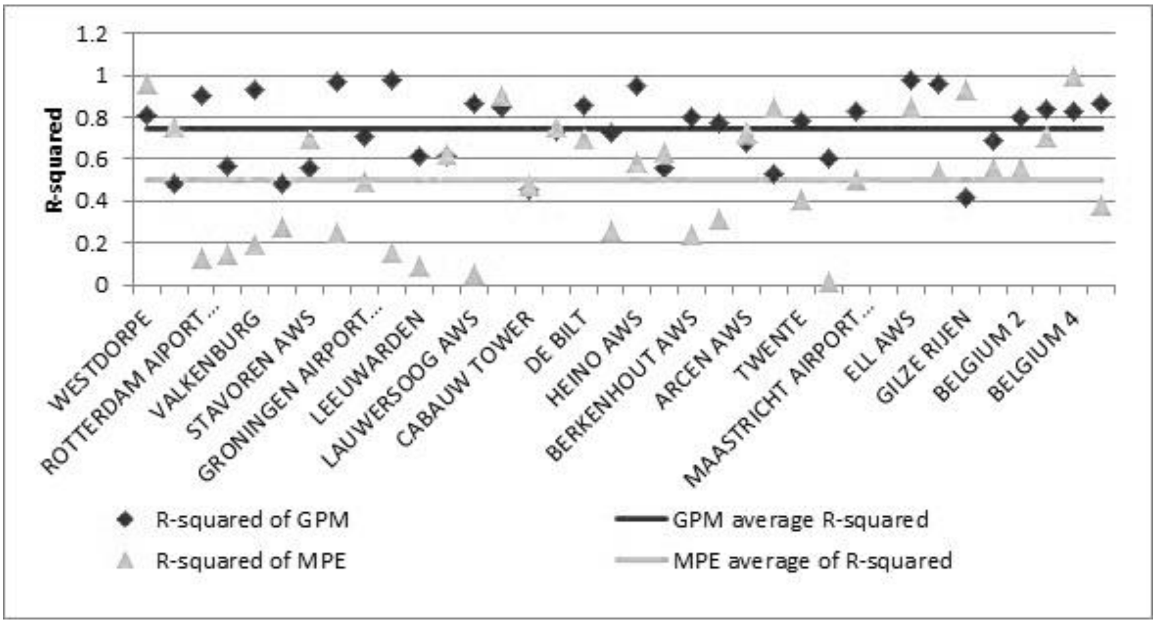

Figure (21): Scatterplot of R-squared for GPM and MPE

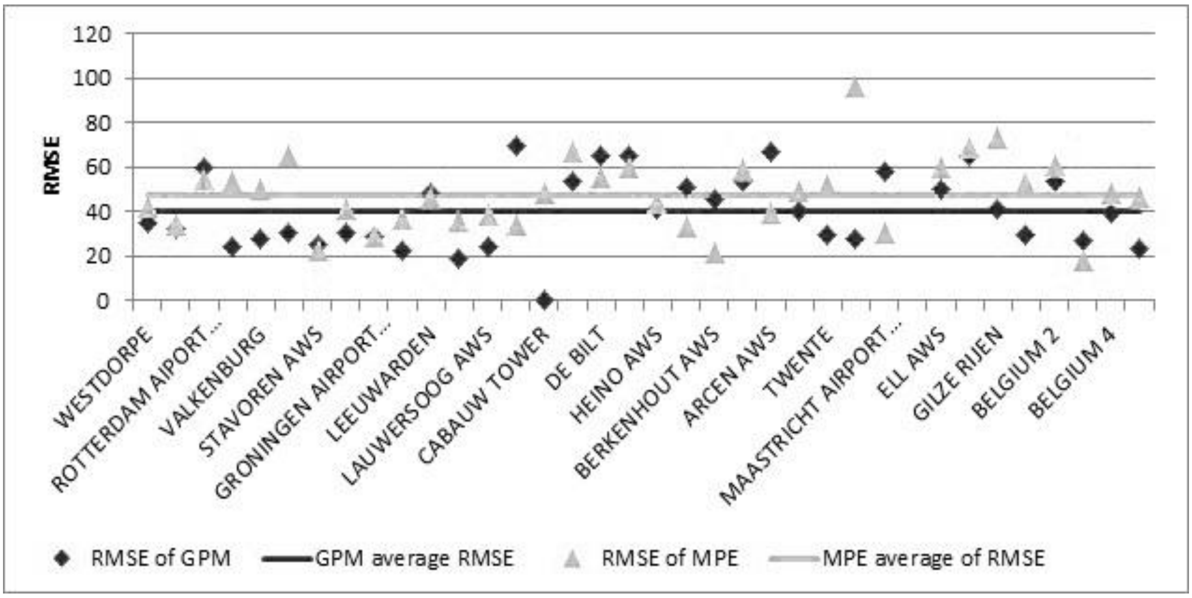

Figure (22): Scatterplot of R-squared for GPM and MPE

Table (3): Statistical parameter of monthly accumulated observation without correction, GPM vs rain gauges

Spatial Distribution	Station Number	Station Name	R2	MBE	MAE	RSME
Coastal	63190	WESTDORPE	0.808	-32.03	32.03	34.62
	63100	VLISSINGEN	0.481	-10.00	26.38	31.88
	63440	ROTTERDAM AIPORT ZESTIE	0.208	-33.13	34.39	47.54
	63300	HOEK VAN HOLLAND	0.02	-20.64	38.93	53.70
	62100	VALKENBURG	0.44	-30.08	30.08	40.50
	62570	WIJK AAN ZEE	0.361	-44.95	49.44	62.29
	62670	STAVOREN AWS	0.062	-33.08	33.83	51.74
	62350	DE KOOIJ	0.77	-32.38	32.38	39.02
	62800	GRONINGEN AIRPORT EELDE	0.35	-13.64	23.95	28.07
	62860	NIEUW BEERTA AWS	0.561	-23.21	23.21	26.93
	62700	LEEUWARDEN	0.01	-23.45	42.56	52.08
	62510	TERSCHELLINGHOORN	0.163	-27.76	30.68	40.46
	62770	LAUWERSOOG AWS	0.58	-15.28	20.34	23.93
Central	63750	VOLKEL	0.403	-51.62	54.13	65.60
	63480	CABAUW TOWER	0.451	-33.45	37.35	45.26
	62750	DEELEN	0.64	-66.11	66.11	84.61
	62600	DE BILT	0.058	-36.53	56.38	67.00
	62400	AMSTERDAM AIRPORT SCHIPHOL	0.274	-42.50	43.75	60.92
	62780	HEINO AWS	0.371	-37.36	37.36	42.71
	62690	LELYSTAD AWS	0.225	-36.14	36.30	44.24
	62490	BERKENHOUT AWS	0.8	-32.18	32.62	45.81
	62730	MARKNESSE AWS	0.771	-46.45	46.45	53.26
East	63910	ARCEN AWS	0.1	-42.03	44.56	58.48
	62830	HUPSEL AWS	0.523	-26.92	28.47	39.83
	62900	TWENTE	0.6	-32.29	32.29	39.97
	62790	HOOGEVEEN	0.6	-35.46	35.46	50.61
South	63800	MAASTRICHT AIRPORT ZUID	0.828	-40.79	41.07	58.39
	63770	ELL AWS	0.981	-39.78	39.78	49.72
	63700	EINDHOVEN	0.6847	-49.16	49.16	61.97
	63500	GILZE RIJEN	0.004	-59.65	64.14	94.84
	64640	BELGIUM 1	0.493	-37.14	37.68	52.67
	64770	BELGIUM 2	0.636	-39.27	40.72	49.97
	64500	BELGIUM 3	0.564	-14.17	-14.17	25.34
	64310	BELGIUM 4	0.831	-36.29	36.29	39.52
	64470	BELGIUM 5	0.445	-27.78	29.16	41.83

Table (4): Statistical parameter of monthly accumulated observation after correction, GPM vs rain gauges

Spatial Distribution	Station Number	Station Name	R2	MBE	MAE	RSME
Coastal	63190	WESTDORPE	0.808	-32.03	32.03	34.62
	63100	VLISSINGEN	0.481	-10.00	26.38	31.88
	63440	ROTTERDAM AIPORT ZESTIE	0.908	-51.36	51.36	59.88
	63300	HOEK VAN HOLLAND	0.5662	-20.89	20.89	24.36
	62100	VALKENBURG	0.9346	-24.24	24.24	27.98
	62570	WIJK AAN ZEE	0.4846	-20.40	26.38	30.10
	62670	STAVOREN AWS	0.5528	-19.20	20.05	25.21
	62350	DE KOOIJ	0.971	-26.43	26.43	30.92
	62800	GRONINGEN AIRPORT EELDE	0.7035	-25.06	25.06	28.88
	62860	NIEUW BEERTA AWS	0.9771	-22.00	22.00	22.20
	62700	LEEUWARDEN	0.614	-37.31	38.13	48.23
	62510	TERSCHELLINGHOORN	0.6176	-12.44	16.33	18.94
	62770	LAUWERSOOG AWS	0.8646	-20.16	20.56	24.57
Central	63750	VOLKEL	0.8487	-60.43	60.43	70.03
	63480	CABAUW TOWER	0.451	-40.45	40.45	0.6974
	62750	DEELEN	0.731	-42.32	42.32	53.17
	62600	DE BILT	0.8523	-49.58	51.68	64.77
	62400	AMSTERDAM AIRPORT SCHIPHOL	0.7245	-48.78	49.79	65.13
	62780	HEINO AWS	0.9486	-37.28	37.28	41.55
	62690	LELYSTAD AWS	0.5573	-47.79	47.79	51.07
	62490	BERKENHOUT AWS	0.8	-32.18	32.62	45.81
	62730	MARKNESSE AWS	0.771	-46.45	46.45	53.26
East	63910	ARCEN AWS	0.6774	-56.18	56.18	67.29
	62830	HUPSEL AWS	0.527	-26.92	28.47	39.83
	62900	TWENTE	0.7787	-25.21	25.21	29.47
	62790	HOOGEVEEN	0.6	-22.93	22.93	27.59
South	63800	MAASTRICHT AIRPORT ZUID	0.828	-40.79	41.07	58.39
	63770	ELL AWS	0.981	-39.78	39.78	49.72
	63700	EINDHOVEN	0.9632	-51.54	51.54	65.10
	63500	GILZE RIJEN	0.4196	-25.64	30.77	41.22
	64640	BELGIUM 1	0.6843	-24.25	24.87	29.22
	64770	BELGIUM 2	0.7974	-45.71	45.71	53.38
	64500	BELGIUM 3	0.8381	-18.32	19.58	26.50
	64310	BELGIUM 4	0.831	-36.29	36.29	39.52
	64470	BELGIUM 5	0.8633	-17.27	18.85	23.10

Table (5): Statistical parameter of monthly accumulated observation for each month without correction, MPE vs rain gauges

Spatial Distribution	Station Number	Station Name	R2	MBE	MAE	RSME
Coastal	63190	WESTDORPE	0.3284	-26.17	33.08	36.89
	63100	VLISSINGEN	0.2969	-20.18	25.72	29.80
	63440	ROTTERDAM AIPORT ZESTIE	0.0328	-25.73	47.78	57.55
	63300	HOEK VAN HOLLAND	0.0068	-24.98	41.81	54.64
	62100	VALKENBURG	0.0003	-25.76	40.91	49.84
	62570	WIJK AAN ZEE	0.0474	-38.12	45.86	61.44
	62670	STAVOREN AWS	0.0106	-18.32	35.51	50.72
	62350	DE KOOIJ	0.2473	-27.53	29.31	41.52
	62800	GRONINGEN AIRPORT EELDE	0.2333	-17.71	22.59	27.86
	62860	NIEUW BEERTA AWS	0.2846	4.27	50.67	77.75
	62700	LEEUWARDEN	0.0359	-9.48	38.11	56.96
	62510	TERSCHELLINGHOORN	0.0007	-15.04	32.27	40.34
	62770	LAUWERSOOG AWS	0.0393	5.46	44.21	63.43
Central	63750	VOLKEL	0.182	-27.42	39.65	49.96
	63480	CABAUW TOWER	0.0003	-23.03	44.28	54.26
	62750	DEELEN	0.3479	-39.35	53.18	65.45
	62600	DE BILT	0.0298	-29.92	47.92	58.06
	62400	AMSTERDAM AIRPORT SCHIPHOL	0.0063	-27.75	49.54	63.28
	62780	HEINO AWS	0.0088	-1.87	54.58	78.00
	62690	LELYSTAD AWS	0.3285	-11.25	29.02	33.76
	62490	BERKENHOUT AWS	0.0012	-28.72	43.16	65.98
	62730	MARKNESSE AWS	0.0417	-20.12	45.06	58.94
East	63910	ARCEN AWS	0.3715	-20.71	35.15	41.28
	62830	HUPSEL AWS	0.2251	-8.01	49.67	60.08
	62900	TWENTE	0.1593	1.01	64.35	87.27
	62790	HOOGEVEEN	0.011	-9.19	64.27	96.60
South	63800	MAASTRICHT AIRPORT ZUID	0.092	-34.39	50.60	70.75
	63770	ELL AWS	0.0575	-27.80	48.34	61.97
	63700	EINDHOVEN				
	63500	GILZE RIJEN	0.9291	-60.14	60.14	73.42
	64640	BELGIUM 1	0.0125	-19.75	38.49	55.57
	64770	BELGIUM 2	0.0131	-23.15	43.92	58.20
	64500	BELGIUM 3	0.0024	-1.39	31.17	46.56
	64310	BELGIUM 4	0.3578	-31.41	34.75	42.16
	64470	BELGIUM 5	0.1755	-15.82	40.04	51.27

Table (6): Statistical parameter of monthly accumulated observation for each month after correction, MPE vs rain gauges

Spatial Distribution	Station Number	Station Name	R2	MBE	MAE	RSME
Coastal	63190	WESTDORPE	0.959	-39.50	39.50	41.83
	63100	VLISSINGEN	0.7505	-30.60	30.60	33.75
	63440	ROTTERDAM AIPORT ZESTIE	0.1255	-40.47	43.54	54.12
	63300	HOEK VAN HOLLAND	0.1447	-37.23	39.10	53.71
	62100	VALKENBURG	0.1905	-36.54	39.66	49.86
	62570	WIJK AAN ZEE	0.2794	-47.21	48.76	64.97
	62670	STAVOREN AWS	0.7007	-17.01	17.01	22.46
	62350	DE KOOIJ	0.2473	-27.53	29.31	41.52
	62800	GRONINGEN AIRPORT EELDE	0.4954	-22.61	23.45	29.12
	62860	NIEUW BEERTA AWS	0.1548	-23.27	29.75	36.87
	62700	LEEUWARDEN	0.0885	-25.68	28.71	46.52
	62510	TERSCHELLINGHOORN	0.6241	-26.47	27.59	35.44
	62770	LAUWERSOOG AWS	0.0543	-14.81	29.47	38.68
Central	63750	VOLKEL	0.9036	-27.58	27.58	34.20
	63480	CABAUW TOWER	0.4691	-38.26	38.66	48.65
	62750	DEELEN	0.7527	-52.87	52.87	66.77
	62600	DE BILT	0.7005	-44.48	44.48	55.78
	62400	AMSTERDAM AIRPORT SCHIPHOL	0.2612	-43.57	44.76	59.94
	62780	HEINO AWS	0.5844	-37.63	37.63	43.40
	62690	LELYSTAD AWS	0.6297	-26.85	26.85	33.13
	62490	BERKENHOUT AWS	0.2364	1.56	17.69	21.55
	62730	MARKNESSE AWS	0.3131	-43.45	43.45	58.73

East	63910	ARCEN AWS	0.7265	-31.09	32.76	39.52
	62830	HUPSEL AWS	0.851	-37.72	39.18	49.33
	62900	TWENTE	0.4091	-40.57	43.88	52.16
	62790	HOOGEVEEN	0.011	-9.19	64.27	96.60
South	63800	MAASTRICHT AIRPORT ZUID	0.4978	-2.21	23.82	30.84
	63770	ELL AWS	0.8518	-42.84	44.19	59.43
	63700	EINDHOVEN	0.5338	-56.20	56.20	68.52
	63500	GILZE RIJEN	0.9291	-60.14	60.14	73.42
	64640	BELGIUM 1	0.5599	-32.88	33.68	52.78
	64770	BELGIUM 2	0.555	-44.71	44.71	60.29
	64500	BELGIUM 3	0.7023	-7.49	12.79	17.66
	64310	BELGIUM 4	0.9957	-44.10	44.10	48.51
	64470	BELGIUM 5	0.3786	-28.95	34.89	46.65

4.2. Raster to Raster analysis

In this method, monthly rainfall maps of TRMM, GPM and MPE are compared to find any correlation between these estimates in the overlapped area. For this task, since we are working in global scale, the overlapped area between these maps will be very wide. On the other hand most parts of these areas are not affected by rainfall which in turn will cause a very high correlation that is mean less. To solve this problem a 2 mm daily precipitation threshold is applied in all daily rainfall maps which mean that all the pixels having a value less than 2 mm are removed in our comparison. As the second step, all daily rainfall maps summed and monthly rainfall maps are generated for each satellite. To be able to do "Cross mapping" task in ILWIS software all maps must have the same georeference. The result of this comparison demonstrates that GPM and TRMM have a good correlation. The correlation coefficient for each month comparison is approximately 0.65.

In order to identify the rainfall field of two satellites, the number of pixels estimated by each of them is calculated in tables and demonstrated in Appendix E. This quantifies the territory of rainfall observed by each satellite. As an example, in table (9), the number of pixels observed in the accumulated rainfall map of GPM and TRMM satellite for the month March is quantified.

Table (7): The result of Cross mapping monthly accumulated GPM data vs TRMM data for each month

	Correlation coefficient	R^2	Sum value of all pixels (GPM)	Sum value of all pixels (TRMM)	Std. of all pixels(GPM)	Std. of all pixels(TRMM)
March	0.613	0.3755	14931552.42	14908712.7	103	107
April	0.671	0.450	19313033.98	18590681.2	119.82	113
May	0.68	0.46	19038956.57	18563729.5	173.89	169.6
June	0.65	0.45	19284719.87	18491525.3	139.4	114.1
July	0.713	0.508	9883265.405	9677406.7	118.1	134.7
August	0.573	0.329	11171874.83	12301207.1	110.7	117.1
September	0.627	0.393	13041148.42	12862879.4	111.6	105.3
October	0.638	0.407	17138611.24	15923383.2	107.52	102.6

Table (8): The result of Cross mapping monthly accumulated GPM data vs MPE data for each month

	Correlation coefficient	R2	Sum of all pixels(GPM)	Sum of all pixels(MPE)	Std. of all pixels(GPM)	Std. of all pixels(MPE)
March	0.07	0.005	99666.741	143720.96	19.15	21.6
April	0.221	0.05	282507.2846	267785.78	28.77	18.04
May	0.22	0.0485	218162.3949	187567.48	21.15	16.16
June	0.259	0.067	185672.5116	139296.99	22.2	19
July	0.31	0.13	183018.2376	147134.9015	26.3	17.1
August	0.412	0.17	196346.7421	172054.16	31.7	26.3
September	0.353	0.12	229950.3746	219342.01	27.56	23.56
October	0.296	0.087	232820.0182	245833.87	21.64	23.18

Table (9): The number of pixels observed by TRMM and GPM in March

MARCH		Estimated values of GPM		TOTAL
		Yes	No	
Estimated values of TRMM	Yes	88843	154924	243767
	NO	20814	311419	332233
TOTAL		109657	466343	576000

5. DISCUSSION AND CONCLUSION

In this part we want to verify to see whether or not our study answered the research questions generated in the introduction.

Question 1. Is there a statistically significant difference between the data retrieved from GPM and the TRMM data in overlapped area?

Answer: The results obtained in the raster to raster comparison clarify that GPM estimations has a good correlation with TRMM estimations. The correlation coefficients between TRMM and GPM for month March, April, May, June, July, August, September and October are 0.613, 0.671, 0.68, 0.713, 0.573, 0.627 and 0.638 which approve a good correlation in satellite observation, especially in a very large overlapped area which is in tropics and subtropics. The sum of all pixel values of the overlapped area between the two rainfalls maps are also very close, which in turn approve that the correlation between two estimates is good and GPM has good capability in detecting convective rainfall. The reason of this good correlation is because both satellites use approximately the same instrument, but that of the GPM is more developed and is able to detect also light rain and snow. For this reason we have a higher total sum from GPM in comparison with TRMM. The rainfall field comparison demonstrates a higher number of pixels detected by TRMM in comparison with GPM for all months. As you can see in Table (9), the number of pixels detected by TRMM is 243767 but for GPM is 109657. But the sum value of all pixels for GPM is higher than TRMM which means that we always have a higher estimation for GPM in comparison to TRMM

Question 2. What is the accuracy of the data retrieved from GPM compared with combined gauge data?

Answer: The point to raster comparison done in The Netherlands and north of Belgium approve that in the majority of these point observations there is an underestimation in detecting rainfall by GPM. As you can see in Appendix A, in most of column bar graph GPM has a lower estimation than rain gauges which are the ground truth. This underestimation is higher May until August. In that months we have a higher amounts of rainfalls compared to other months of the time series of this study. In months we have light precipitation, GPM estimations are approximately close to rain gauge observations. It approves that GPM has a good accuracy in detecting light rainfall.

The significant part of this comparison is that before doing a correction on scatterplots the correlation between GPM and gauge is moderate and in some cases it is very good, but after applying the correction and removing 1 or 2 plots we can observe a very good correlation between GPM and gauge. Since we are sure that our data processing and computing does not have any error, we can conclude that in some cases we have significant errors in gauge observing.

Another significant result of this study is that we have the best correlation in south parts, then in coastal regions and after that in central parts of The Netherlands and finally the lowest correlation is done in east part of the country. This means that the best GPM observation is done in south parts, and then in central parts, and after that in central parts and finally the less accurate observation is done in east part of The Netherlands. For MPE the best observation is done in south parts, then in east parts, and after that in central parts, and finally the less accurate observation is done in coastal parts.

An issues detected in GPM comparison is that in certain month the error of estimates over the study area varies very much. For example as you can see in Figure (20) in month June at station number 3 we have approximately 48 millimetre of underestimation and at the same month in station number 11 there is 22 millimetre overestimation.

Question 3. How much is the difference between the GPM data and the data of the near real time EUMETSAT MPE regarding rainfall intensity?

Answer: Contrary to the GPM, the majority of MPE estimations have overestimation in a comparison with rain gauge as ground truth. As you can see in Appendix A, most of MPE observations have higher value in comparison with rain gauge observation as well as GPM estimations. As it is based on cloud top temperature, the MPE is more suitable for detecting convective rainfall and not for frontal rainfall which is our study area in point to raster analysis.

Question 4. How good is GPM in detecting frontal rainfall intensities?

Answer: In The Netherlands and north of Belgium, in where we mostly have frontal rainfall events, the point to raster analysis approve that GPM has mostly an underestimation in detecting high precipitation rain events. On the other hand, in month we have light precipitation, the estimation of GPM in approximately close to that of rain gauges.

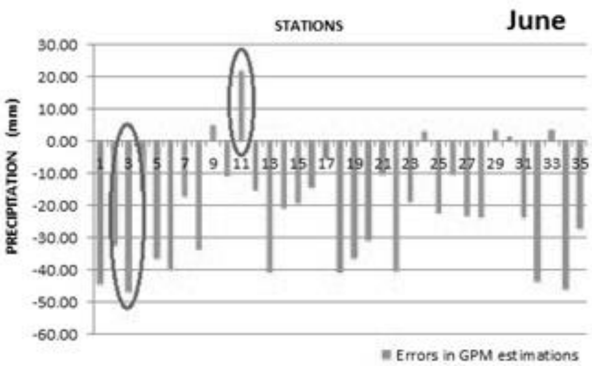

Figure (23): Error bar of GPM for June

6. RECOMMENDATION AND FUTURE WORK

The goal of this assessment on GPM is to demonstrate the strengths and weakness points and the probable lake of accuracy of the new GPM mission to algorithm developers in order to make a revision on it and make it more precise and solve the systematic problems.
The other issue is that in certain month the error of estimates over the study area varies very much. It is recommended for future work to find the reason behind this. For example in month June at station number 3 we have approximately 48 millimeter of underestimation and at the same month in station number 11 there is 22 millimeter overestimation.

It is also recommended to use some interpolation techniques like Thiessen polygon method, IDW, Spline, Kriging and TW to change the point map of rainfall measurement to a raster map and doing the raster to raster analysis and comparing the results versus radar values to find the more accurate technique to develop a raster map of precipitation distribution.

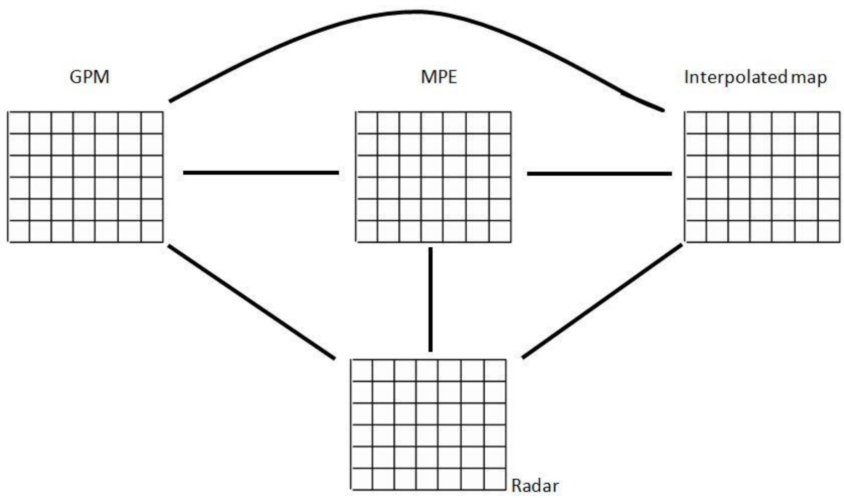

Figure (24): Different raster comparison

Since the results of this study is obtained in The Netherlands and north of Belgium, in where we mostly have frontal rainfall, and other part of this research is done on the tropics and sub-tropics, in where we mostly have convective rainfall, it is highly recommended to verify the accuracy of GPM estimations in mountainous areas in where we mostly have orographic precipitation. This task is very essential because contrary to TRMM that only with tropics and sub0tropics, the GPM do measurement in global scale so to better understand the accuracy of GPM estimates we need to do comparison in all types of rainfall which consist of convective, frontal and orographic precipitation.

7. REFERENCES

Allcroft, D. J., Glasbey, C. A., & Durban, M. (2001). Modelling weather data, 192–195.

Aly, A. (2008). *Construction of Complete Daily Precipitation Records for Rain Gauges in Central and South Florida*.

Amitai, E., Llort, X., & Sempere-Torres, D. (2006). Opportunities and challenges for evaluating precipitation estimates during GPM mission. *Meteorologische Zeitschrift*, *15*(5), 551–557. doi:10.1127/0941-2948/2006/0157

Animation of groundwater processes > Water Balance. (n.d.). Retrieved July 25, 2014, from http://iwmi.dhigroup.com/hydrological_cycle/waterbalance.html

B. Geerts and E. Linacre. (2010). Global precipitation. Retrieved January 27, 2015, from http://www-das.uwyo.edu/~geerts/cwx/notes/chap10/global_precip.html

Bajracharya, S. R., Shrestha, M. S., Mool, K., & Thapa, R. (2010). Validation of Satellite Rainfall Estimation in the Summer monsoon Dominated Area of the Hindu Kush Himalayan Region, 281–290.

Barcelona Field Studies Centre. (2013). U.K. Weather: Frontal Rain. Retrieved September 14, 2014, from http://geographyfieldwork.com/FrontalRain.htm

Burrows, W. R. (1871). Henry R . Stanski Laurence J . Wilson 1 . 1 A Verification Model, 1–12.

Catto, J. L., Jakob, C., Berry, G., & Nicholls, N. (2012). Relating global precipitation to atmospheric fronts. *Geophysical Research Letters*, *39*(10), n/a–n/a. doi:10.1029/2012GL051736

Collins, F. (2005). Combined Radar and Radiometer Analysis of Precipitation Profiles for a Parametric, (2000), 909–929.

comet. (2011). Introduction to Tropical Meteorology, Ch. 2: Remote Sensing. Retrieved January 27, 2015, from http://www.goes-r.gov/users/comet/tropical/textbook_2nd_edition/print_2.htm#page_12.2.2

Convectional Rainfall. (2006). Retrieved September 14, 2014, from http://weather.about.com/od/lessonplanshighschool/a/ConvRain.htm

Dimitris. (2014). Frontal systems. Retrieved September 15, 2014, from http://users.otenet.gr/~meteo/frontal-systems.html

Earth Gauge » Tips Archive » Climate Fact: Frontal System Precipitation. (n.d.). Retrieved September 14, 2014, from http://www.earthgauge.net/2012/climate-fact-frontal-system-precipitation

Ebert, E. E. (1997). Methods for verifying satellite precipitation estimates, 1–12.

Fang, H., Beaudoing, H. K., Rodell, M., Teng, W. L., Vollmer, B. E., Earth, G., … Systems, W. I. (2009). Global Land Data Assimilation System (GLDAS) Products , Services and Application from NASA Hydrology Data and Information Services Center (HDISC) ASPRS 2009 Annual Conference Baltimore , Maryland Š March 8-13 , 2009 ASPRS 2009 Annual Conference Baltim.

Furukawa, K., Hanado, H., Ishii, Y., Kojima, M., Takahashi, N., Iguchi, T., & Okumura, M. (2007). Dual-Frequency Precipitation Radar for the Global Precipitation Measurement, (1), 3551–3554.

Geerts, B. (2010). Satellite-based rainfall estimation. Retrieved January 27, 2015, from http://www-das.uwyo.edu/~geerts/cwx/notes/chap10/satellite_rain.html

Giovanni-3 Online Users Manual: 5. Services and Operations — GES DISC. (2011). Retrieved September 15, 2014, from http://disc.sci.gsfc.nasa.gov/giovanni/additional/users-manual/G3_manual_Chapter_5_services.shtml#latlon

Goddard Space Flight Center. (2014). GPM Data Downloads | Precipitation Measurement Missions. Retrieved September 18, 2014, from http://pmm.nasa.gov/data-access/downloads/gpm

Gómez, M. R. S. (2007). *Spatial and temporal rainfall gauge data analysis and comparison with TRMM microwave radiometer surface rainfall retrievals*. *ITC*. ITC, University of Twente. Retrieved from http://medcontent.metapress.com/index/A65RM03P4874243N.pdf

Han, W. S., Burian, S. J., & Shepherd, J. M. (2010). Assessment of satellite-based rainfall estimates in urban areas in different geographic and climatic regions. *Natural Hazards*, *56*(3), 733–747. doi:10.1007/s11069-010-9585-7

Hanson, H., & Bensusen, S. (2013). *Global Precipitation Measurement: Core Observatory*.

Harris, T. (2014). Celebrating the Upcoming Launch of Global Precipitation Measurement (GPM) Mission. Retrieved September 09, 2014, from https://www.exelisvis.com/Learn/EventsTraining/Webinars/TabId/397/ArtMID/1694/ArticleID/13826/Celebrating-the-Upcoming-Launch-of-Global-Precipitation-Measurement-GPM-Mission.aspx

Heinemann, T., Lattanzio, A., & Roveda, F. (2007). THE EUMETSAT MULTI-SENSOR PRECIPITATION ESTIMATE (MPE), 1–8.

Huffman, G. J., & Bolvin, D. T. (2014a). August 2013, (October 2012), 1–46.

Huffman, G. J., & Bolvin, D. T. (2014b). May 2014, (May), 1–42.

Islam, T., Rico-Ramirez, M. a., Han, D., Srivastava, P. K., & Ishak, A. M. (2012). Performance evaluation of the TRMM precipitation estimation using ground-based radars from the GPM validation network. *Journal of Atmospheric and Solar-Terrestrial Physics*, *77*, 194–208. doi:10.1016/j.jastp.2012.01.001

Kidd, C., & Hou, A. (n.d.). The Global Precipitation Measurement (GPM) mission : Hydrological applications.

Kidd, C., & Levizzani, V. (2011). Status of satellite precipitation retrievals, 1109–1116. doi:10.5194/hess-15-1109-2011

Kidd, C., & Levizzani, V. (2011). Status of satellite precipitation retrievals. *Hydrology and Earth System Sciences*, *15*(4), 1109–1116. doi:10.5194/hess-15-1109-2011

Levizzani, V., Bauer, P., & Turk, F. J. (2007). *MEASURING PRECIPITATION FROM SPACE*. Springer.

Liu, Z., Ostrenga, D., Teng, W., & Kempler, S. (2012). Tropical Rainfall Measuring Mission (TRMM) Precipitation Data and Services for Research and Applications. *Bulletin of the American Meteorological Society*, *93*(9), 1317–1325. doi:10.1175/BAMS-D-11-00152.1

Maxwell, R. (2014). NASA's Global Precipitation Measurement - GIS Lounge. Retrieved September 09, 2014, from http://www.gislounge.com/nasas-global-precipitation-measurement/

Michaelides, S. C. (2008). *Precipitation : Advances in Measurement, Estimation and Prediction*. Dordrecht: Springer.

Morris, K. R., & Schwaller, M. R. (2010). Data visualization and analysis tools for the Global Precipitation Measurement (GPM) Validation Network. In *2010 IEEE International Geoscience and Remote Sensing Symposium* (pp. 847–850). IEEE. doi:10.1109/IGARSS.2010.5654248

Murphy, A. H. (1995). The coefficients of correlation and determination as measures of performance in forecast verification.

National Weather Service. (2010). Education Resource - Airmasses and Fronts. Retrieved from http://www.srh.noaa.gov/crp/?n=education-airmasses

NEWR/WRF EMS - Frequently Asked Questions [FAQ] : WRF EMS Info. (n.d.). Retrieved July 17, 2014, from http://www.wrfems.info/viewtopic.php?f=3&t=148

Novella, N., & Thiaw, W. (2009). Validation of Satellite-Derived Rainfall Products over the Sahel, *2*(1).

Olson, W. S., & Masunaga, H. (2011). GPM Combined Radar-Radiometer Precipitation Algorithm Theoretical Basis Document, (Version 2).

Reed, J. (2014, January 16). The Global Precipitation Measurement Mission. Retrieved from http://www.nasa.gov/mission_pages/GPM/overview/

Rodell, M., Houser, P. R., Jambor, U., Gottschalck, J., Mitchell, K., Meng, C.-J., … Toll, D. (2004). The Global Land Data Assimilation System. *Bulletin of the American Meteorological Society*, *85*(3), 381–394. doi:10.1175/BAMS-85-3-381

Rosenfeld, D., Wolff, D. B., & Amitai, E. (1994). 1520-0450(1994)033-0682-twpmmf-2.0.co;2.pdf.

Schaake et al. JGR 1996(1).pdf. (n.d.).

Schwaller, M. R., & Morris, K. R. (2011). A Ground Validation Network for the Global Precipitation Measurement Mission. *Journal of Atmospheric and Oceanic Technology*, *28*(3), 301–319. doi:10.1175/2010JTECHA1403.1

Smith, E. A., Asrar, G., Furuhama, Y., Ginati, A., Mugnai, A., Nakamura, K., … Zhang, W. (2007). *Measuring Precipitation From Space*. (V. Levizzani, P. Bauer, & F. J. Turk, Eds.) (pp. 611–653). Dordrecht: Springer Netherlands. doi:10.1007/978-1-4020-5835-6

Star, B. K. (2014). GOES-R AWG Product Validation Tool Development Hydrology Application Team, 1–13.

Troutman, T. W., Nws, N., Headquarters, S. R., Worth, F., Rose, M. A., & Office, W. F. (2001). A Comprehensive Heavy Precipitation Climatology for Middle Tennessee.

Vela, N., Cremonini, R., Oberto, E., & Giorcelli, M. (2013). COSMO model validation using the Italian radar mosaic and the rain gauges estimated precipitation 3 Reconstruction of the precipitation field 4 Validation, (13), 83–92.

Wang, J., & Wolff, D. B. (2009). Evaluation of TRMM Ground-Validation Radar-Rain Errors Using Rain Gauge Measurements, (April).

Worqlul, a. W., Maathuis, B., Adem, a. a., Demissie, S. S., Langan, S., & Steenhuis, T. S. (2014). Comparison of rainfall estimations by TRMM 3B42, MPEG and CFSR with ground-observed data for the Lake Tana basin in Ethiopia. *Hydrology and Earth System Sciences*, *18*(12), 4871–4881. doi:10.5194/hess-18-4871-2014

Ymeti, I. (2007). Rainfall estimation by Remote Sensing for conceptual rainfall-runoff modeling in the Upper Blue Nile basin Rainfall estimation by Remote Sensing for conceptual rainfall-runoff modeling in the Upper Blue Nile basin.

Appendix A.

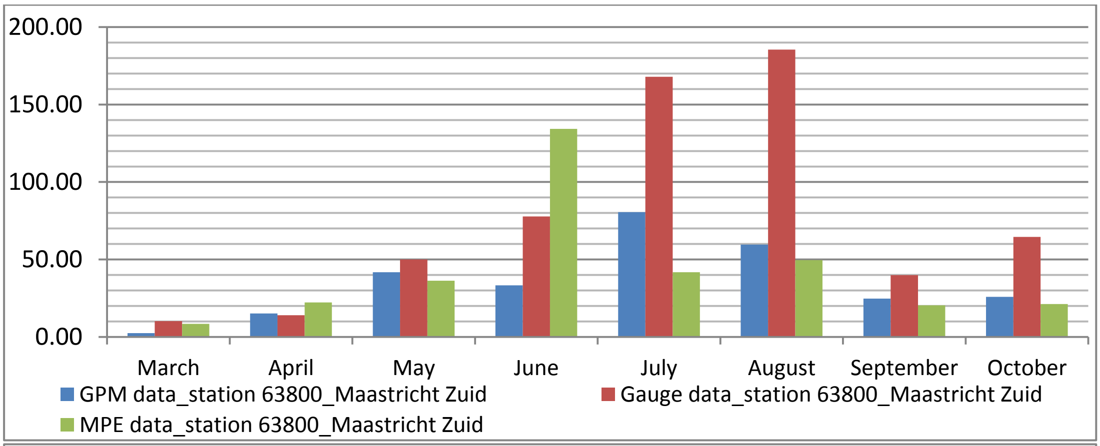
200.00
150.00
100.00
50.00
0.00
March
April
May
June
July
August
September
October
GPM data_station 63800_Maastricht Zuid
Gauge data_station 63800_Maastricht Zuid
MPE data_station 63800_Maastricht Zuid

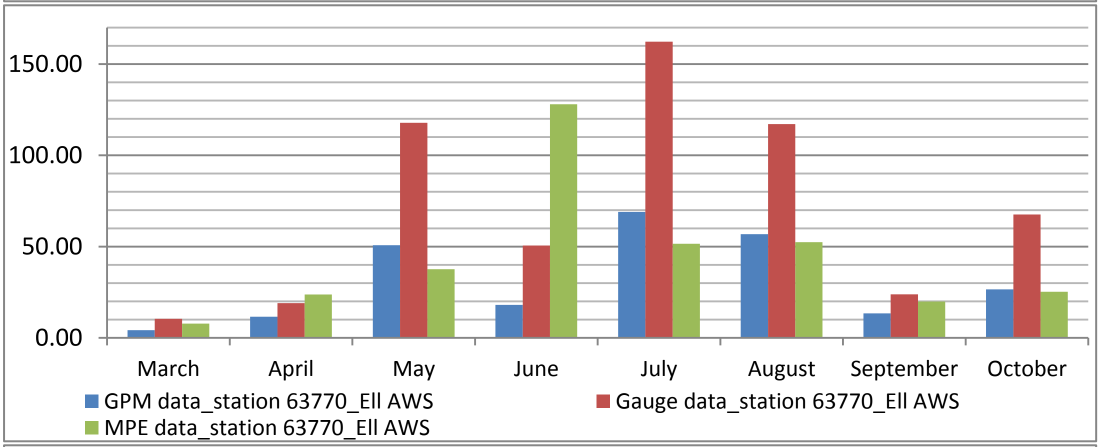
150.00
100.00
50.00
0.00
March
April
May
June
July
August
September
October
GPM data_station 63770_Ell AWS
Gauge data_station 63770_Ell AWS
MPE data_station 63770_Ell AWS

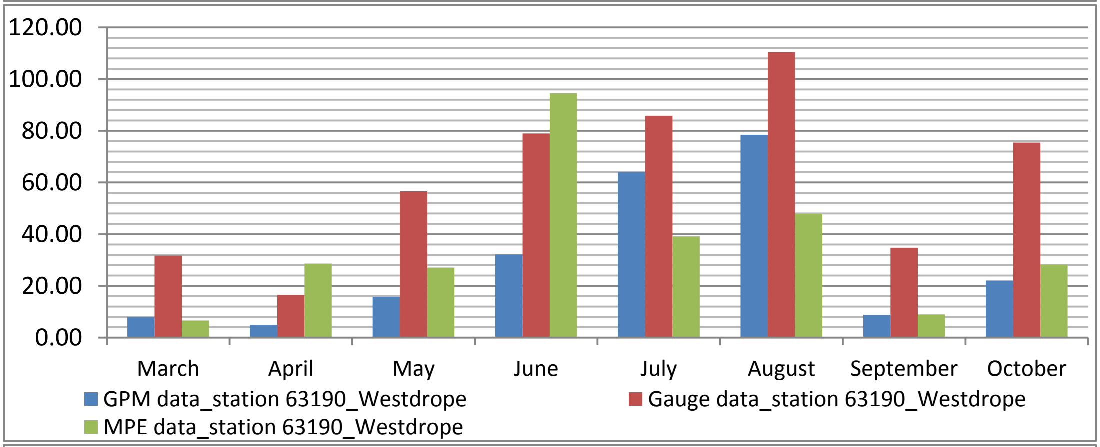
120.00
100.00
80.00
60.00
40.00
20.00
0.00
March
April
May
June
July
August
September
October
GPM data_station 63190_Westdrope
Gauge data_station 63190_Westdrope
MPE data_station 63190_Westdrope

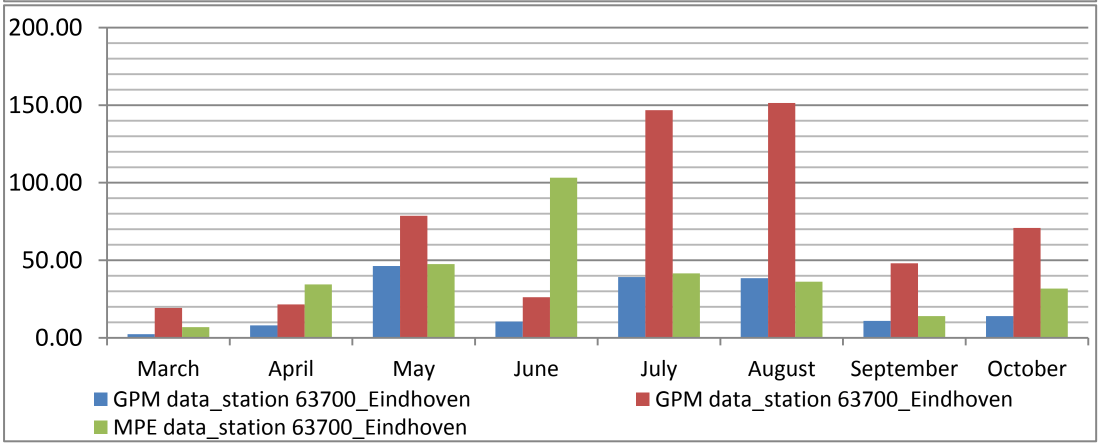
200.00
150.00
100.00
50.00
0.00
March
April
May
June
July
August
September
October
GPM data_station 63700_Eindhoven
GPM data_station 63700_Eindhoven
MPE data_station 63700_Eindhoven

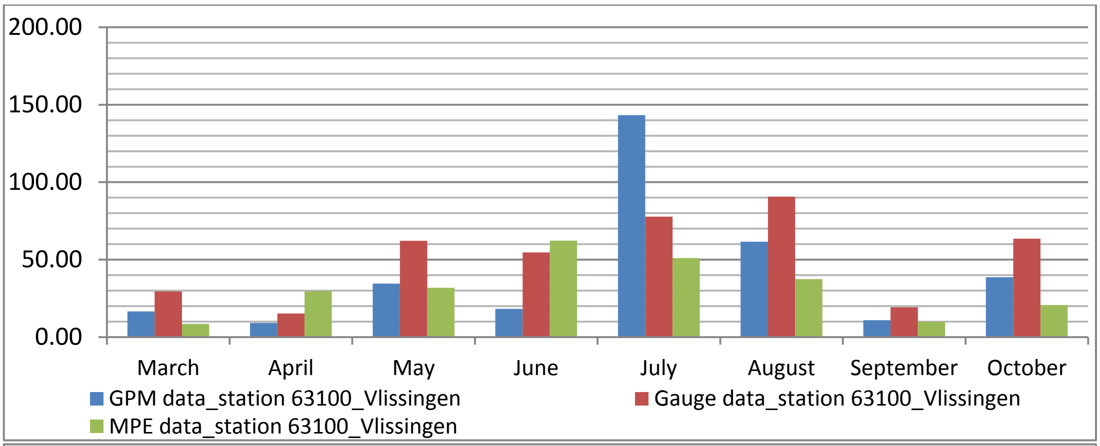
200.00
150.00
100.00
50.00
0.00
March
April
May
June
July
August
September
October
GPM data_station 63100_Vlissingen
Gauge data_station 63100_Vlissingen
MPE data_station 63100_Vlissingen

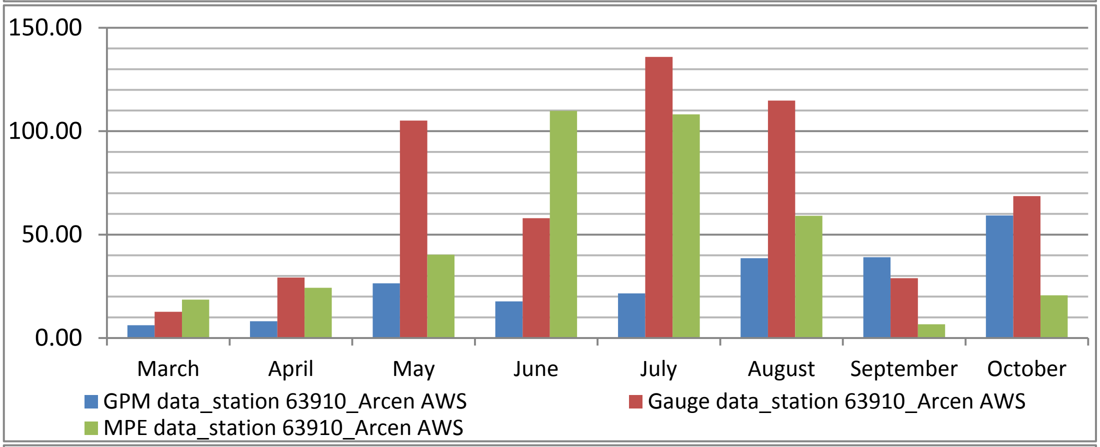
150.00
100.00
50.00
0.00
March
April
May
June
July
August
September
October
GPM data_station 63910_Arcen AWS
Gauge data_station 63910_Arcen AWS
MPE data_station 63910_Arcen AWS

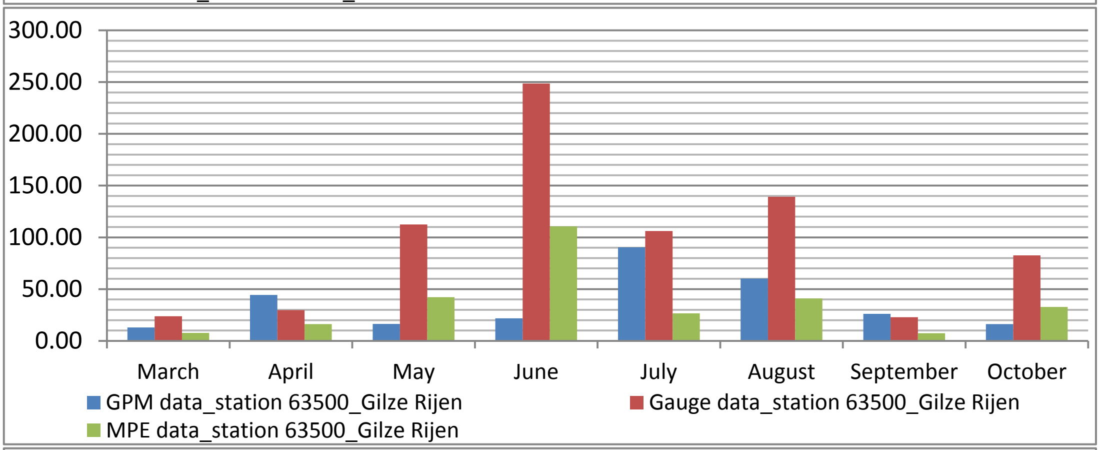
300.00
250.00
200.00
150.00
100.00
50.00
0.00
March
April
May
June
July
August
September
October
GPM data_station 63500_Gilze Rijen
Gauge data_station 63500_Gilze Rijen
MPE data_station 63500_Gilze Rijen

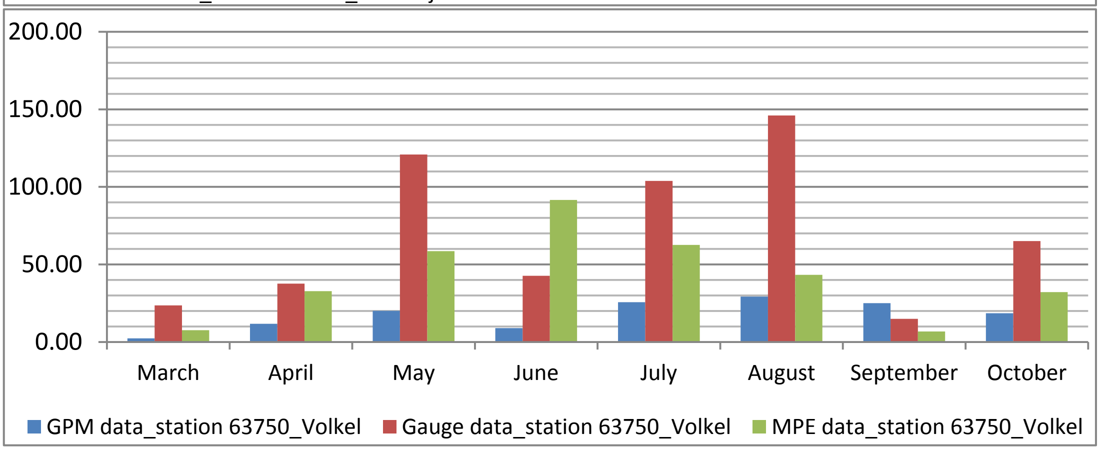
200.00
150.00
100.00
50.00
0.00
March
April
May
June
July
August
September
October
GPM data_station 63750_Volkel
Gauge data_station 63750_Volkel
MPE data_station 63750_Volkel

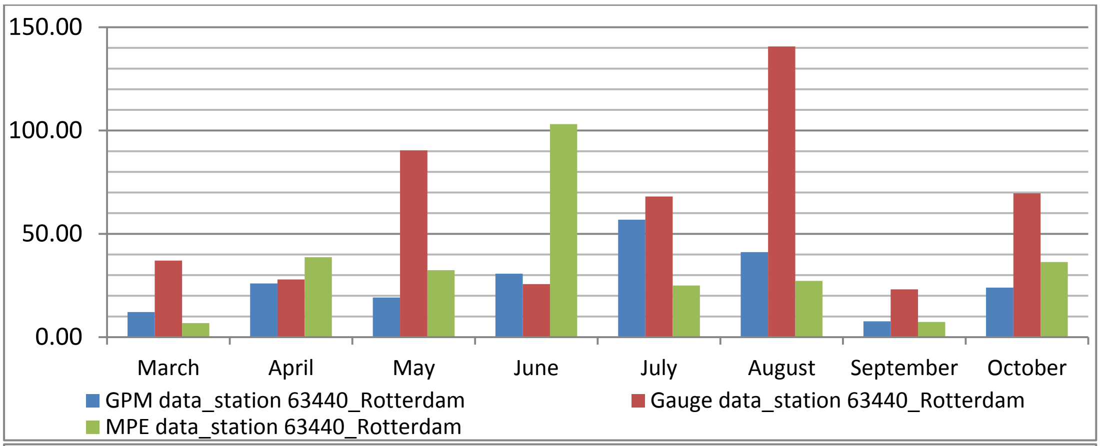
150.00
100.00
50.00
0.00
March
April
May
June
July
August
September
October
GPM data_station 63440_Rotterdam
Gauge data_station 63440_Rotterdam
MPE data_station 63440_Rotterdam

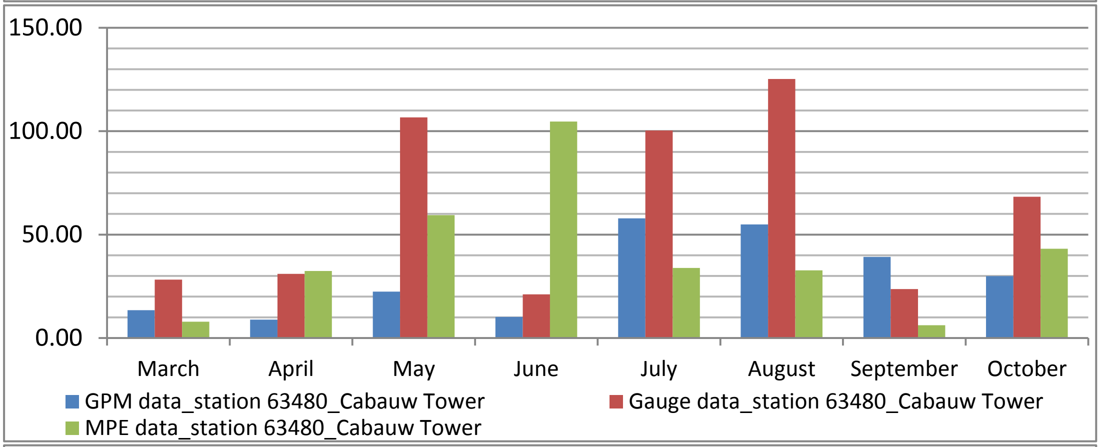
150.00
100.00
50.00
0.00
March
April
May
June
July
August
September
October
GPM data_station 63480_Cabauw Tower
Gauge data_station 63480_Cabauw Tower
MPE data_station 63480_Cabauw Tower

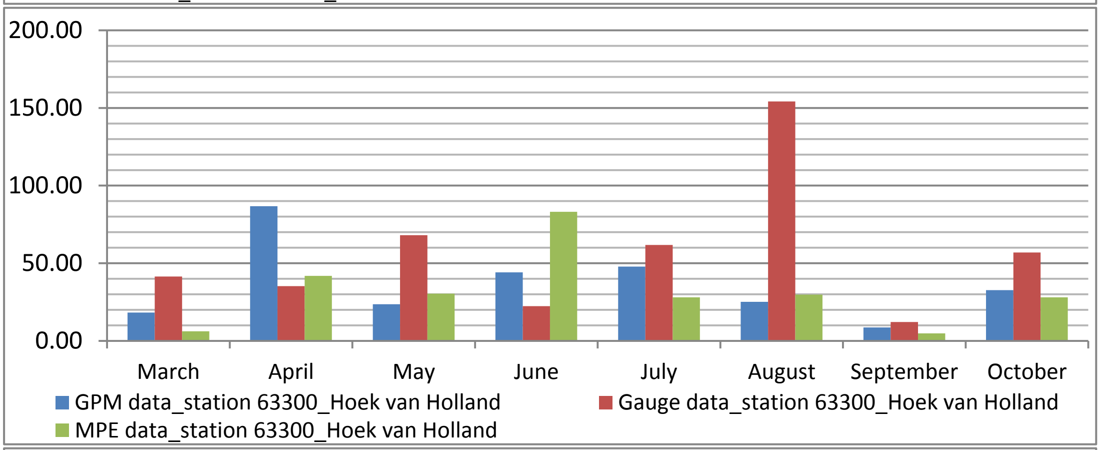
200.00
150.00
100.00
50.00
0.00
March
April
May
June
July
August
September
October
GPM data_station 63300_Hoek van Holland
Gauge data_station 63300_Hoek van Holland
MPE data_station 63300_Hoek van Holland

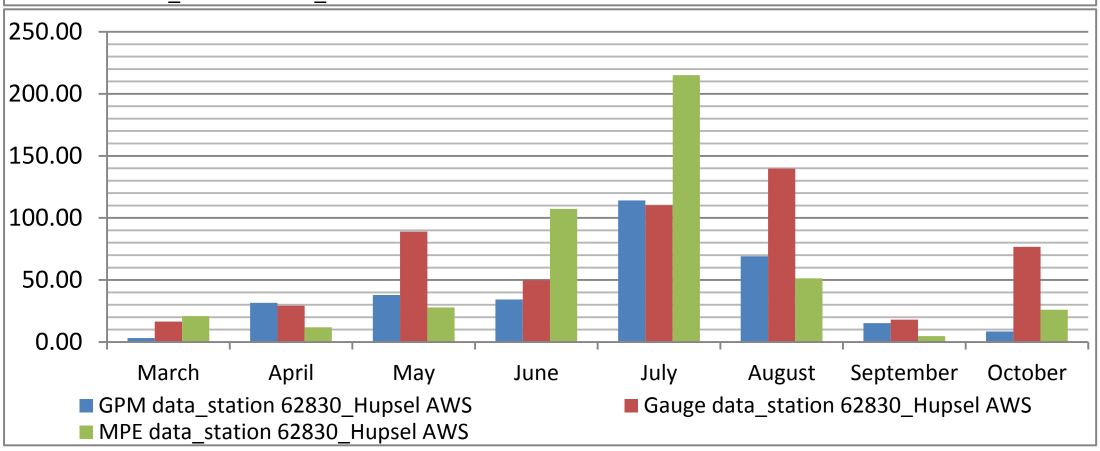
250.00
200.00
150.00
100.00
50.00
0.00
March
April
May
June
July
August
September
October
GPM data_station 62830_Hupsel AWS
Gauge data_station 62830_Hupsel AWS
MPE data_station 62830_Hupsel AWS

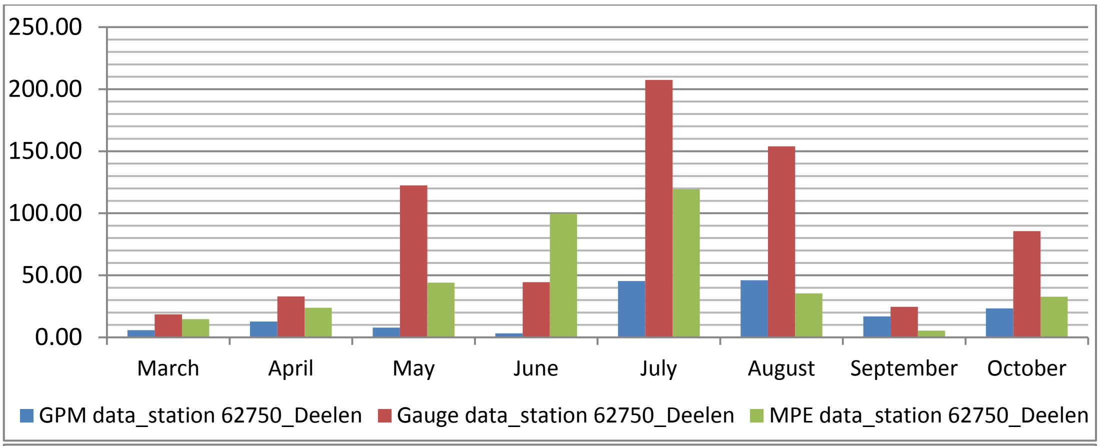
250.00
200.00
150.00
100.00
50.00
0.00
March
April
May
June
July
August
September
October
GPM data_station 62750_Deelen
Gauge data_station 62750_Deelen
MPE data_station 62750_Deelen

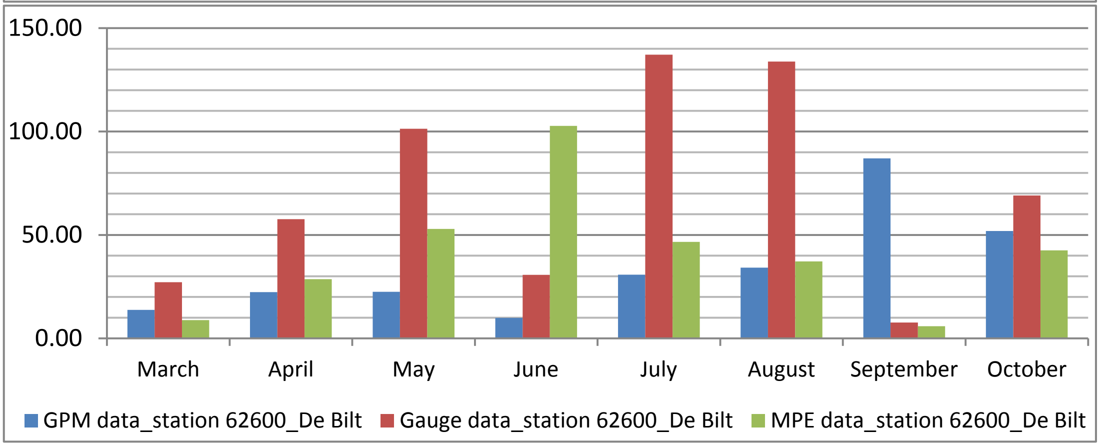
150.00
100.00
50.00
0.00
March
April
May
June
July
August
September
October
GPM data_station 62600_De Bilt
Gauge data_station 62600_De Bilt
MPE data_station 62600_De Bilt

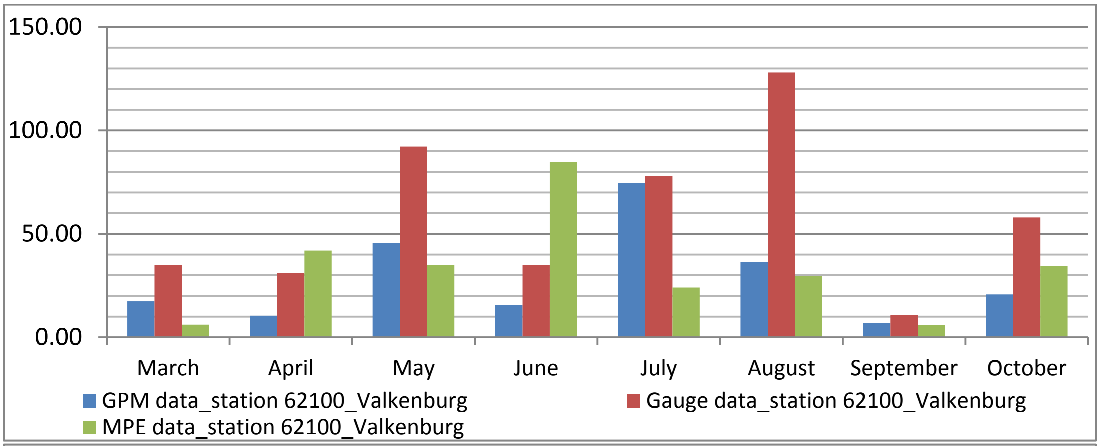
150.00
100.00
50.00
0.00
March
April
May
June
July
August
September
October
GPM data_station 62100_Valkenburg
Gauge data_station 62100_Valkenburg
MPE data_station 62100_Valkenburg

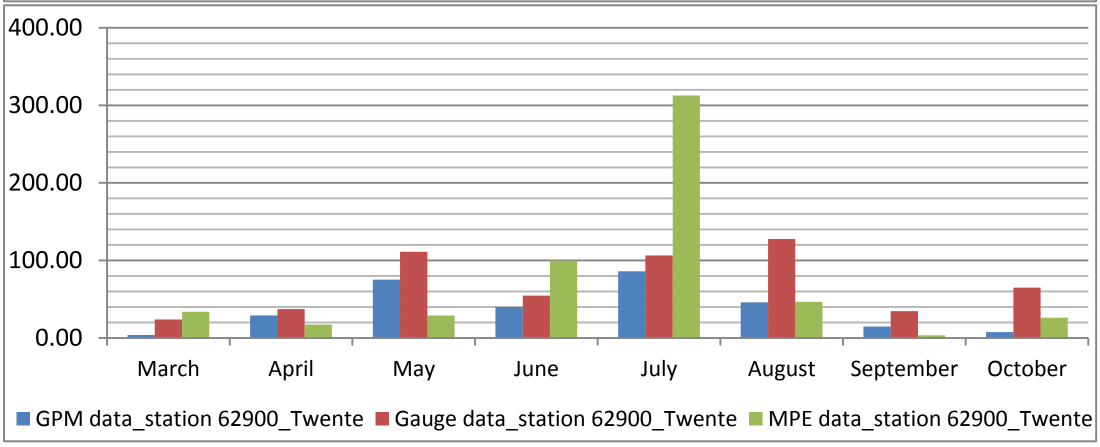
400.00
300.00
200.00
100.00
0.00
March
April
May
June
July
August
September
October
GPM data_station 62900_Twente
Gauge data_station 62900_Twente
MPE data_station 62900_Twente

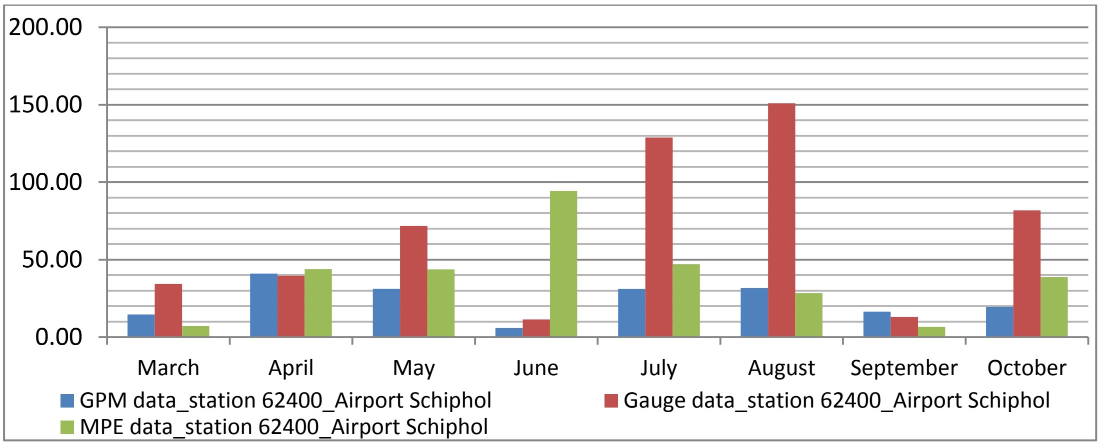
200.00
150.00
100.00
50.00
0.00
March
April
May
June
July
August
September
October
GPM data_station 62400_Airport Schiphol
Gauge data_station 62400_Airport Schiphol
MPE data_station 62400_Airport Schiphol

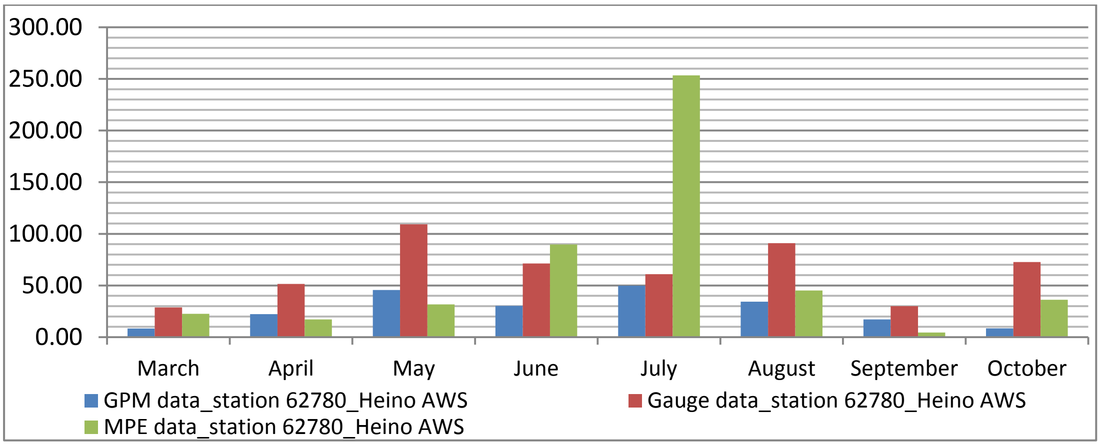
300.00
250.00
200.00
150.00
100.00
50.00
0.00
March
April
May
June
July
August
September
October
GPM data_station 62780_Heino AWS
Gauge data_station 62780_Heino AWS
MPE data_station 62780_Heino AWS

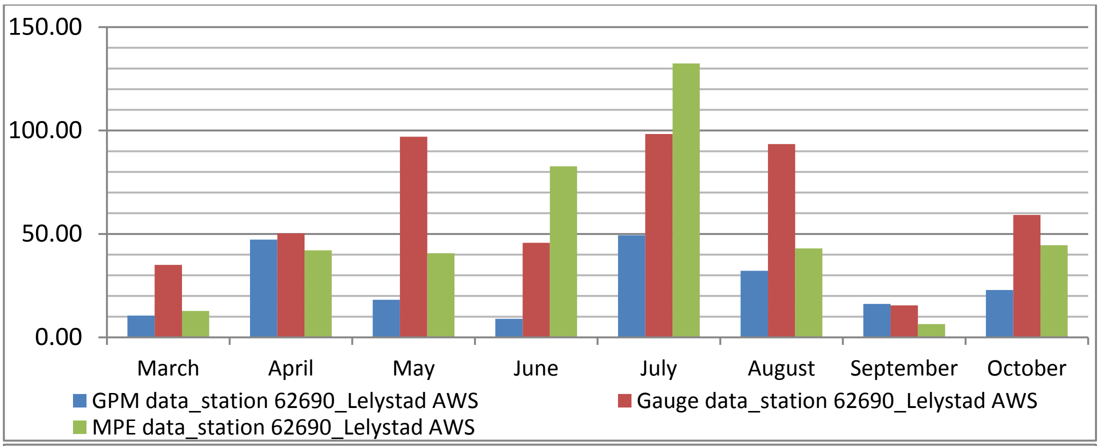
150.00
100.00
50.00
0.00
March
April
May
June
July
August
September
October
GPM data_station 62690_Lelystad AWS
Gauge data_station 62690_Lelystad AWS
MPE data_station 62690_Lelystad AWS

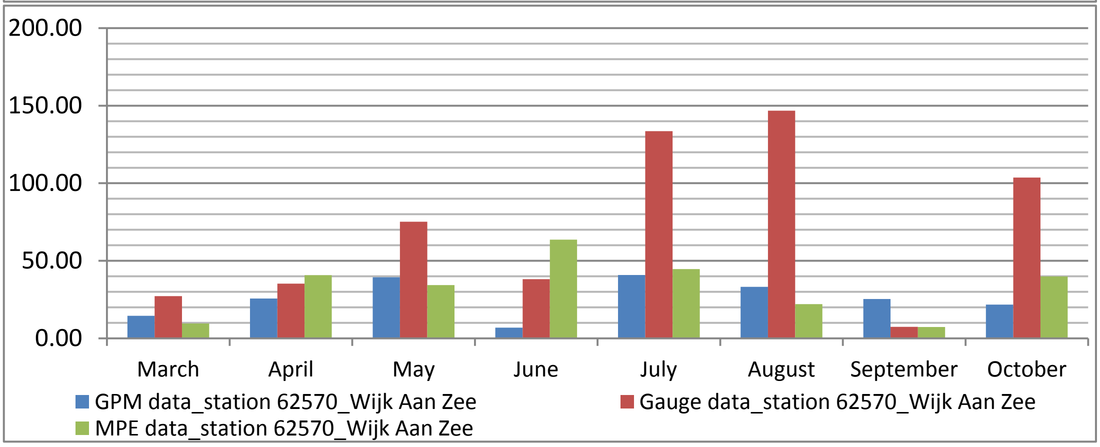
200.00
150.00
100.00
50.00
0.00
March
April
May
June
July
August
September
October
GPM data_station 62570_Wijk Aan Zee
Gauge data_station 62570_Wijk Aan Zee
MPE data_station 62570_Wijk Aan Zee

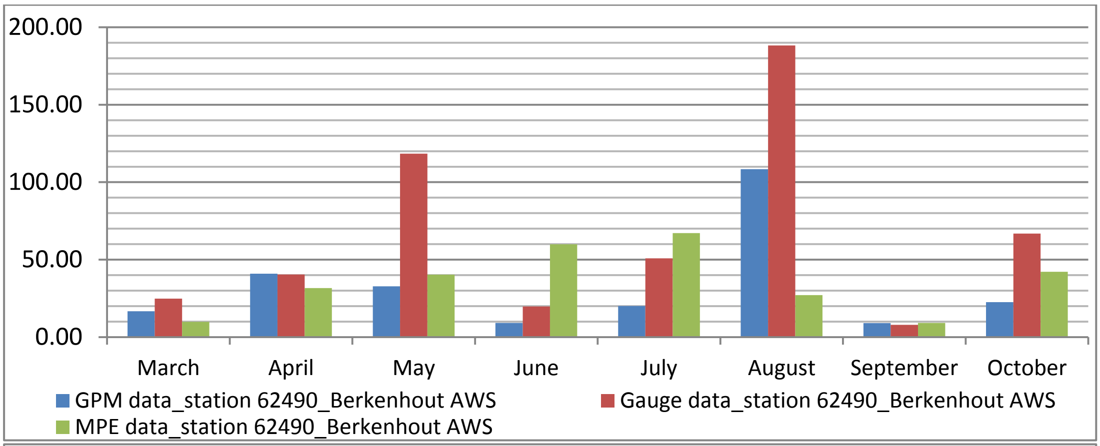
200.00
150.00
100.00
50.00
0.00
March
April
May
June
July
August
September
October
GPM data_station 62490_Berkenhout AWS
Gauge data_station 62490_Berkenhout AWS
MPE data_station 62490_Berkenhout AWS

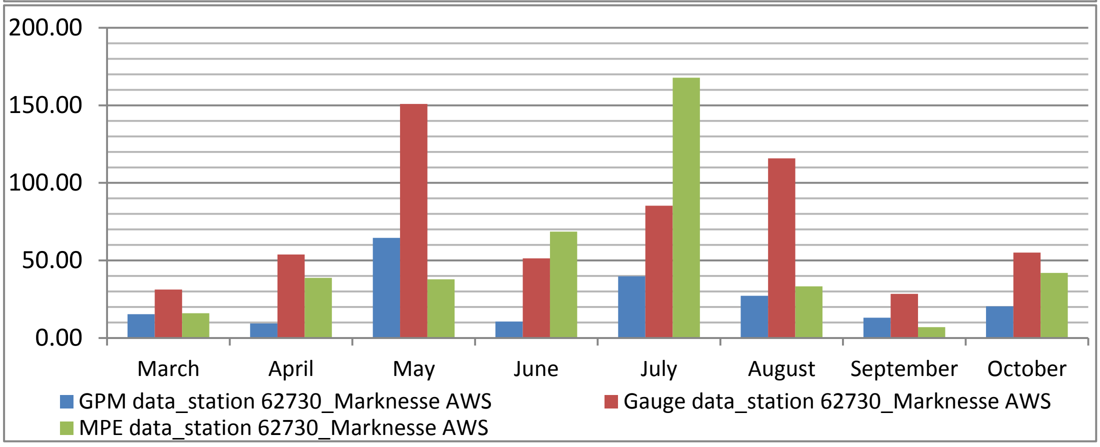
200.00
150.00
100.00
50.00
0.00
March
April
May
June
July
August
September
October
GPM data_station 62730_Marknesse AWS
Gauge data_station 62730_Marknesse AWS
MPE data_station 62730_Marknesse AWS

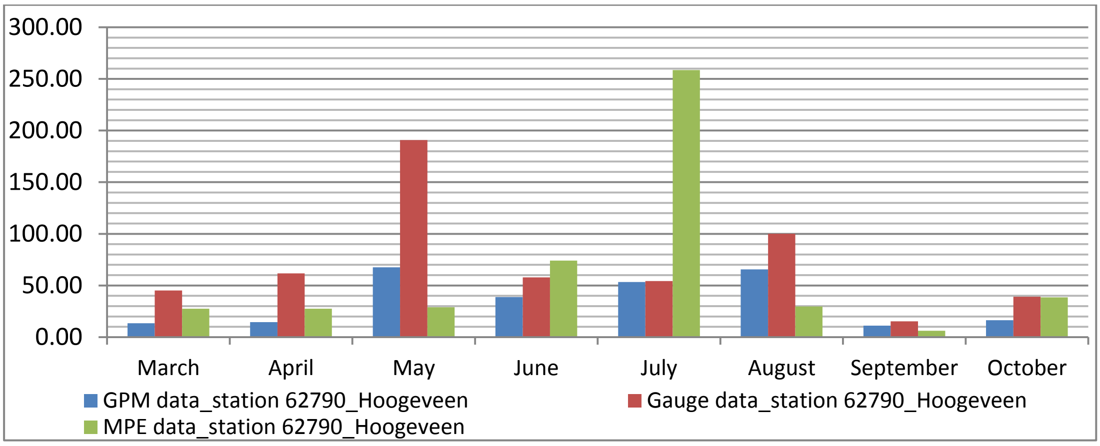
300.00
250.00
200.00
150.00
100.00
50.00
0.00
March
April
May
June
July
August
September
October
GPM data_station 62790_Hoogeveen
Gauge data_station 62790_Hoogeveen
MPE data_station 62790_Hoogeveen

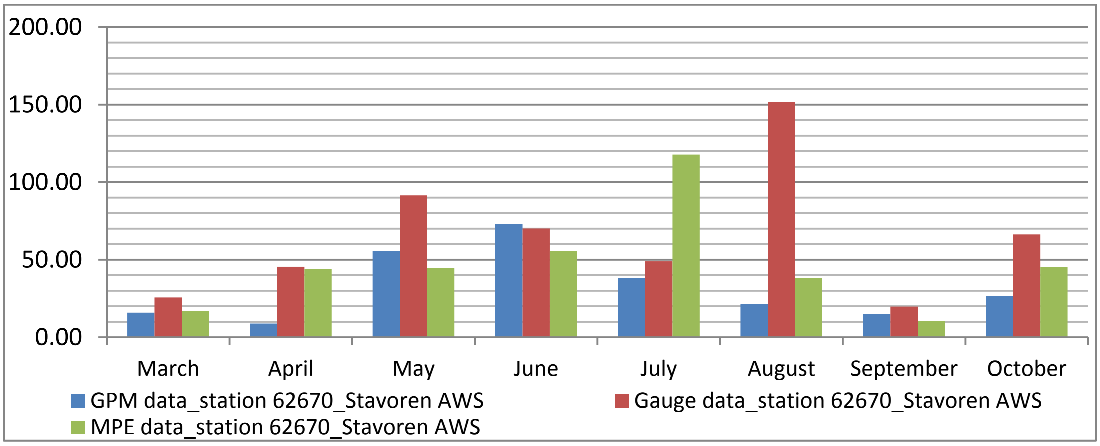
200.00
150.00
100.00
50.00
0.00
March
April
May
June
July
August
September
October
GPM data_station 62670_Stavoren AWS
Gauge data_station 62670_Stavoren AWS
MPE data_station 62670_Stavoren AWS

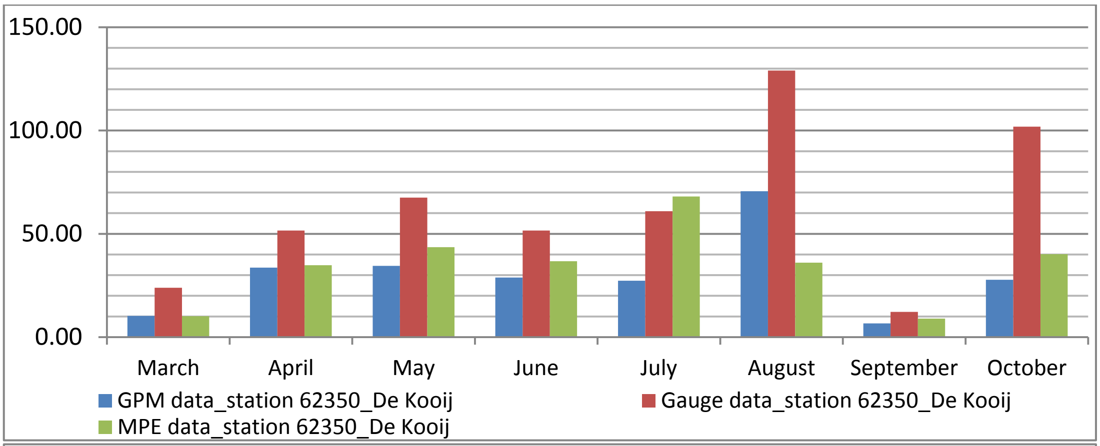
150.00
100.00
50.00
0.00
March
April
May
June
July
August
September
October
GPM data_station 62350_De Kooij
Gauge data_station 62350_De Kooij
MPE data_station 62350_De Kooij

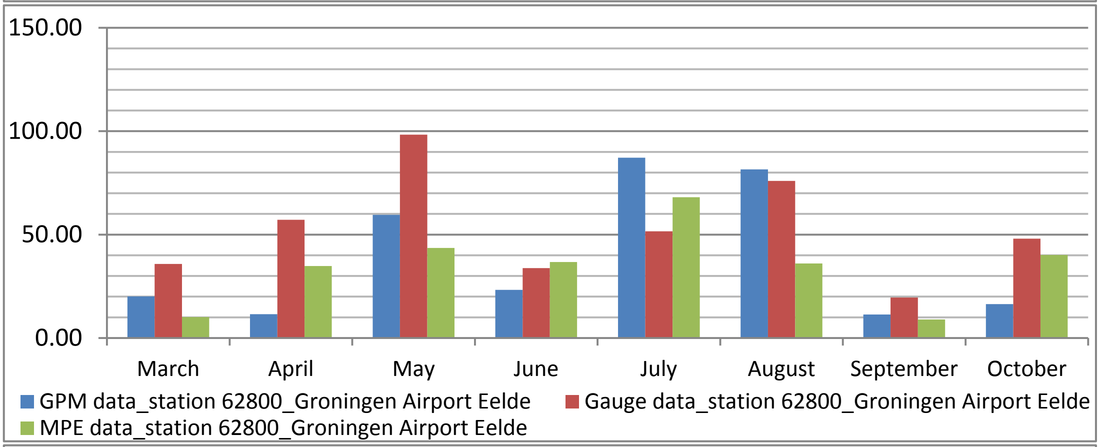
150.00
100.00
50.00
0.00
March
April
May
June
July
August
September
October
GPM data_station 62800_Groningen Airport Eelde
Gauge data_station 62800_Groningen Airport Eelde
MPE data_station 62800_Groningen Airport Eelde

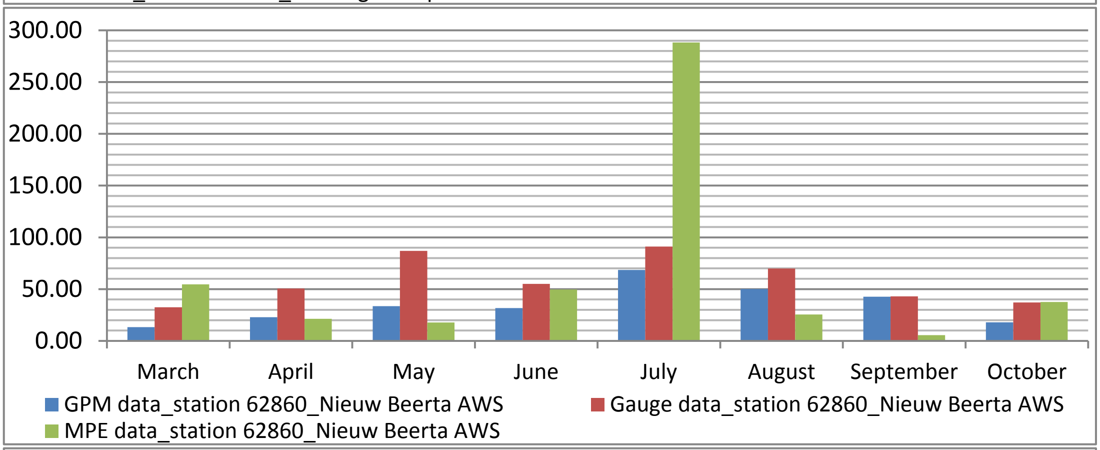
300.00
250.00
200.00
150.00
100.00
50.00
0.00
March
April
May
June
July
August
September
October
GPM data_station 62860_Nieuw Beerta AWS
Gauge data_station 62860_Nieuw Beerta AWS
MPE data_station 62860_Nieuw Beerta AWS

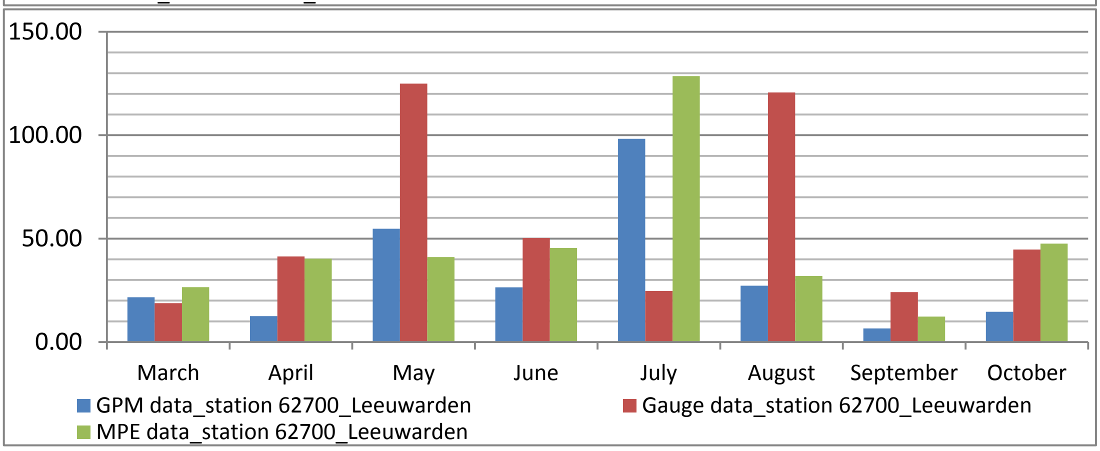
150.00
100.00
50.00
0.00
March
April
May
June
July
August
September
October
GPM data_station 62700_Leeuwarden
Gauge data_station 62700_Leeuwarden
MPE data_station 62700_Leeuwarden

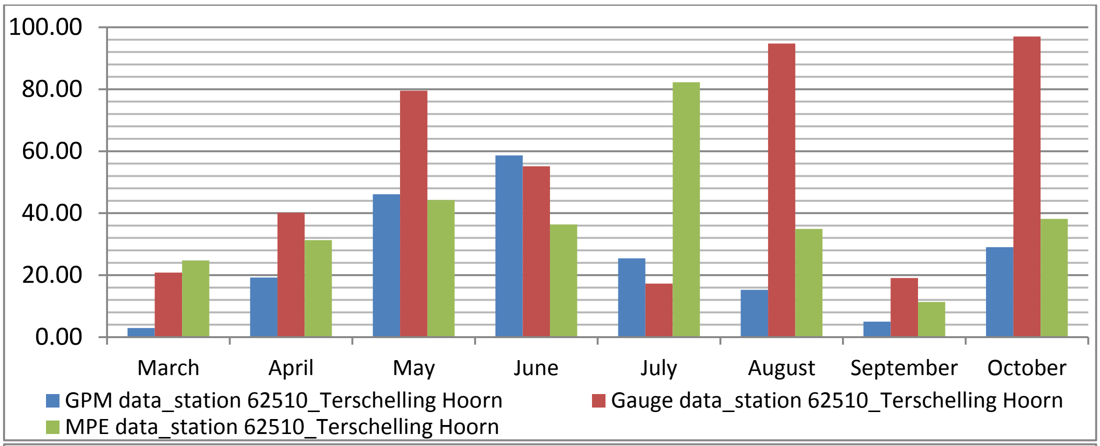
100.00
80.00
60.00
40.00
20.00
0.00
March
April
May
June
July
August
September
October
GPM data_station 62510_Terschelling Hoorn
Gauge data_station 62510_Terschelling Hoorn
MPE data_station 62510_Terschelling Hoorn

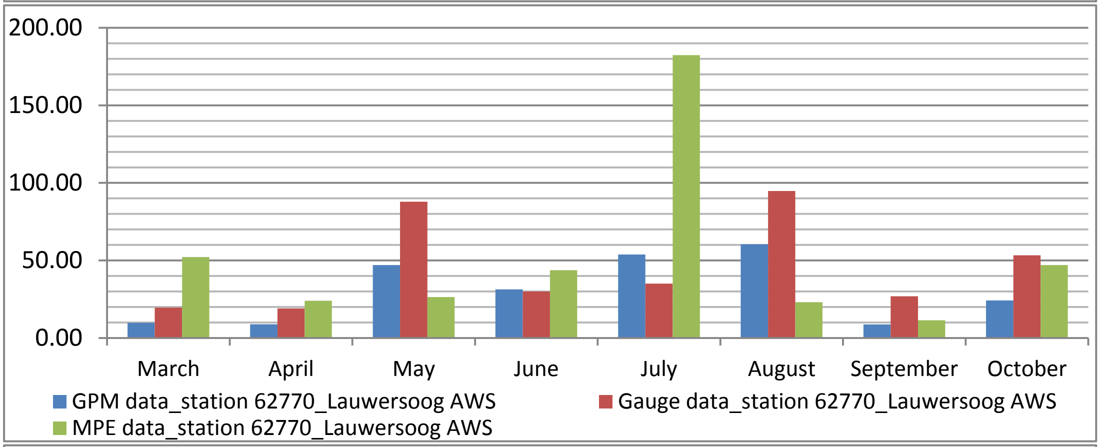
200.00
150.00
100.00
50.00
0.00
March
April
May
June
July
August
September
October
GPM data_station 62770_Lauwersoog AWS
Gauge data_station 62770_Lauwersoog AWS
MPE data_station 62770_Lauwersoog AWS

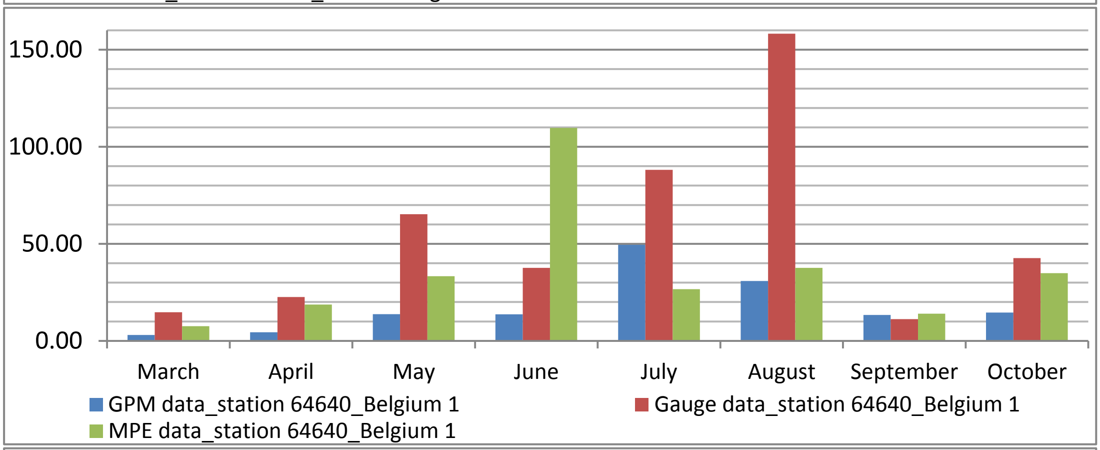
150.00
100.00
50.00
0.00
March
April
May
June
July
August
September
October
GPM data_station 64640_Belgium 1
Gauge data_station 64640_Belgium 1
MPE data_station 64640_Belgium 1

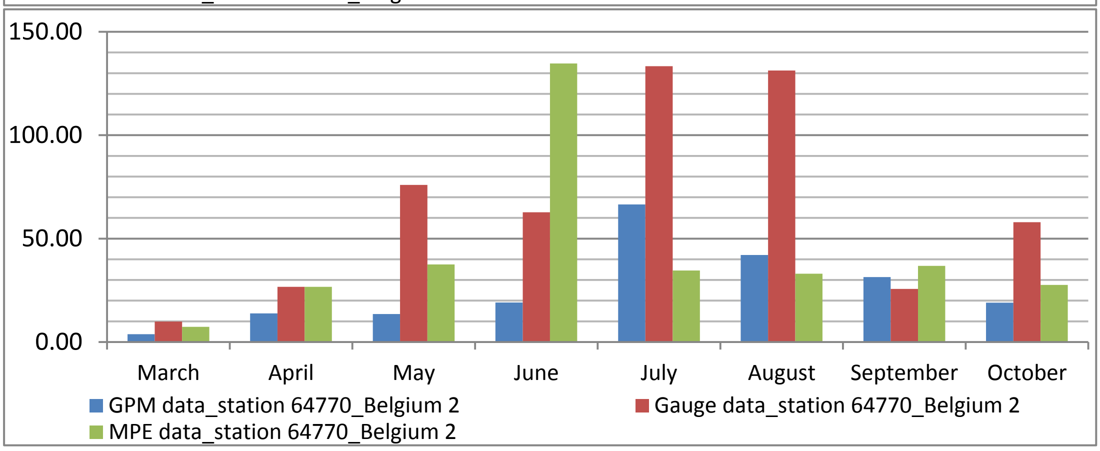
150.00
100.00
50.00
0.00
March
April
May
June
July
August
September
October
GPM data_station 64770_Belgium 2
Gauge data_station 64770_Belgium 2
MPE data_station 64770_Belgium 2

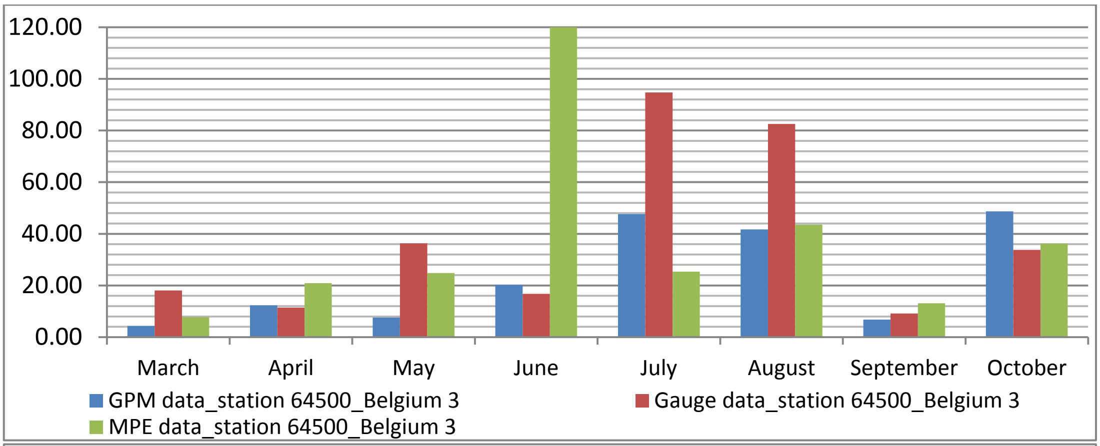
120.00
100.00
80.00
60.00
40.00
20.00
0.00
March
April
May
June
July
August
September
October
GPM data_station 64500_Belgium 3
Gauge data_station 64500_Belgium 3
MPE data_station 64500_Belgium 3

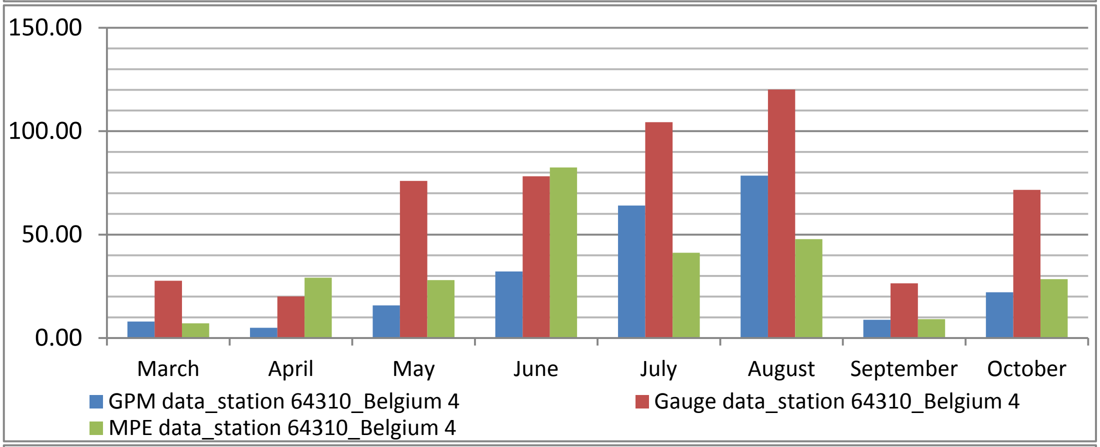
150.00
100.00
50.00
0.00
March
April
May
June
July
August
September
October
GPM data_station 64310_Belgium 4
Gauge data_station 64310_Belgium 4
MPE data_station 64310_Belgium 4

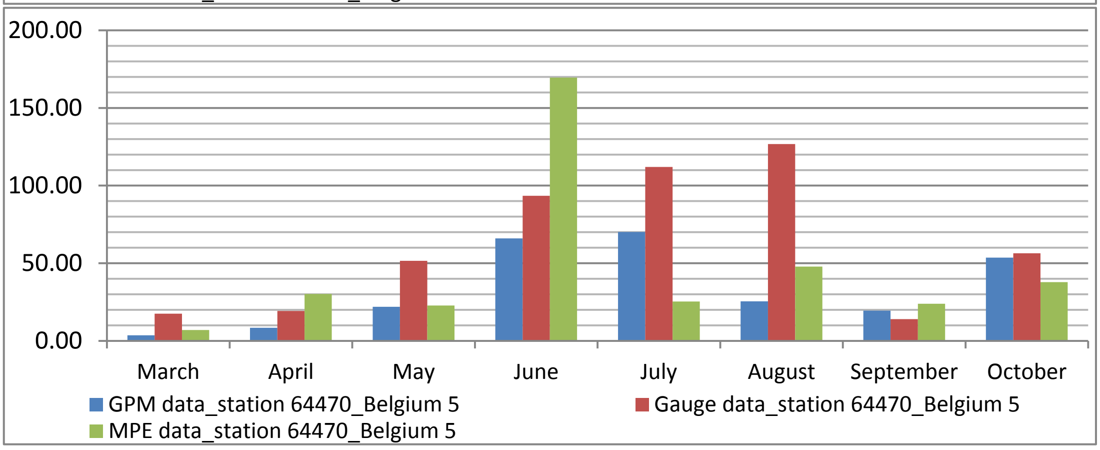
200.00
150.00
100.00
50.00
0.00
March
April
May
June
July
August
September
October
GPM data_station 64470_Belgium 5
Gauge data_station 64470_Belgium 5
MPE data_station 64470_Belgium 5

Appendix B.

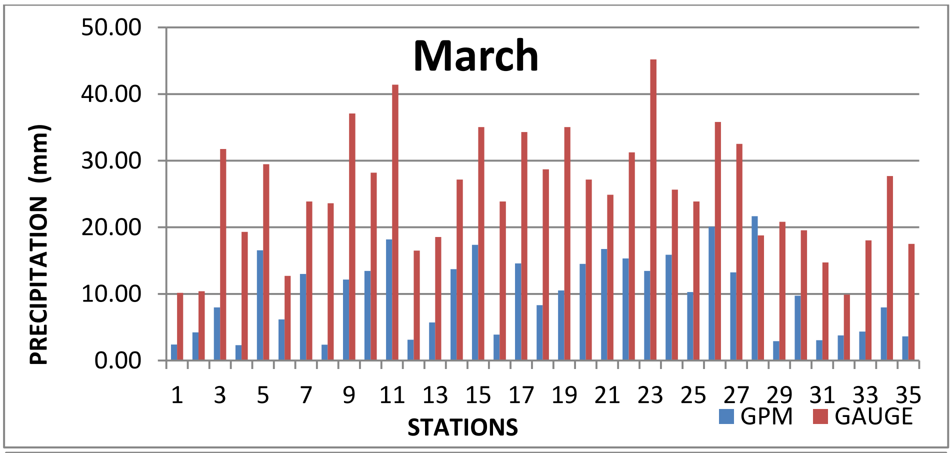
March
PRECIPITATION (mm)
50.00
40.00
30.00
20.00
10.00
0.00
1 3 5 7 9 11 13 15 17 19 21 23 25 27 29 31 33 35
STATIONS
GPM
GAUGE

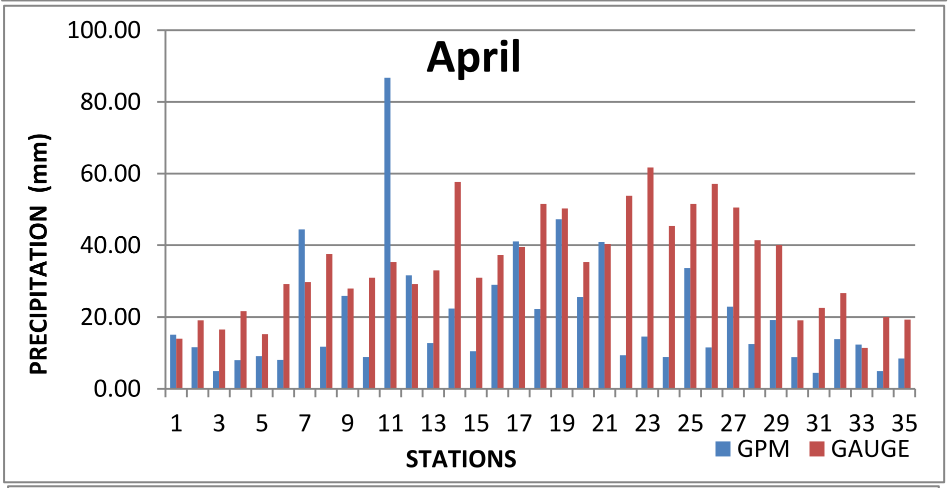
April
PRECIPITATION (mm)
100.00
80.00
60.00
40.00
20.00
0.00
1 3 5 7 9 11 13 15 17 19 21 23 25 27 29 31 33 35
STATIONS
GPM
GAUGE

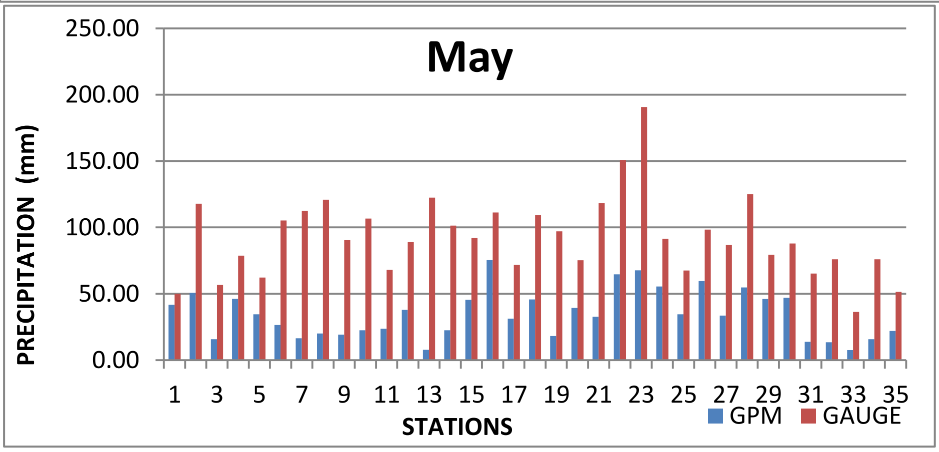
May
PRECIPITATION (mm)
250.00
200.00
150.00
100.00
50.00
0.00
1 3 5 7 9 11 13 15 17 19 21 23 25 27 29 31 33 35
STATIONS
GPM
GAUGE

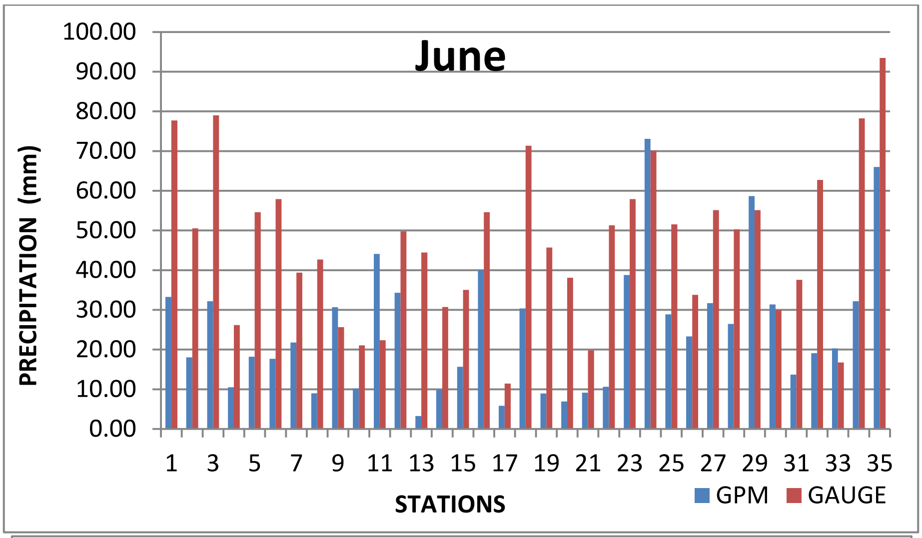
June
PRECIPITATION (mm)
100.00
90.00
80.00
70.00
60.00
50.00
40.00
30.00
20.00
10.00
0.00
1 3 5 7 9 11 13 15 17 19 21 23 25 27 29 31 33 35
STATIONS
GPM
GAUGE

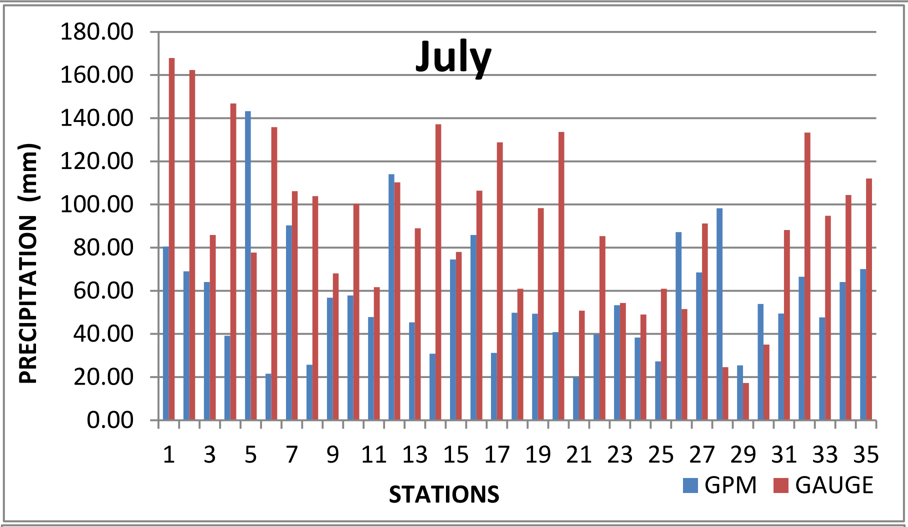
July
PRECIPITATION (mm)
180.00
160.00
140.00
120.00
100.00
80.00
60.00
40.00
20.00
0.00
1 3 5 7 9 11 13 15 17 19 21 23 25 27 29 31 33 35
STATIONS
GPM
GAUGE

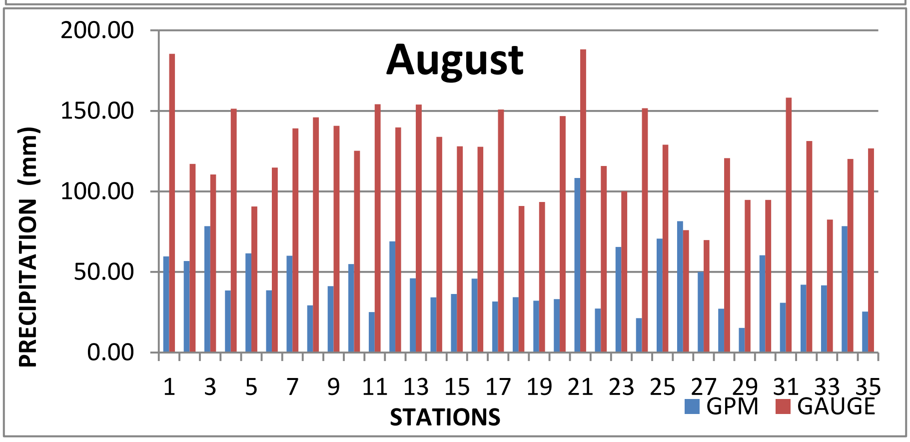
August
PRECIPITATION (mm)
200.00
150.00
100.00
50.00
0.00
1 3 5 7 9 11 13 15 17 19 21 23 25 27 29 31 33 35
STATIONS
GPM
GAUGE

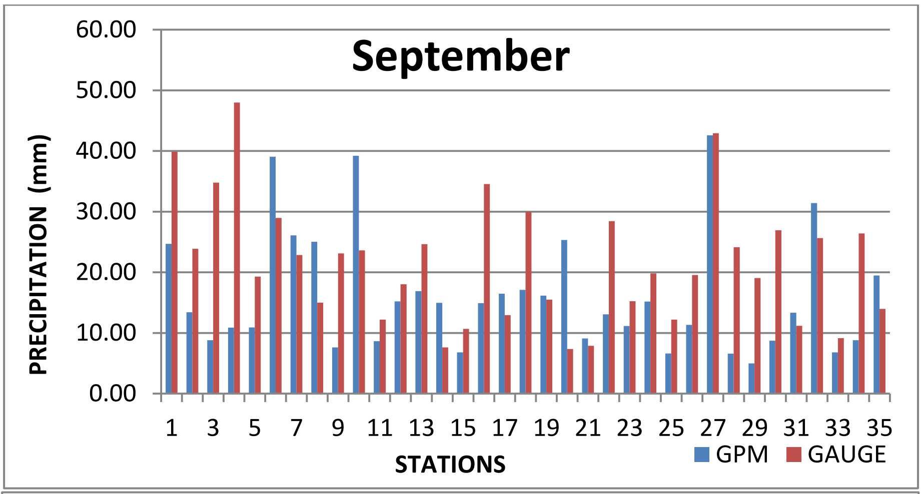
September
PRECIPITATION (mm)
60.00
50.00
40.00
30.00
20.00
10.00
0.00
1 3 5 7 9 11 13 15 17 19 21 23 25 27 29 31 33 35
STATIONS
GPM
GAUGE

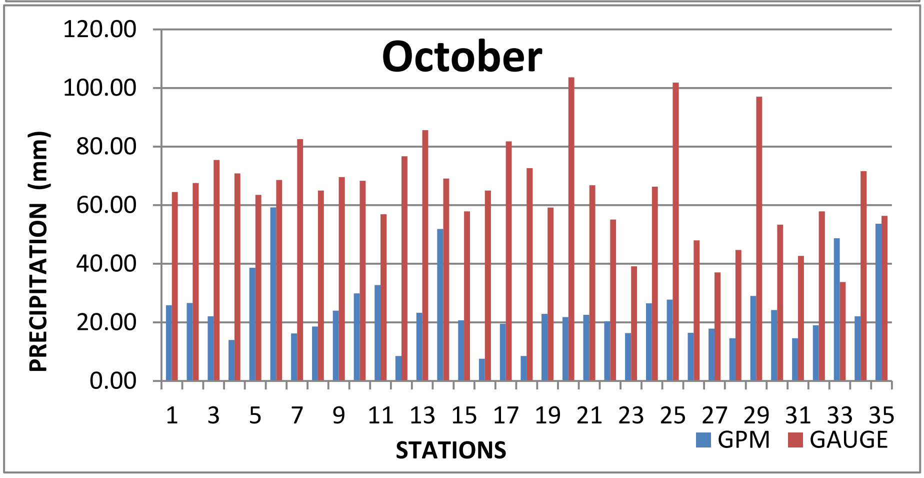
October
PRECIPITATION (mm)
120.00
100.00
80.00
60.00
40.00
20.00
0.00
1 3 5 7 9 11 13 15 17 19 21 23 25 27 29 31 33 35
STATIONS
GPM
GAUGE

Appendix C.

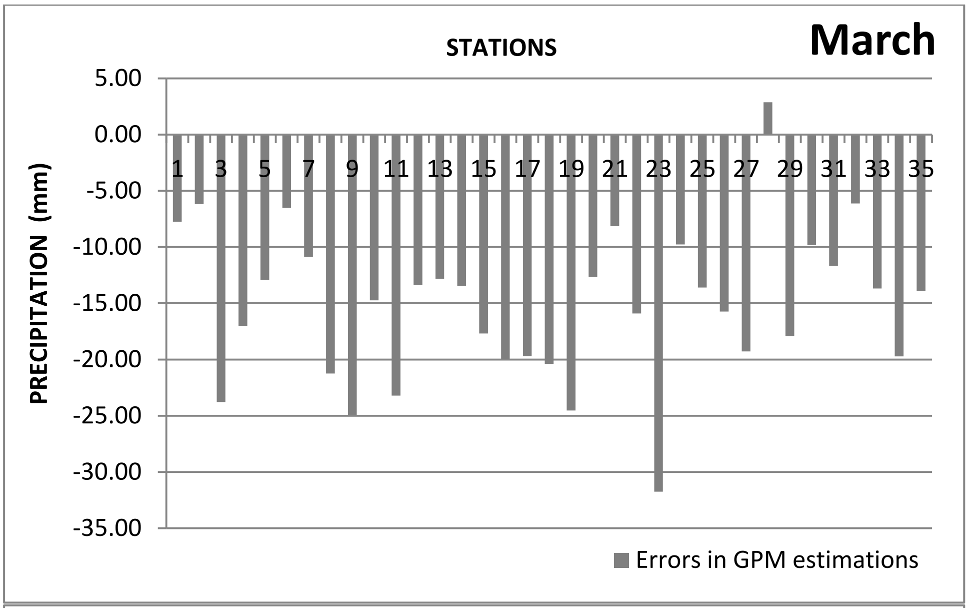
March
STATIONS
PRECIPITATION (mm)
5.00
0.00
-5.00
-10.00
-15.00
-20.00
-25.00
-30.00
-35.00
1 3 5 7 9 11 13 15 17 19 21 23 25 27 29 31 33 35
Errors in GPM estimations

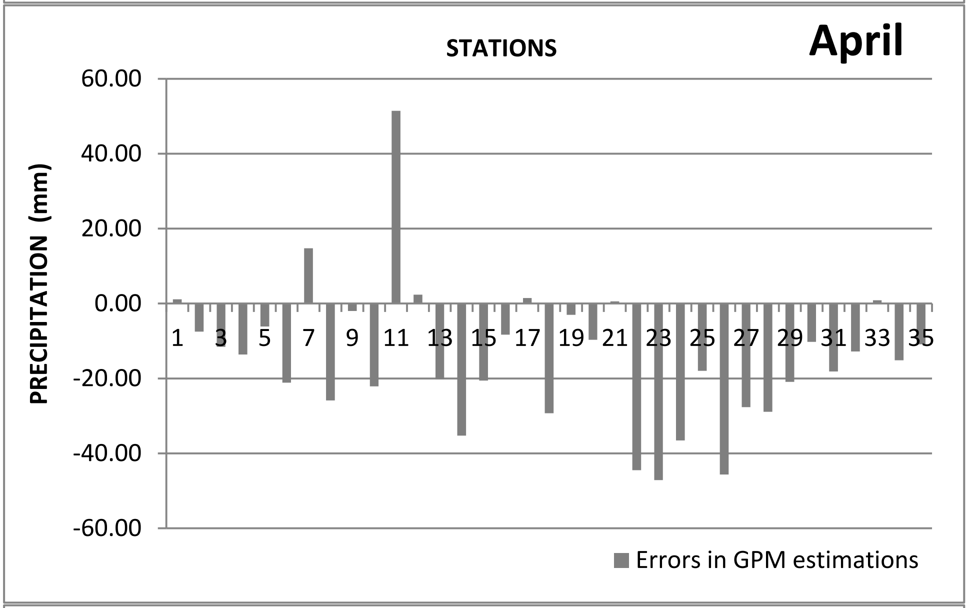
April
STATIONS
PRECIPITATION (mm)
60.00
40.00
20.00
0.00
-20.00
-40.00
-60.00
1 3 5 7 9 11 13 15 17 19 21 23 25 27 29 31 33 35
Errors in GPM estimations

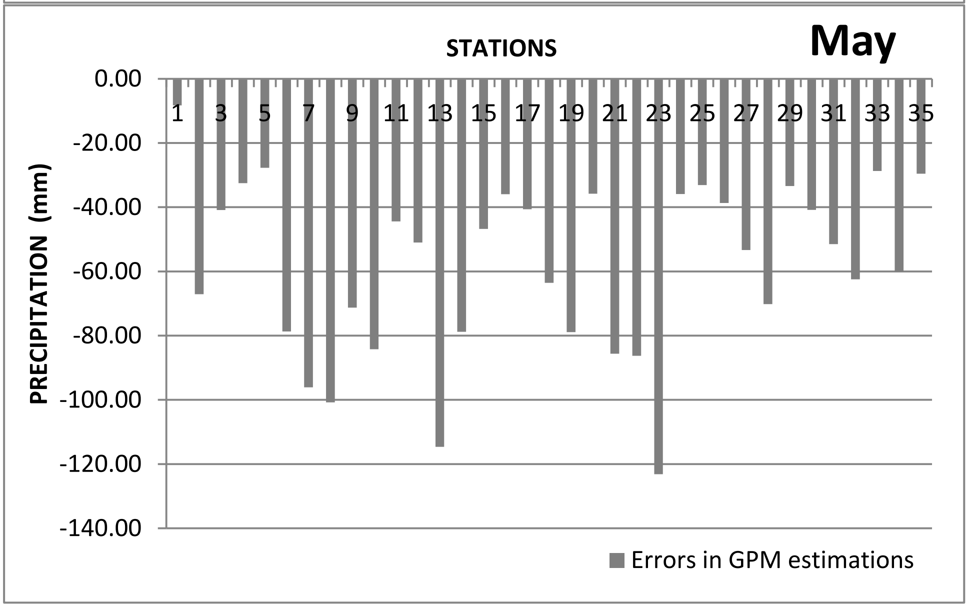
May
STATIONS
PRECIPITATION (mm)
0.00
-20.00
-40.00
-60.00
-80.00
-100.00
-120.00
-140.00
1 3 5 7 9 11 13 15 17 19 21 23 25 27 29 31 33 35
Errors in GPM estimations

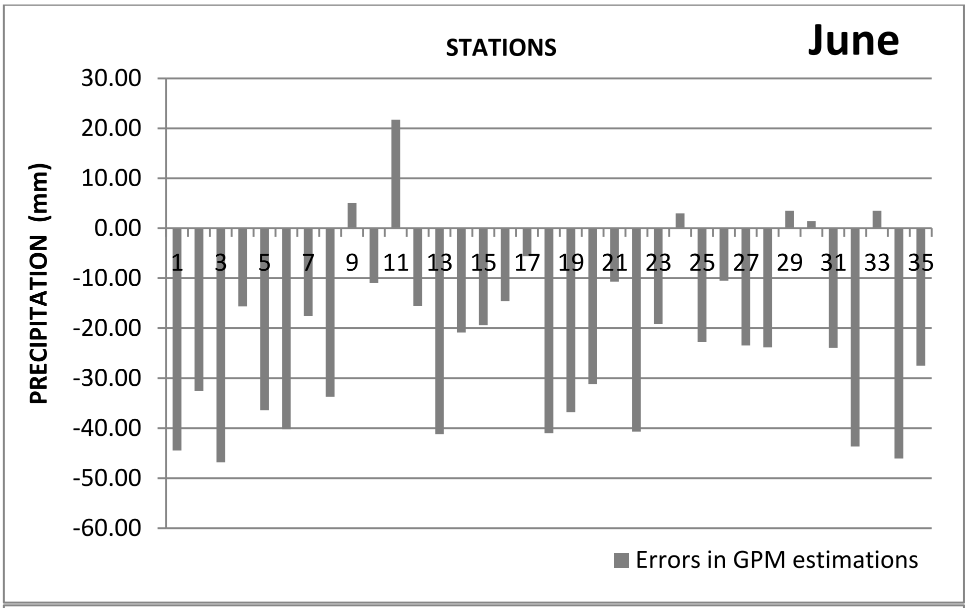
June
STATIONS
PRECIPITATION (mm)
30.00
20.00
10.00
0.00
-10.00
-20.00
-30.00
-40.00
-50.00
-60.00
1 3 5 7 9 11 13 15 17 19 21 23 25 27 29 31 33 35
Errors in GPM estimations

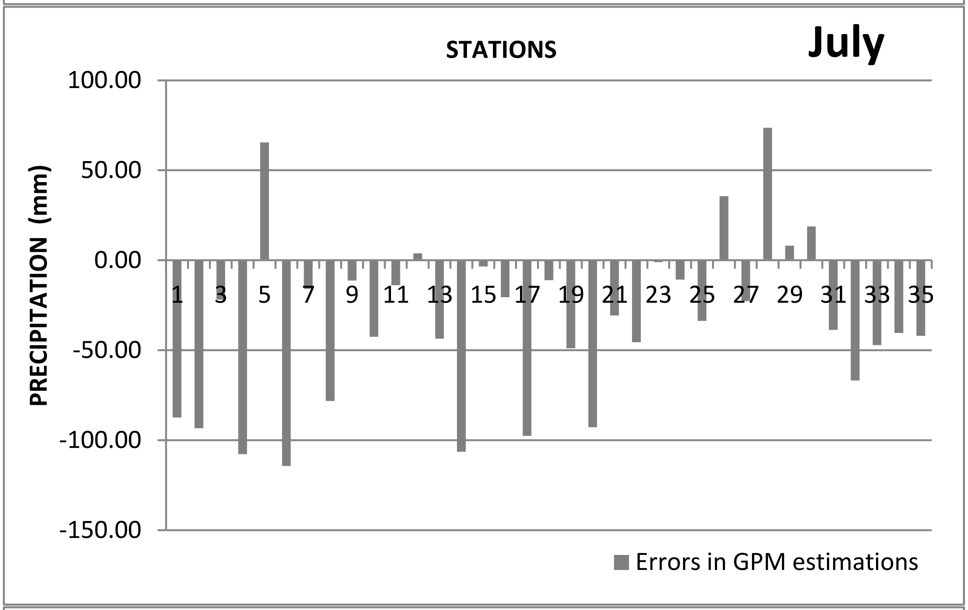
July
STATIONS
PRECIPITATION (mm)
100.00
50.00
0.00
-50.00
-100.00
-150.00
1 3 5 7 9 11 13 15 17 19 21 23 25 27 29 31 33 35
Errors in GPM estimations

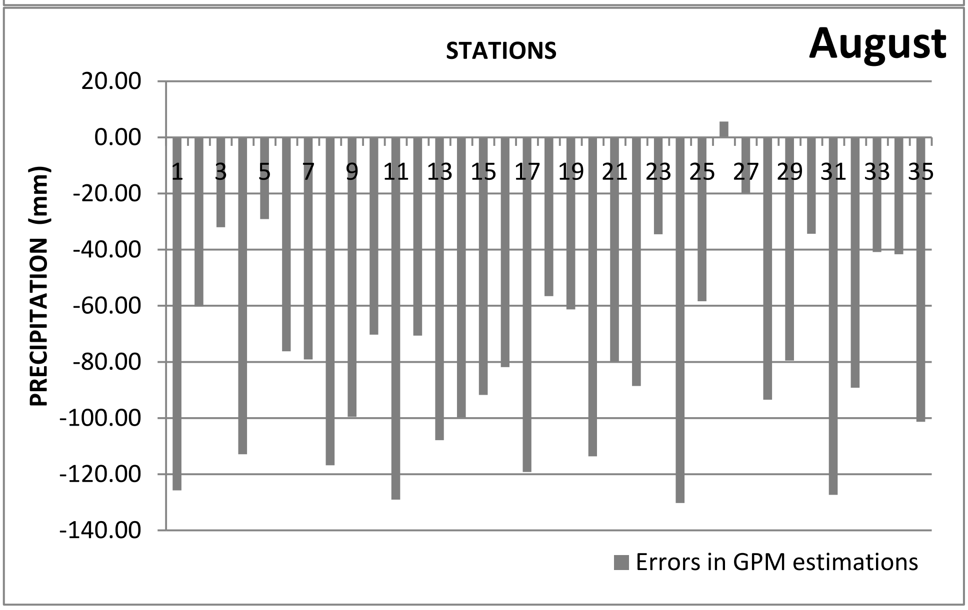
August
STATIONS
PRECIPITATION (mm)
20.00
0.00
-20.00
-40.00
-60.00
-80.00
-100.00
-120.00
-140.00
1 3 5 7 9 11 13 15 17 19 21 23 25 27 29 31 33 35
Errors in GPM estimations

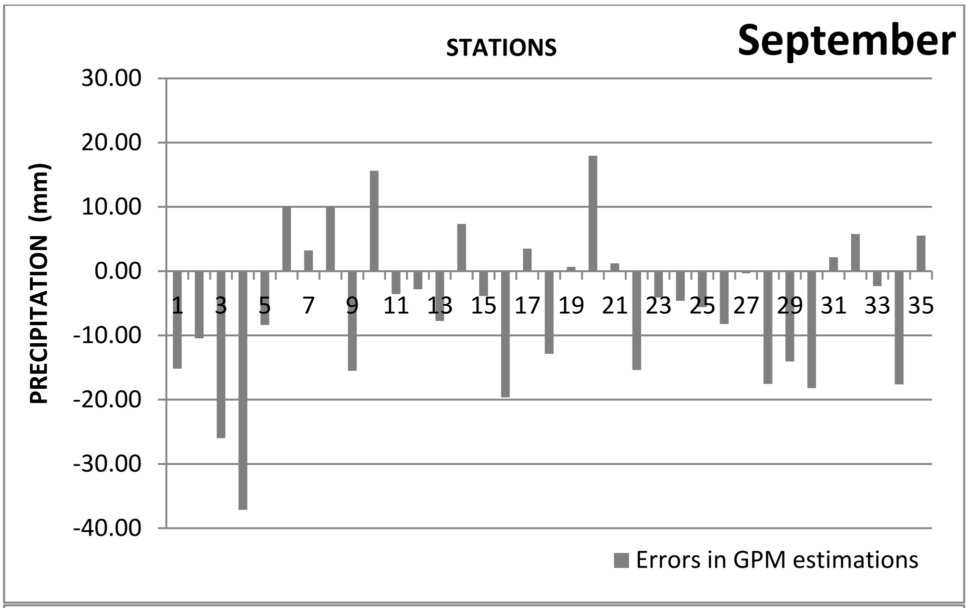

STATIONS
September
30.00
20.00
10.00
0.00
-10.00
-20.00
-30.00
-40.00
PRECIPITATION (mm)
1 3 5 7 9 11 13 15 17 19 21 23 25 27 29 31 33 35
Errors in GPM estimations

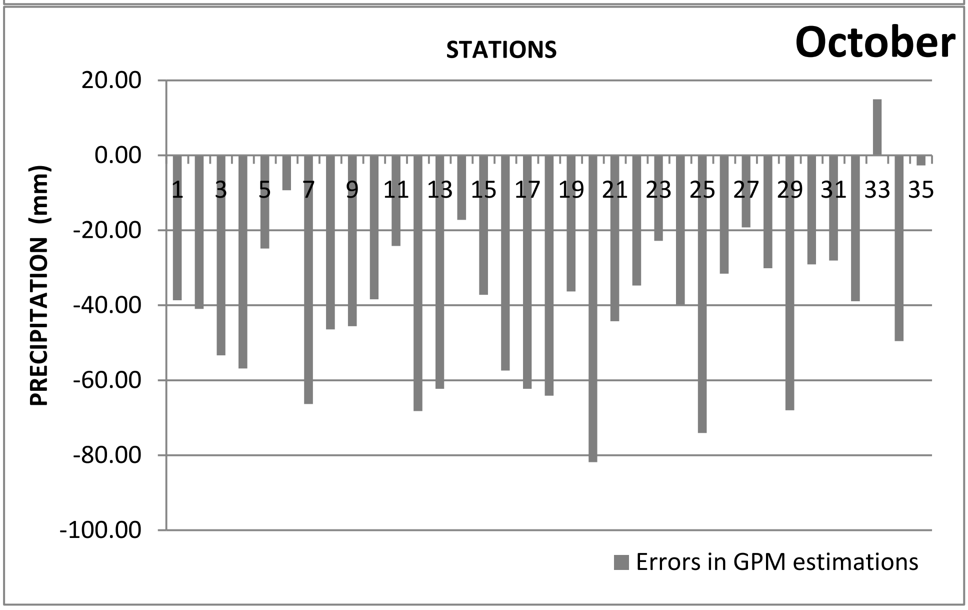

STATIONS
October
20.00
0.00
-20.00
-40.00
-60.00
-80.00
-100.00
PRECIPITATION (mm)
1 3 5 7 9 11 13 15 17 19 21 23 25 27 29 31 33 35
Errors in GPM estimations

Appendix D.

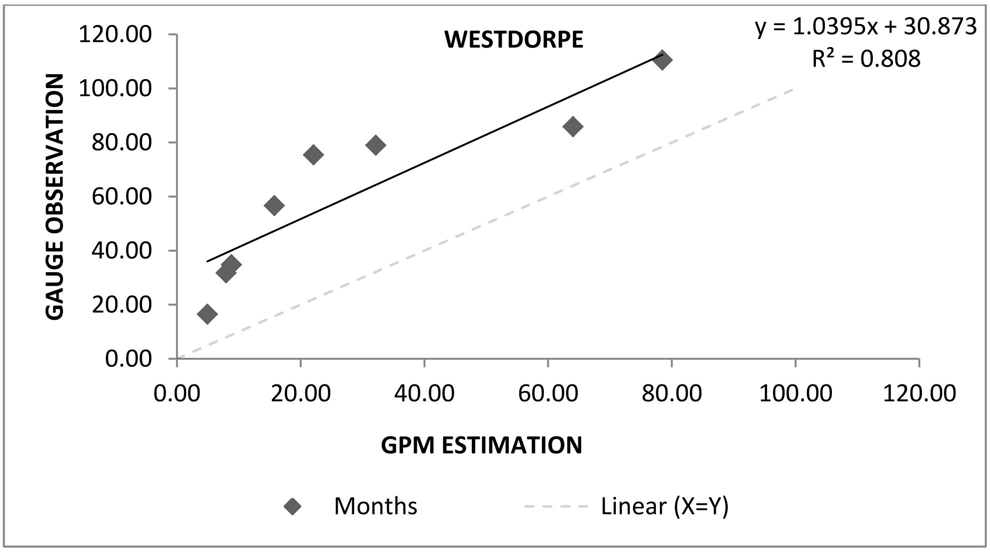

WESTDORPE
y = 1.0395x + 30.873
R² = 0.808
GAUGE OBSERVATION
120.00
100.00
80.00
60.00
40.00
20.00
0.00
0.00
20.00
40.00
60.00
80.00
100.00
120.00
GPM ESTIMATION
Months
Linear (X=Y)

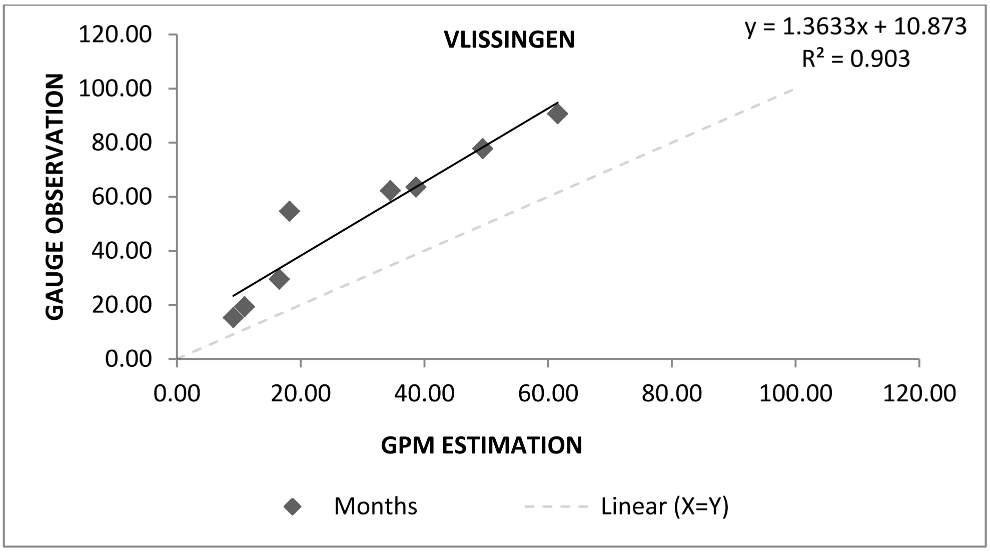

VLISSINGEN
y = 1.3633x + 10.873
R² = 0.903
GAUGE OBSERVATION
120.00
100.00
80.00
60.00
40.00
20.00
0.00
0.00
20.00
40.00
60.00
80.00
100.00
120.00
GPM ESTIMATION
Months
Linear (X=Y)

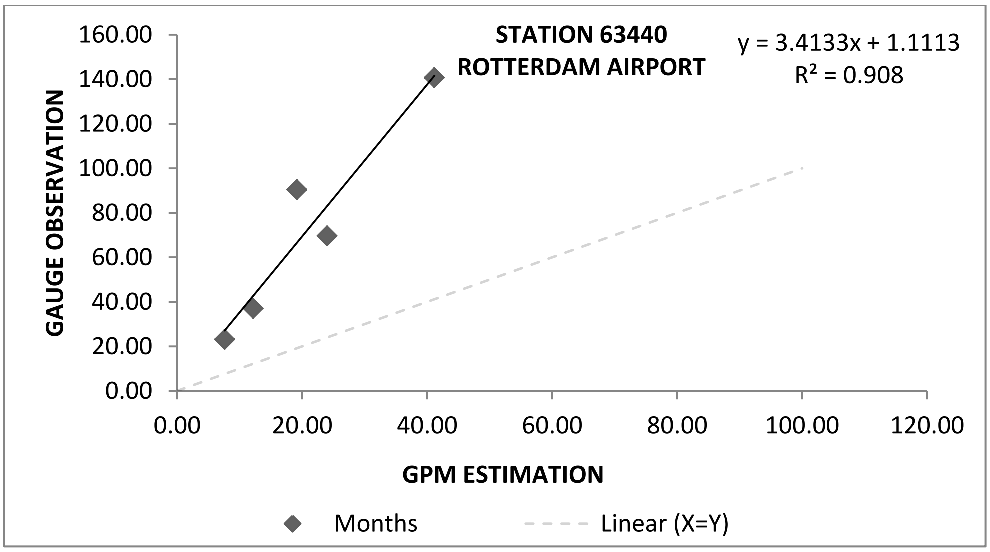

STATION 63440
ROTTERDAM AIRPORT
y = 3.4133x + 1.1113
R² = 0.908
GAUGE OBSERVATION
160.00
140.00
120.00
100.00
80.00
60.00
40.00
20.00
0.00
0.00
20.00
40.00
60.00
80.00
100.00
120.00
GPM ESTIMATION
Months
Linear (X=Y)

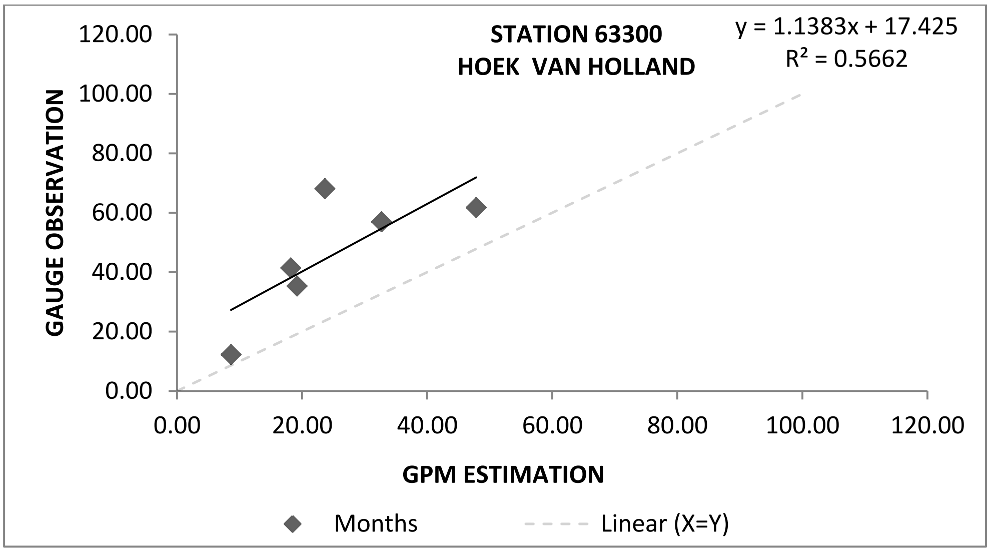
STATION 63300
HOEK VAN HOLLAND
y = 1.1383x + 17.425
R² = 0.5662
GAUGE OBSERVATION
GPM ESTIMATION
0.00
20.00
40.00
60.00
80.00
100.00
120.00
Months
Linear (X=Y)

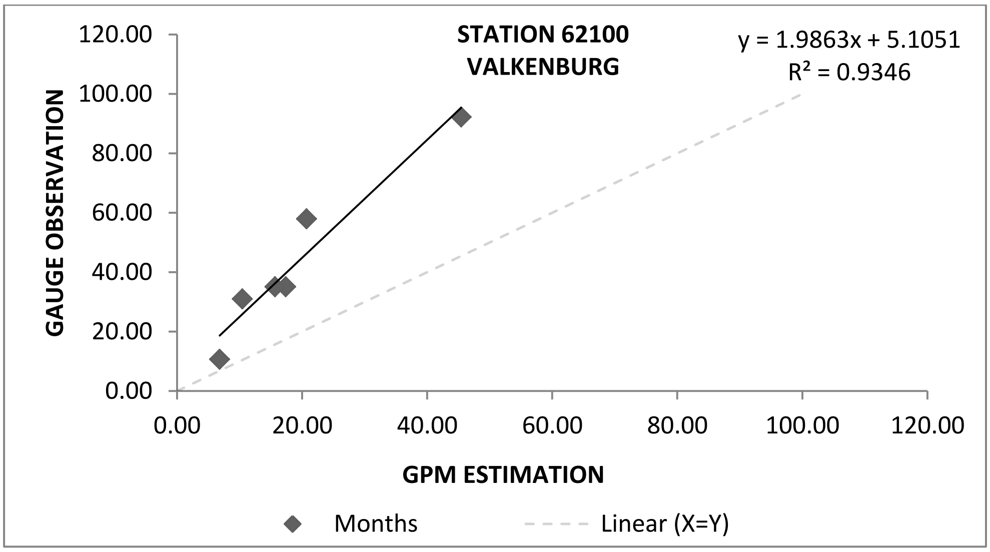
STATION 62100
VALKENBURG
y = 1.9863x + 5.1051
R² = 0.9346
GAUGE OBSERVATION
GPM ESTIMATION
0.00
20.00
40.00
60.00
80.00
100.00
120.00
Months
Linear (X=Y)

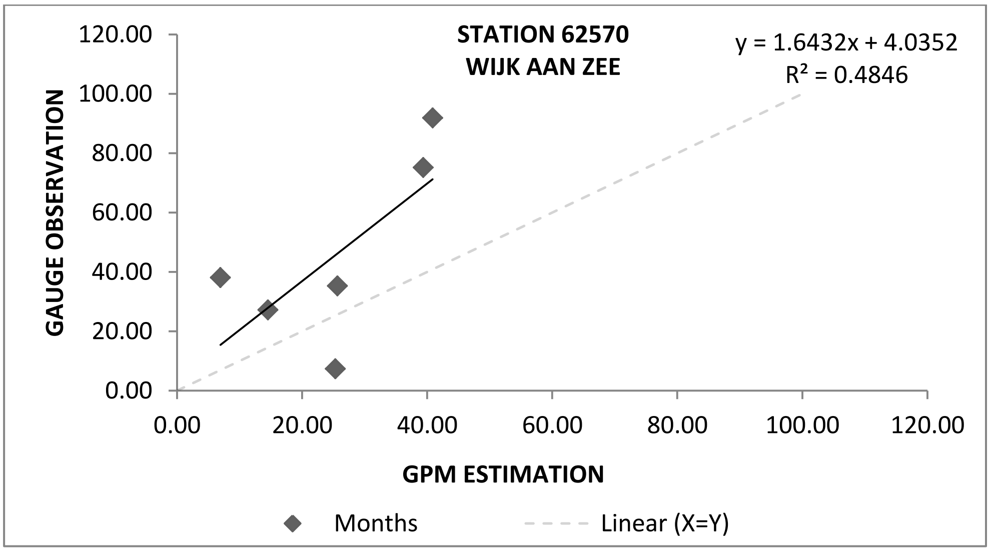
STATION 62570
WIJK AAN ZEE
y = 1.6432x + 4.0352
R² = 0.4846
GAUGE OBSERVATION
GPM ESTIMATION
0.00
20.00
40.00
60.00
80.00
100.00
120.00
Months
Linear (X=Y)

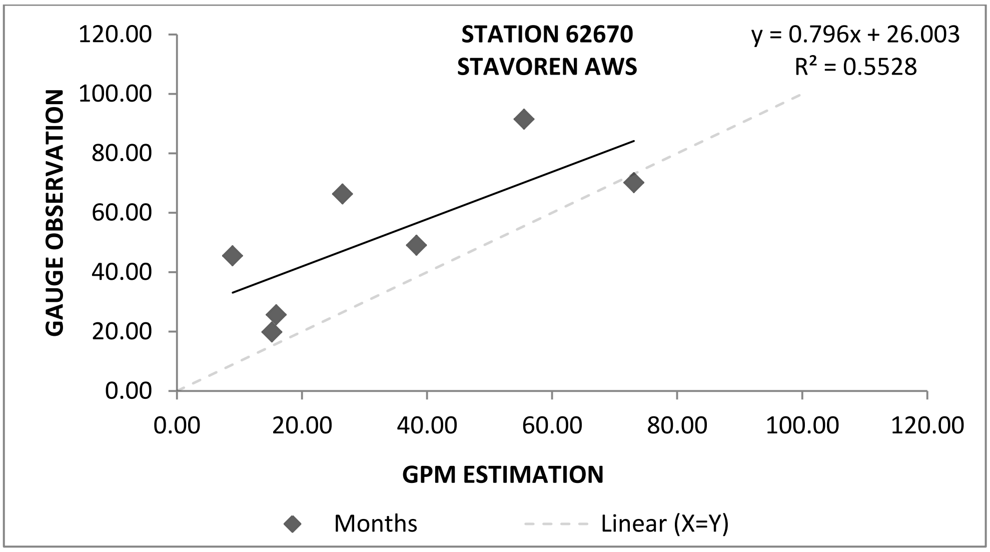

STATION 62670
STAVOREN AWS
y = 0.796x + 26.003
R² = 0.5528
GAUGE OBSERVATION
GPM ESTIMATION
0.00
20.00
40.00
60.00
80.00
100.00
120.00
Months
Linear (X=Y)

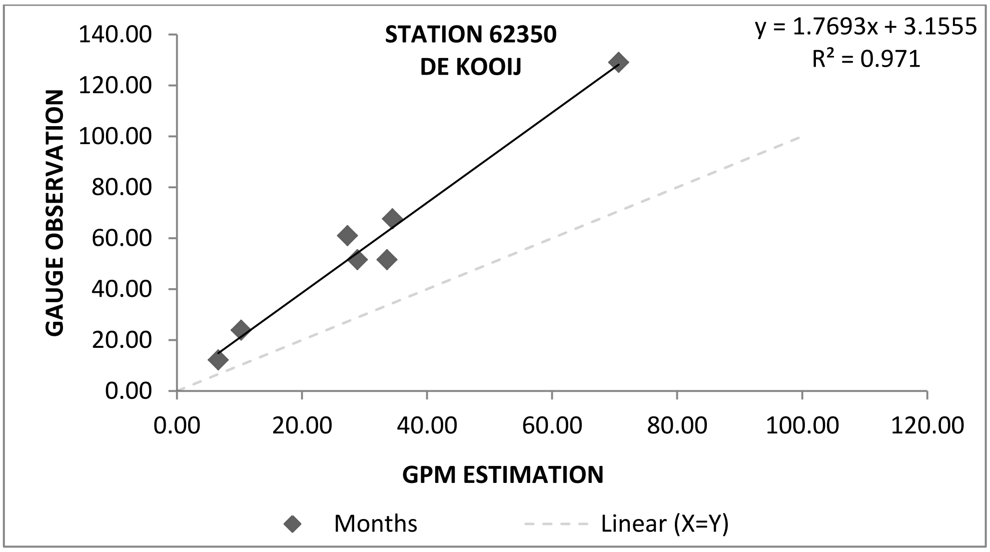

STATION 62350
DE KOOIJ
y = 1.7693x + 3.1555
R² = 0.971
GAUGE OBSERVATION
GPM ESTIMATION
0.00
20.00
40.00
60.00
80.00
100.00
120.00
140.00
Months
Linear (X=Y)

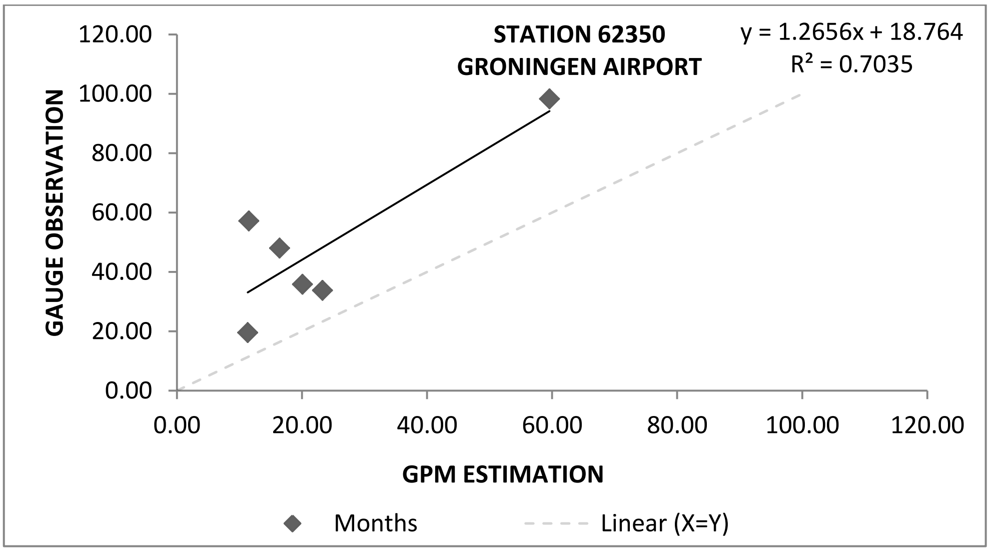

STATION 62350
GRONINGEN AIRPORT
y = 1.2656x + 18.764
R² = 0.7035
GAUGE OBSERVATION
GPM ESTIMATION
0.00
20.00
40.00
60.00
80.00
100.00
120.00
Months
Linear (X=Y)

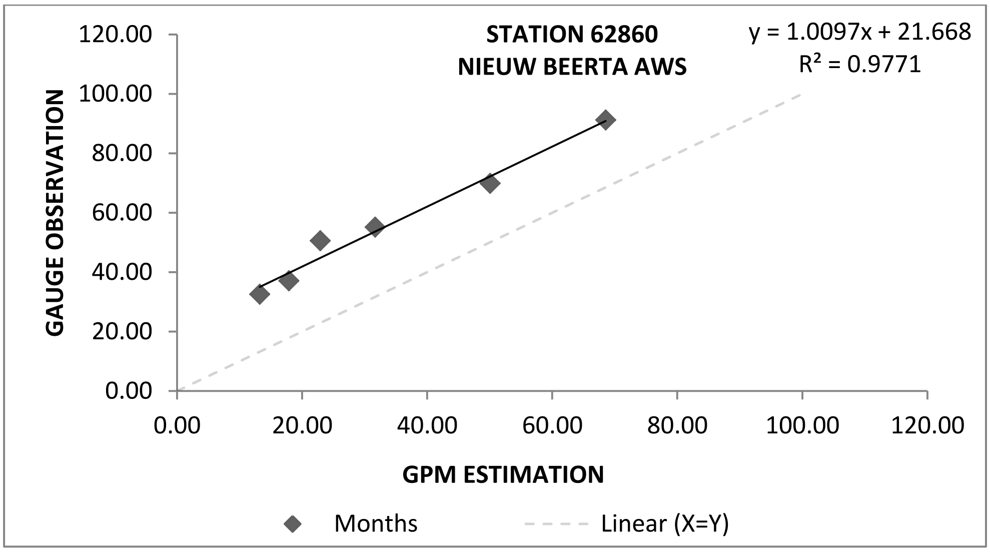
STATION 62860
NIEUW BEERTA AWS
y = 1.0097x + 21.668
R² = 0.9771
GAUGE OBSERVATION
120.00
100.00
80.00
60.00
40.00
20.00
0.00
0.00
20.00
40.00
60.00
80.00
100.00
120.00
GPM ESTIMATION
Months
Linear (X=Y)

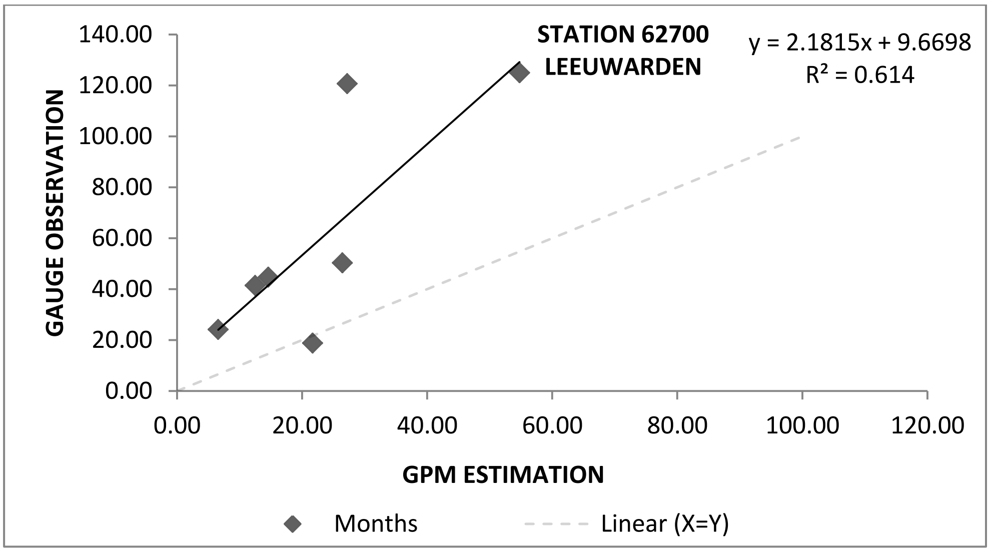
STATION 62700
LEEUWARDEN
y = 2.1815x + 9.6698
R² = 0.614
GAUGE OBSERVATION
140.00
120.00
100.00
80.00
60.00
40.00
20.00
0.00
0.00
20.00
40.00
60.00
80.00
100.00
120.00
GPM ESTIMATION
Months
Linear (X=Y)

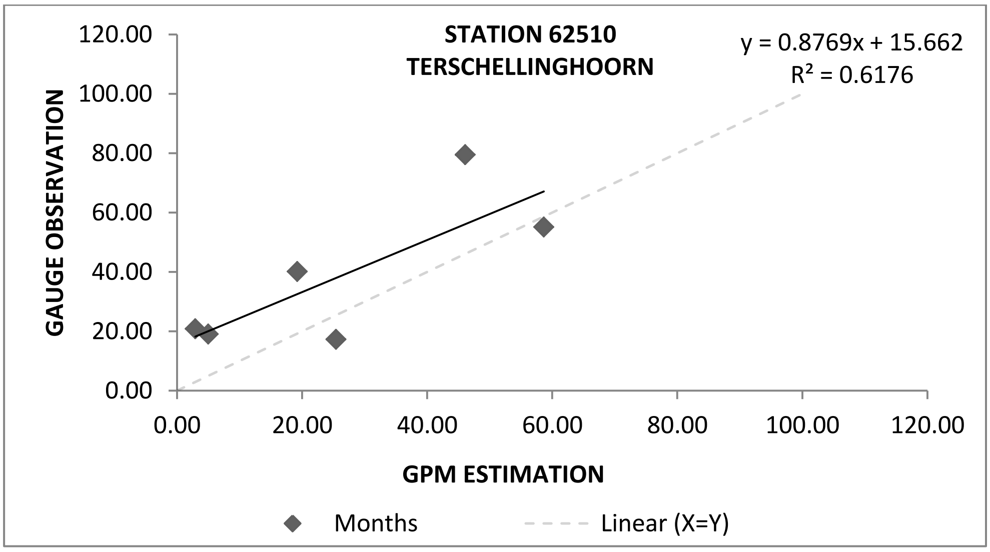
STATION 62510
TERSCHELLINGHOORN
y = 0.8769x + 15.662
R² = 0.6176
GAUGE OBSERVATION
120.00
100.00
80.00
60.00
40.00
20.00
0.00
0.00
20.00
40.00
60.00
80.00
100.00
120.00
GPM ESTIMATION
Months
Linear (X=Y)

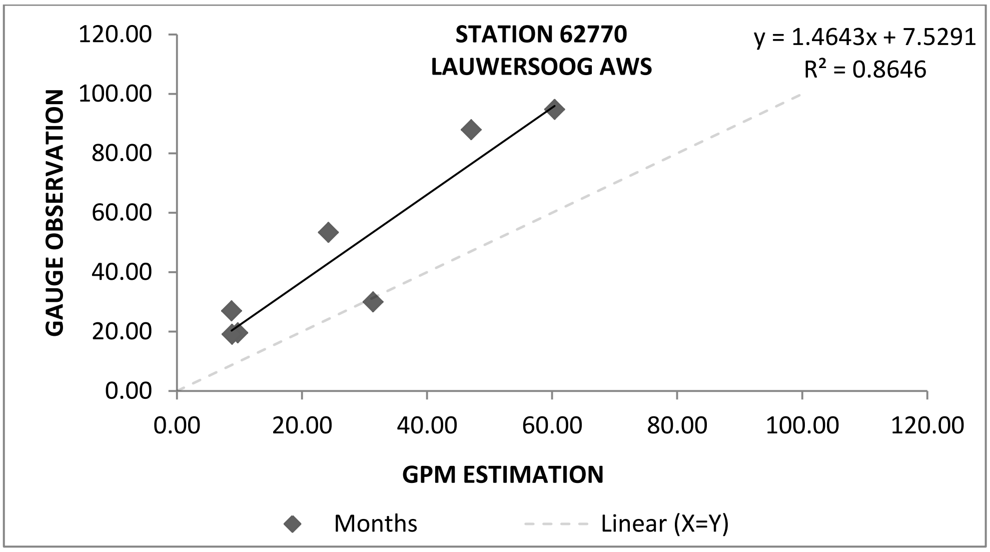
STATION 62770
LAUWERSOOG AWS
y = 1.4643x + 7.5291
R² = 0.8646
GAUGE OBSERVATION
GPM ESTIMATION
Months
Linear (X=Y)

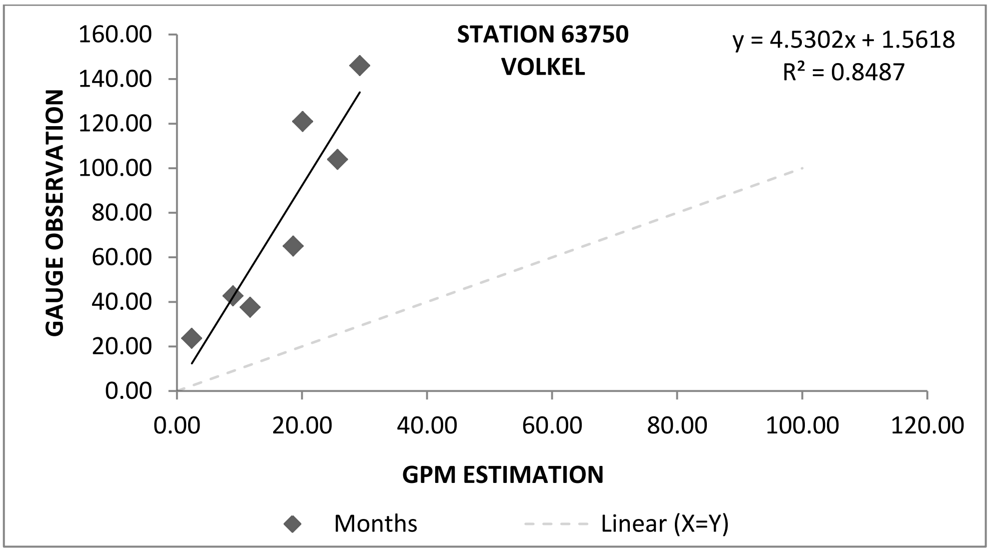
STATION 63750
VOLKEL
y = 4.5302x + 1.5618
R² = 0.8487
GAUGE OBSERVATION
GPM ESTIMATION
Months
Linear (X=Y)

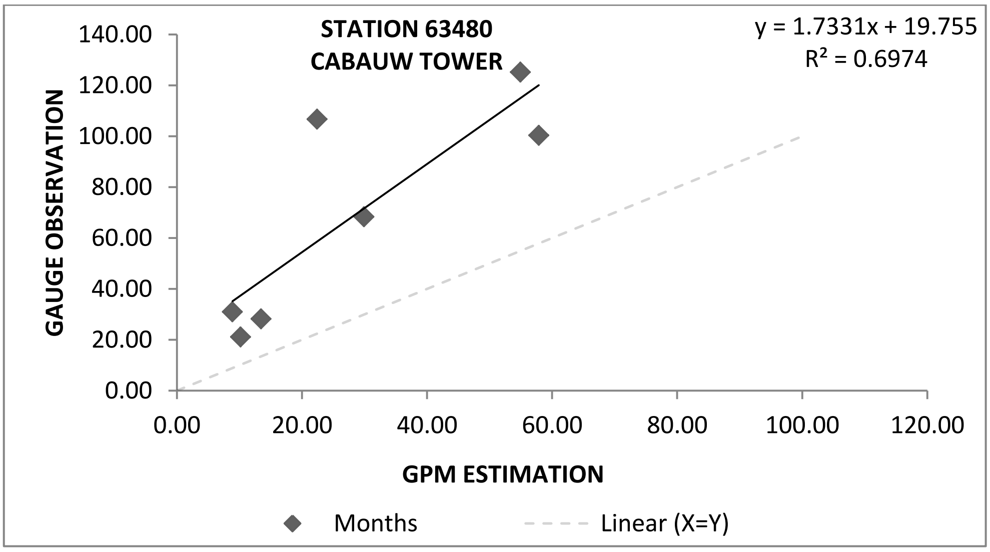
STATION 63480
CABAUW TOWER
y = 1.7331x + 19.755
R² = 0.6974
GAUGE OBSERVATION
GPM ESTIMATION
Months
Linear (X=Y)

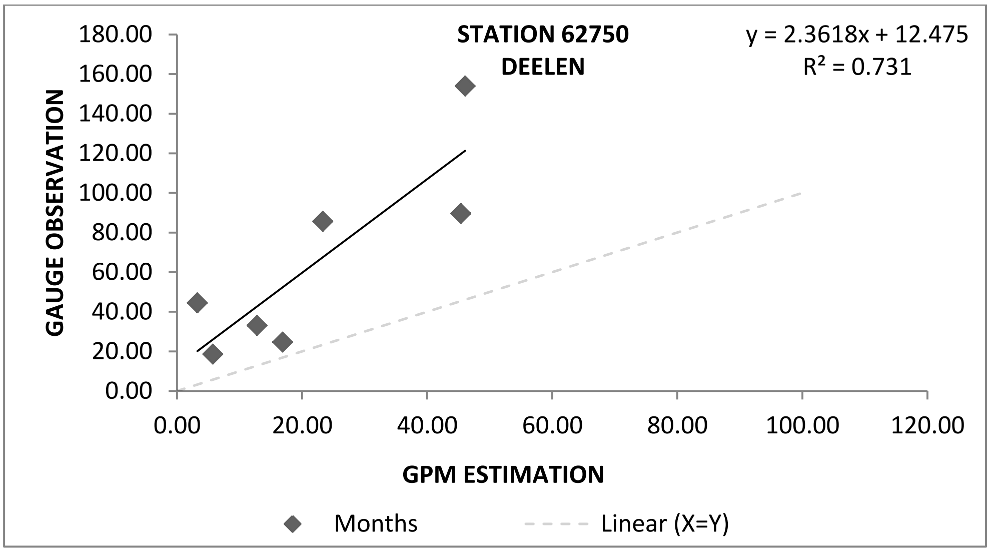

STATION 62750
DEELEN
y = 2.3618x + 12.475
R² = 0.731
GAUGE OBSERVATION
180.00
160.00
140.00
120.00
100.00
80.00
60.00
40.00
20.00
0.00
0.00
20.00
40.00
60.00
80.00
100.00
120.00
GPM ESTIMATION
Months
Linear (X=Y)

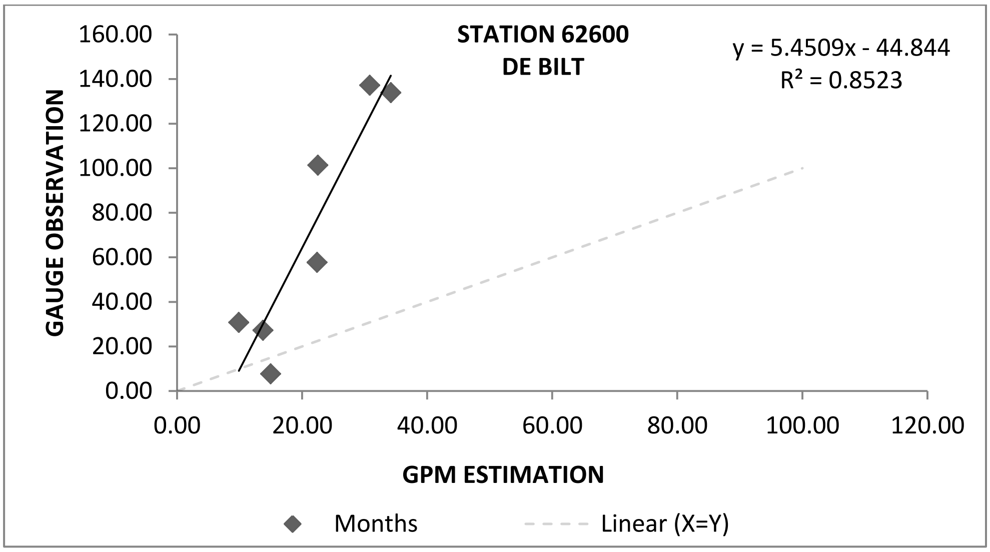

STATION 62600
DE BILT
y = 5.4509x - 44.844
R² = 0.8523
GAUGE OBSERVATION
160.00
140.00
120.00
100.00
80.00
60.00
40.00
20.00
0.00
0.00
20.00
40.00
60.00
80.00
100.00
120.00
GPM ESTIMATION
Months
Linear (X=Y)

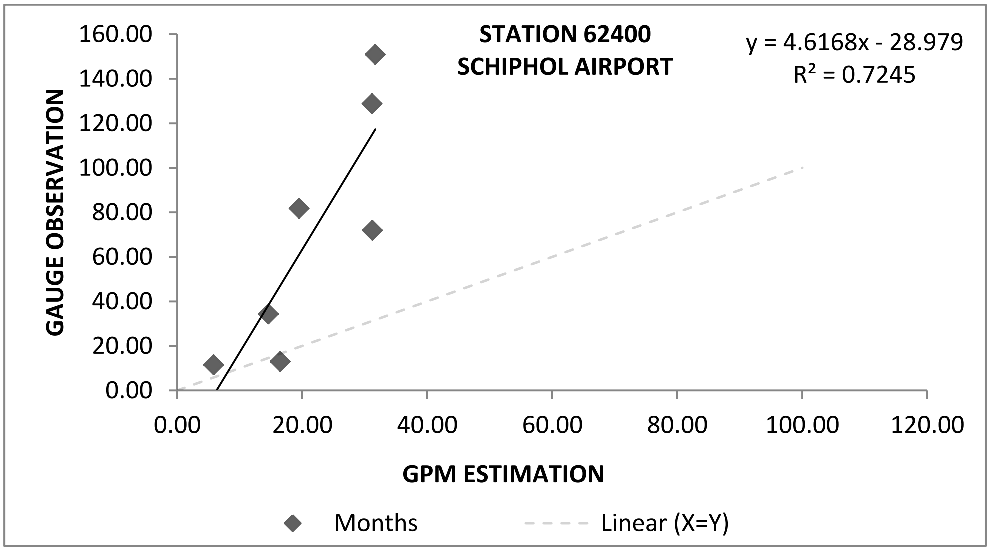

STATION 62400
SCHIPHOL AIRPORT
y = 4.6168x - 28.979
R² = 0.7245
GAUGE OBSERVATION
160.00
140.00
120.00
100.00
80.00
60.00
40.00
20.00
0.00
0.00
20.00
40.00
60.00
80.00
100.00
120.00
GPM ESTIMATION
Months
Linear (X=Y)

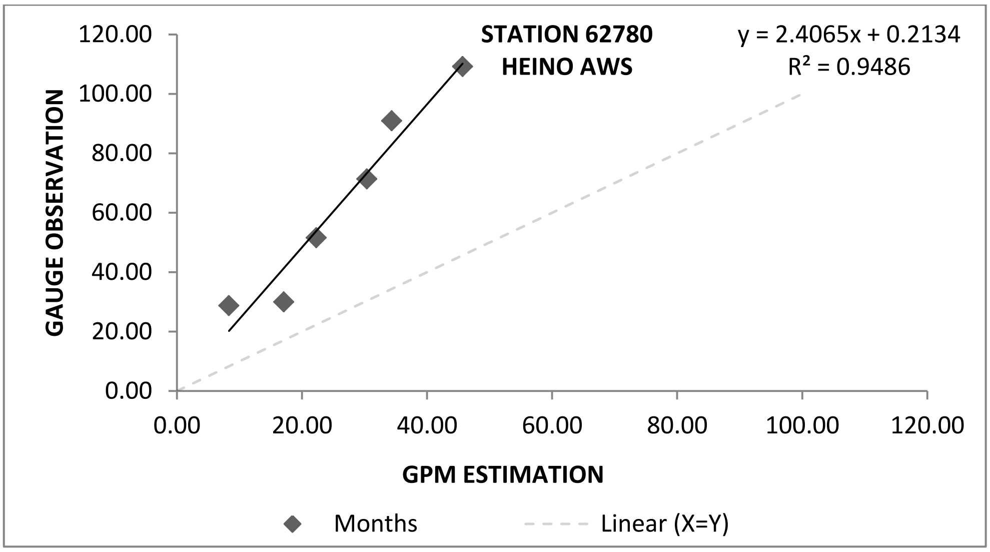
STATION 62780
HEINO AWS
y = 2.4065x + 0.2134
R² = 0.9486
GAUGE OBSERVATION
GPM ESTIMATION
Months
Linear (X=Y)

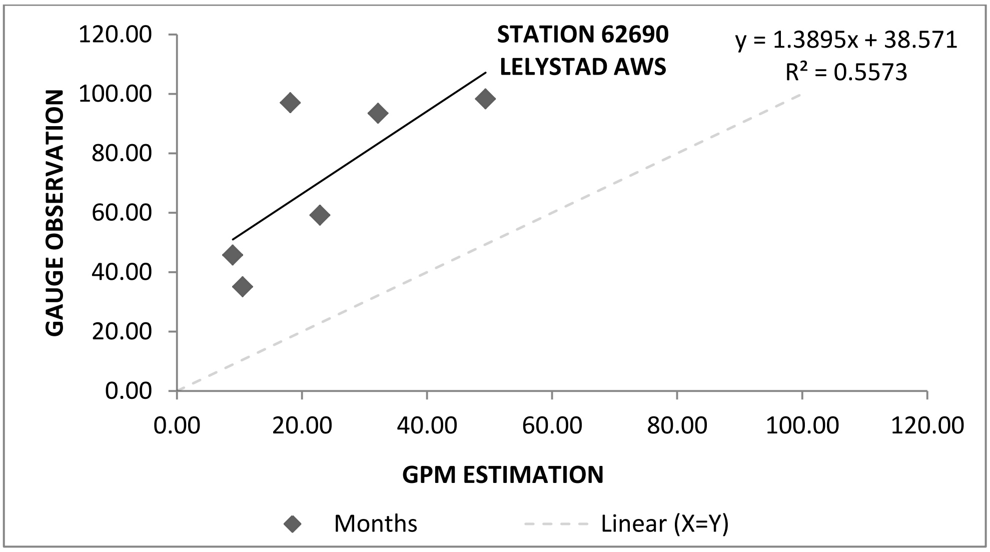
STATION 62690
LELYSTAD AWS
y = 1.3895x + 38.571
R² = 0.5573
GAUGE OBSERVATION
GPM ESTIMATION
Months
Linear (X=Y)

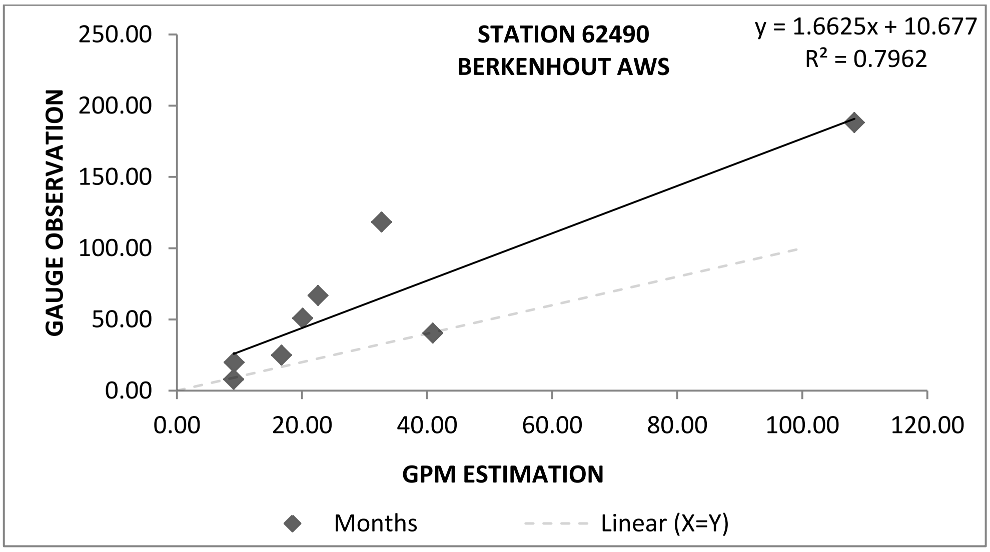
STATION 62490
BERKENHOUT AWS
y = 1.6625x + 10.677
R² = 0.7962
GAUGE OBSERVATION
GPM ESTIMATION
Months
Linear (X=Y)

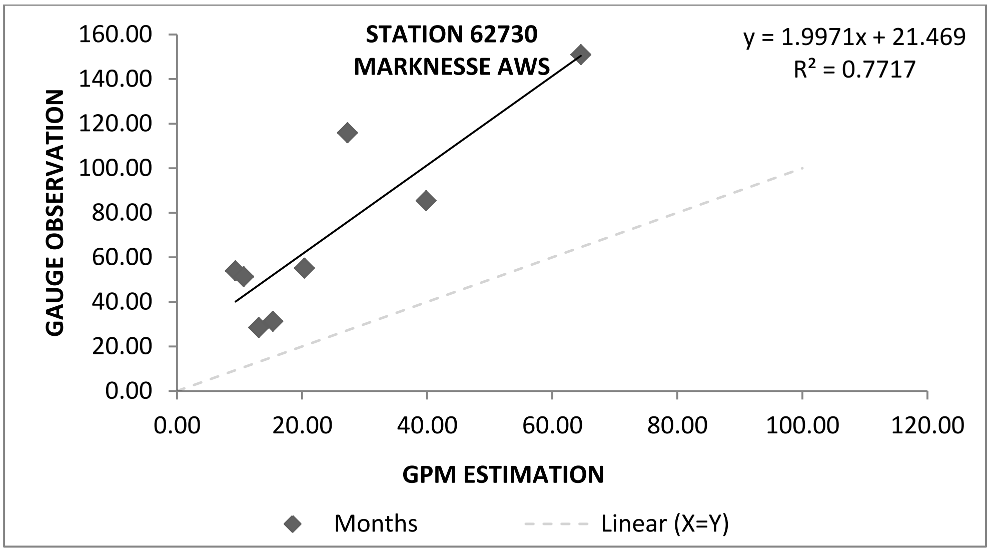
STATION 62730
MARKNESSE AWS
y = 1.9971x + 21.469
R² = 0.7717
GAUGE OBSERVATION
160.00
140.00
120.00
100.00
80.00
60.00
40.00
20.00
0.00
0.00
20.00
40.00
60.00
80.00
100.00
120.00
GPM ESTIMATION
Months
Linear (X=Y)

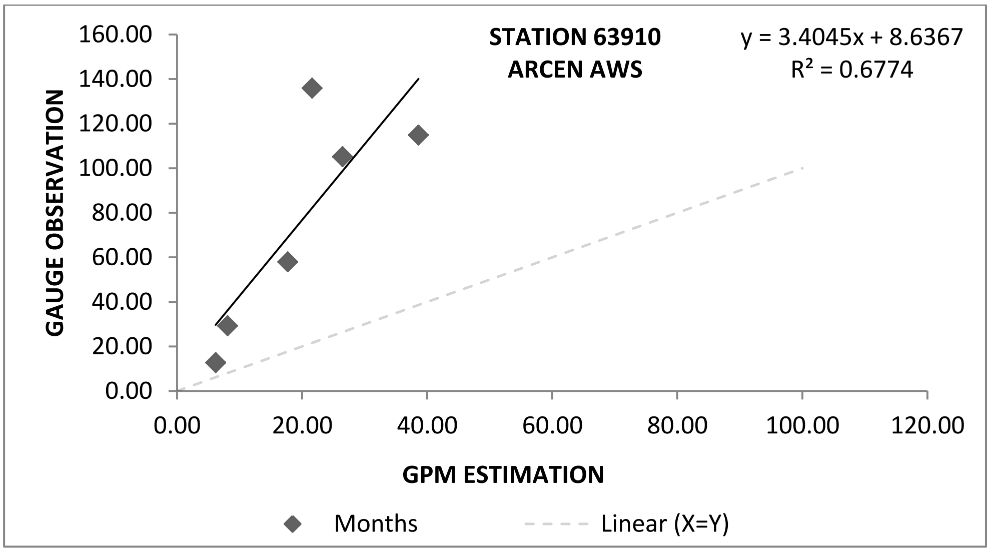
STATION 63910
ARCEN AWS
y = 3.4045x + 8.6367
R² = 0.6774
GAUGE OBSERVATION
160.00
140.00
120.00
100.00
80.00
60.00
40.00
20.00
0.00
0.00
20.00
40.00
60.00
80.00
100.00
120.00
GPM ESTIMATION
Months
Linear (X=Y)

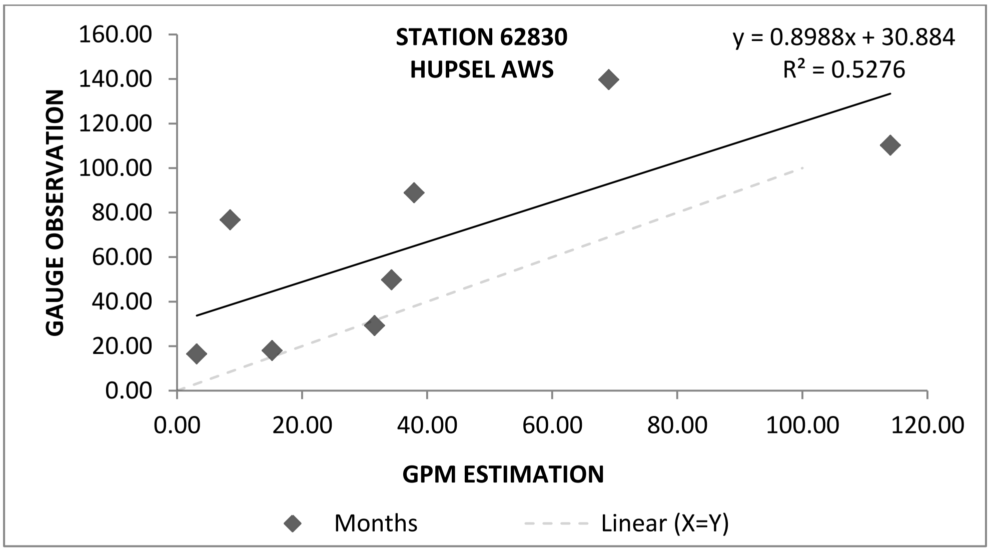
STATION 62830
HUPSEL AWS
y = 0.8988x + 30.884
R² = 0.5276
GAUGE OBSERVATION
160.00
140.00
120.00
100.00
80.00
60.00
40.00
20.00
0.00
0.00
20.00
40.00
60.00
80.00
100.00
120.00
GPM ESTIMATION
Months
Linear (X=Y)

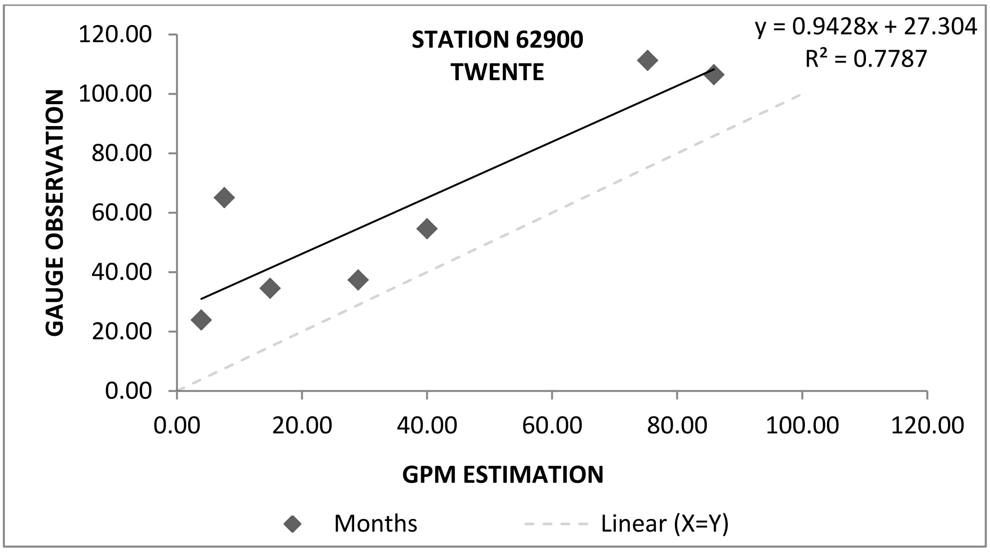

STATION 62900
TWENTE
y = 0.9428x + 27.304
R² = 0.7787
GAUGE OBSERVATION
GPM ESTIMATION
Months
Linear (X=Y)

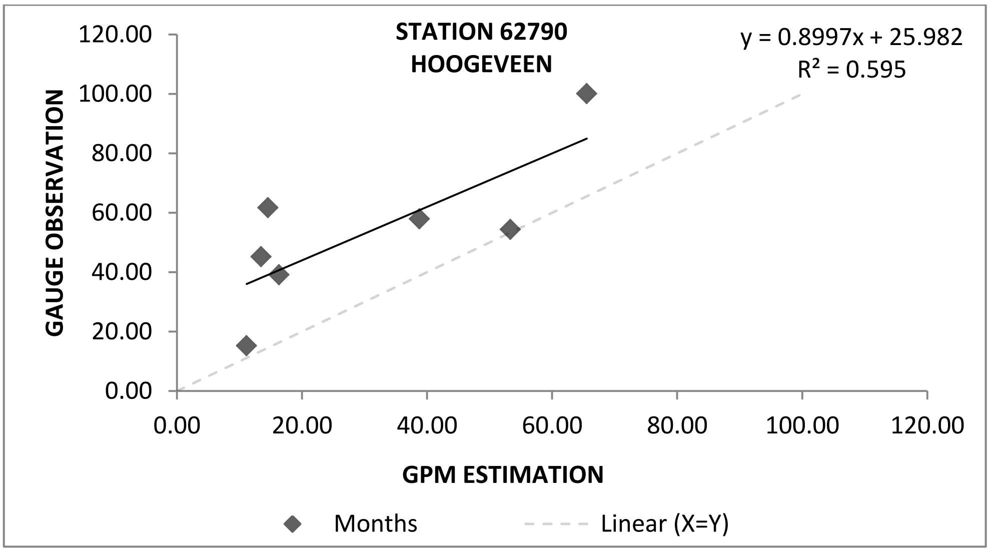

STATION 62790
HOOGEVEEN
y = 0.8997x + 25.982
R² = 0.595
GAUGE OBSERVATION
GPM ESTIMATION
Months
Linear (X=Y)

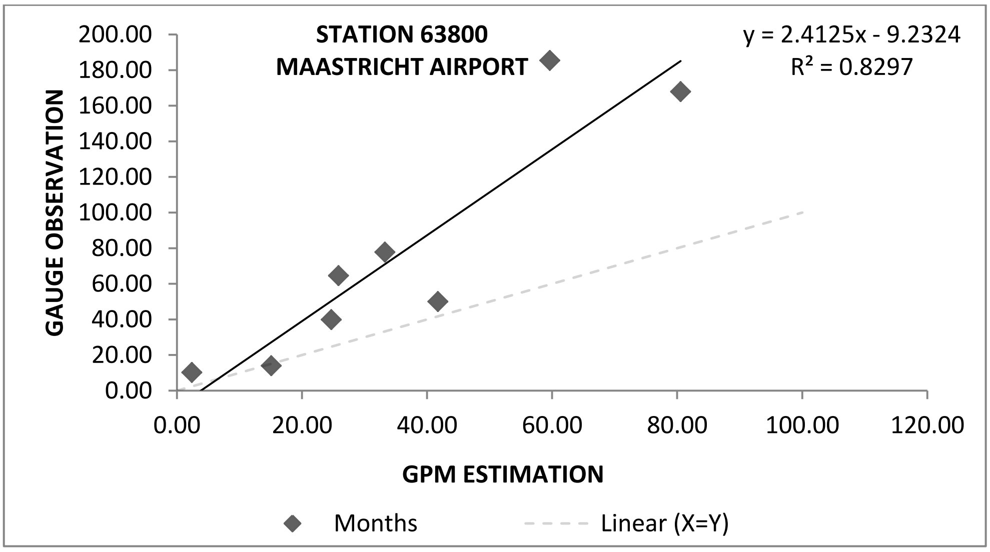

STATION 63800
MAASTRICHT AIRPORT
y = 2.4125x - 9.2324
R² = 0.8297
GAUGE OBSERVATION
GPM ESTIMATION
Months
Linear (X=Y)

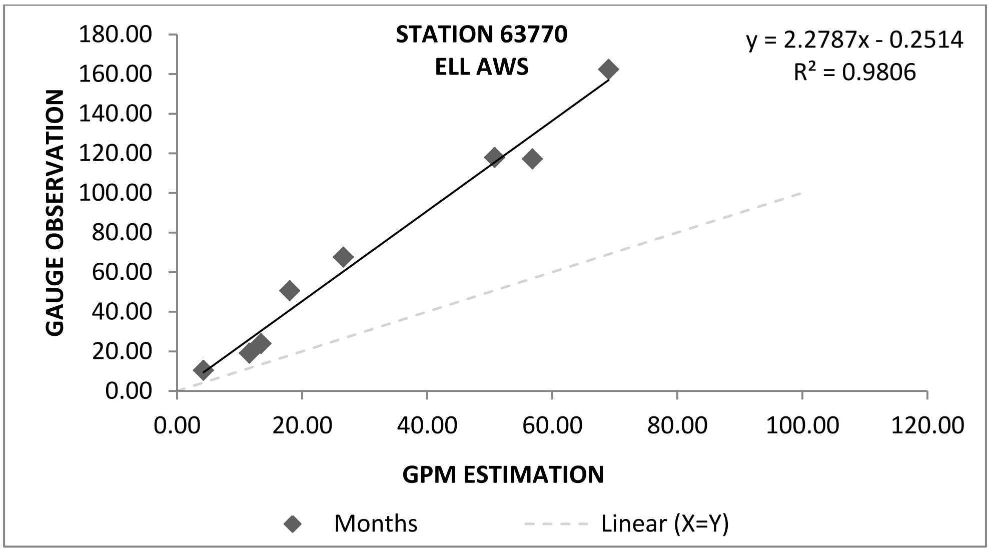
STATION 63770
ELL AWS
y = 2.2787x - 0.2514
R² = 0.9806
GAUGE OBSERVATION
180.00
160.00
140.00
120.00
100.00
80.00
60.00
40.00
20.00
0.00
0.00
20.00
40.00
60.00
80.00
100.00
120.00
GPM ESTIMATION
Months
Linear (X=Y)

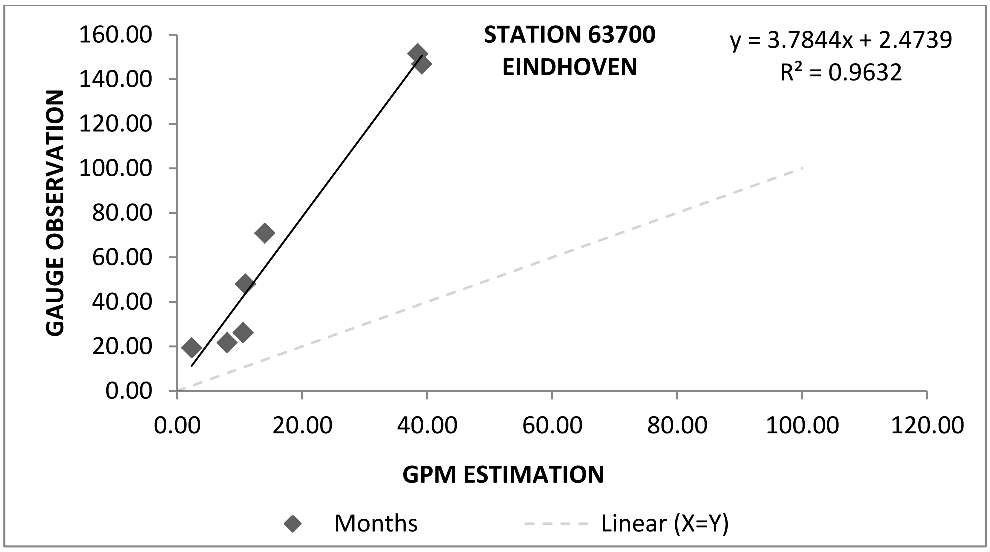
STATION 63700
EINDHOVEN
y = 3.7844x + 2.4739
R² = 0.9632
GAUGE OBSERVATION
160.00
140.00
120.00
100.00
80.00
60.00
40.00
20.00
0.00
0.00
20.00
40.00
60.00
80.00
100.00
120.00
GPM ESTIMATION
Months
Linear (X=Y)

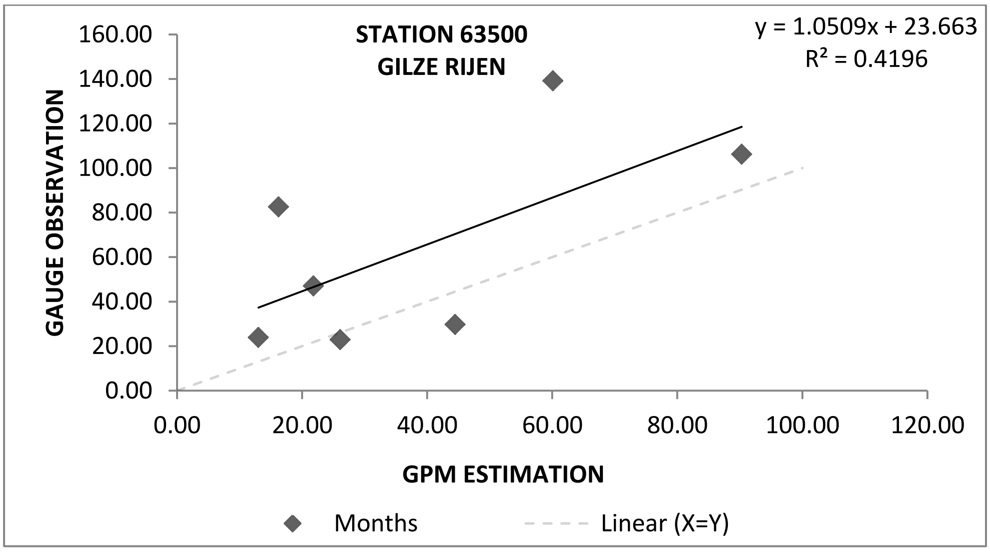
STATION 63500
GILZE RIJEN
y = 1.0509x + 23.663
R² = 0.4196
GAUGE OBSERVATION
160.00
140.00
120.00
100.00
80.00
60.00
40.00
20.00
0.00
0.00
20.00
40.00
60.00
80.00
100.00
120.00
GPM ESTIMATION
Months
Linear (X=Y)

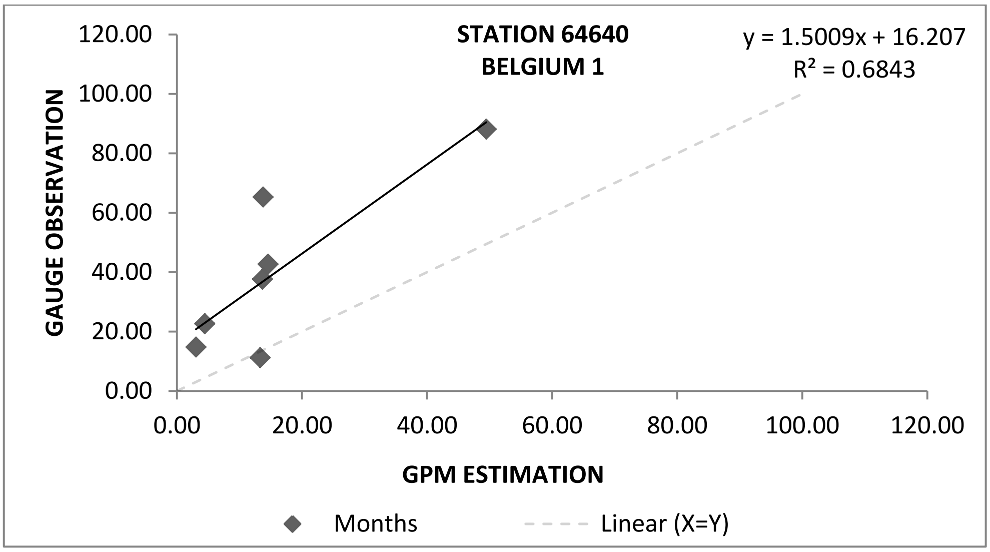
STATION 64640
BELGIUM 1
y = 1.5009x + 16.207
R² = 0.6843
GAUGE OBSERVATION
GPM ESTIMATION
120.00
100.00
80.00
60.00
40.00
20.00
0.00
0.00
20.00
40.00
60.00
80.00
100.00
120.00
Months
Linear (X=Y)

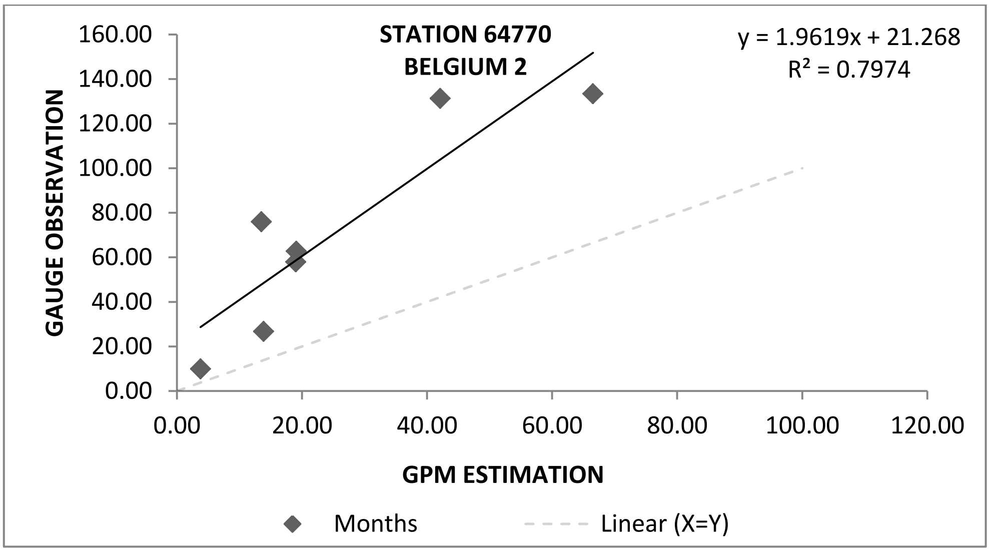
STATION 64770
BELGIUM 2
y = 1.9619x + 21.268
R² = 0.7974
GAUGE OBSERVATION
GPM ESTIMATION
160.00
140.00
120.00
100.00
80.00
60.00
40.00
20.00
0.00
0.00
20.00
40.00
60.00
80.00
100.00
120.00
Months
Linear (X=Y)

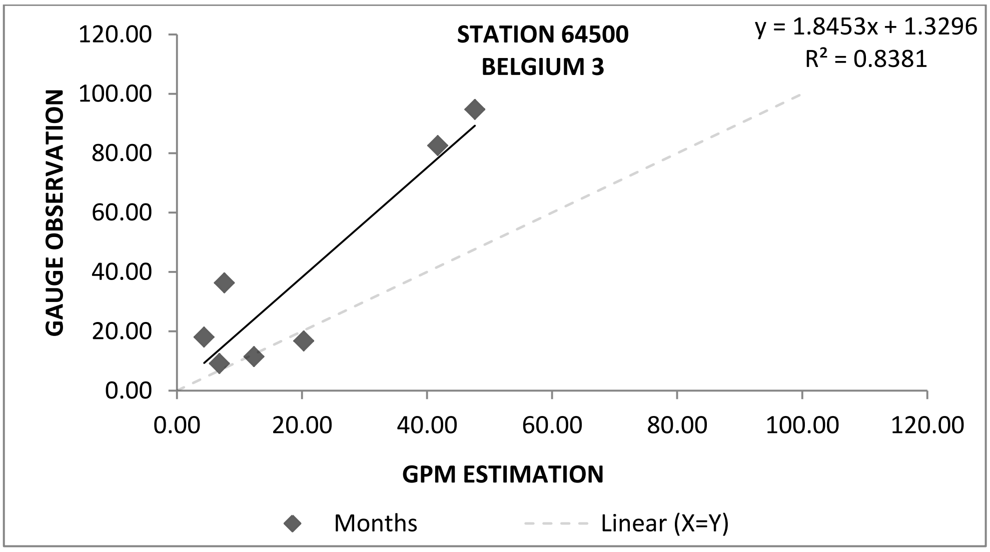
STATION 64500
BELGIUM 3
y = 1.8453x + 1.3296
R² = 0.8381
GAUGE OBSERVATION
GPM ESTIMATION
120.00
100.00
80.00
60.00
40.00
20.00
0.00
0.00
20.00
40.00
60.00
80.00
100.00
120.00
Months
Linear (X=Y)

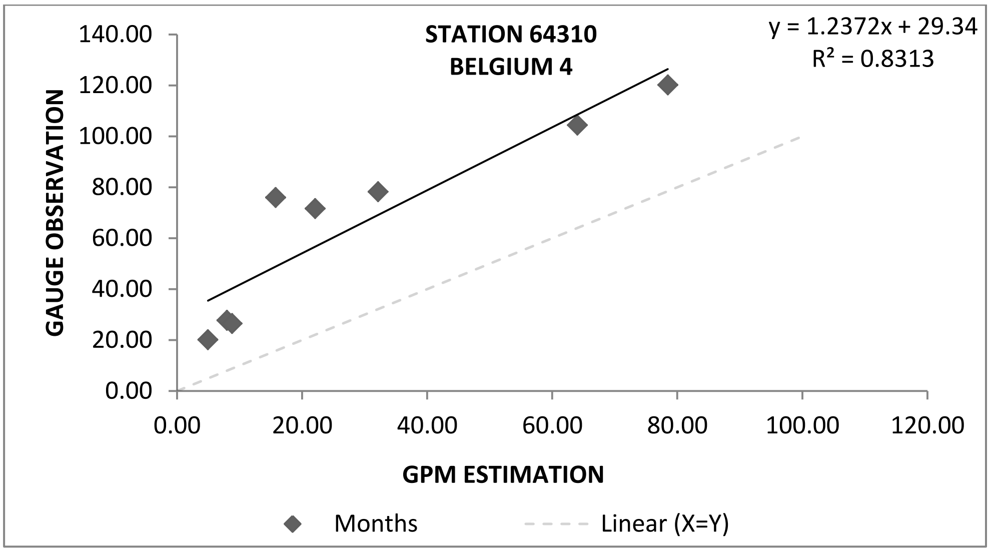
STATION 64310
BELGIUM 4
y = 1.2372x + 29.34
R² = 0.8313
GAUGE OBSERVATION
140.00
120.00
100.00
80.00
60.00
40.00
20.00
0.00
0.00
20.00
40.00
60.00
80.00
100.00
120.00
GPM ESTIMATION
Months
Linear (X=Y)

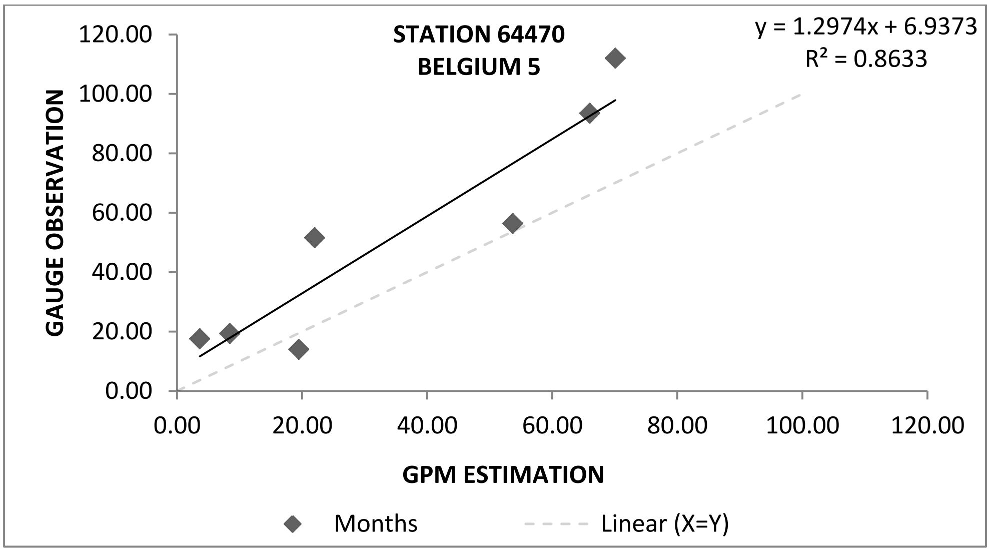
STATION 64470
BELGIUM 5
y = 1.2974x + 6.9373
R² = 0.8633
GAUGE OBSERVATION
120.00
100.00
80.00
60.00
40.00
20.00
0.00
0.00
20.00
40.00
60.00
80.00
100.00
120.00
GPM ESTIMATION
Months
Linear (X=Y)

MPE

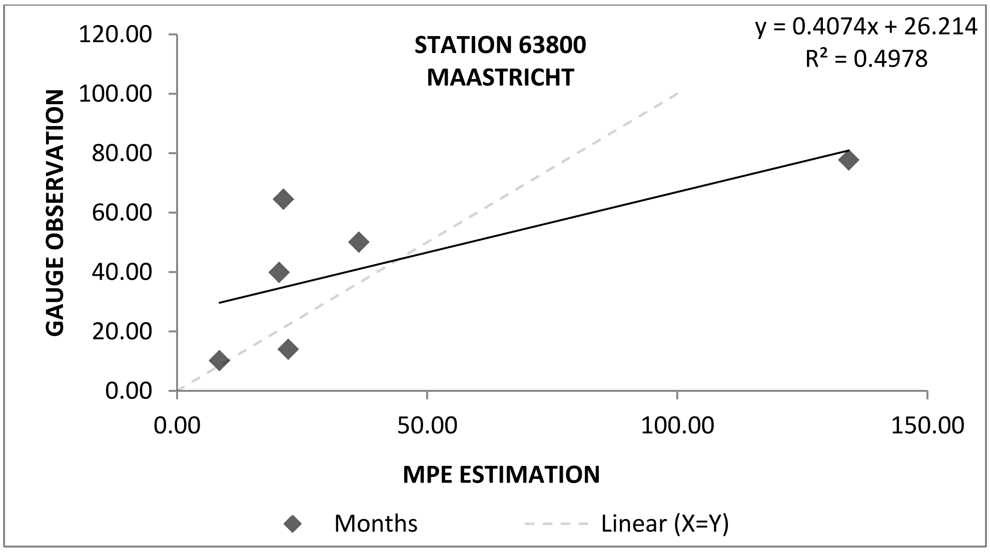
STATION 63800
MAASTRICHT
y = 0.4074x + 26.214
R² = 0.4978
GAUGE OBSERVATION
120.00
100.00
80.00
60.00
40.00
20.00
0.00
0.00
50.00
100.00
150.00
MPE ESTIMATION
Months
Linear (X=Y)

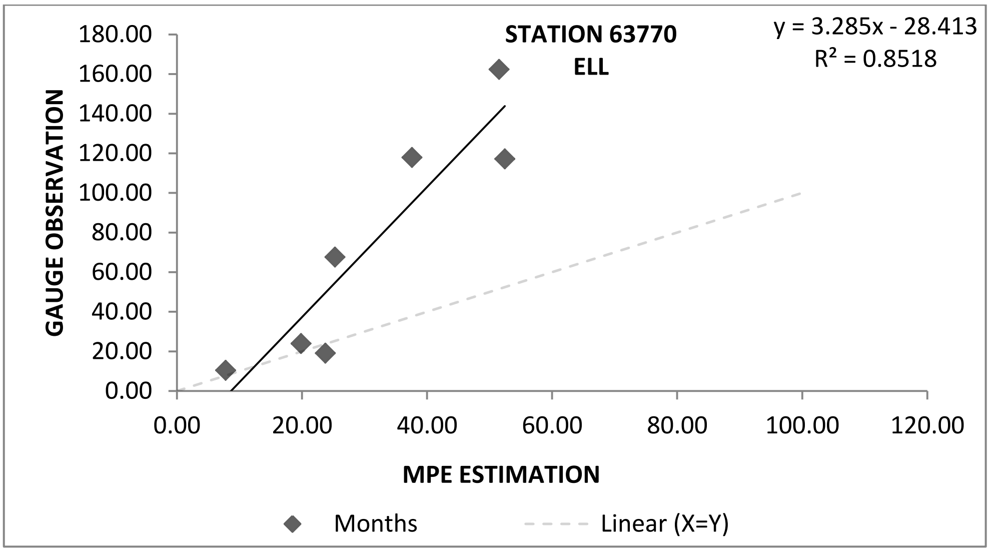
STATION 63770
ELL
y = 3.285x - 28.413
R² = 0.8518
GAUGE OBSERVATION
MPE ESTIMATION
Months
Linear (X=Y)

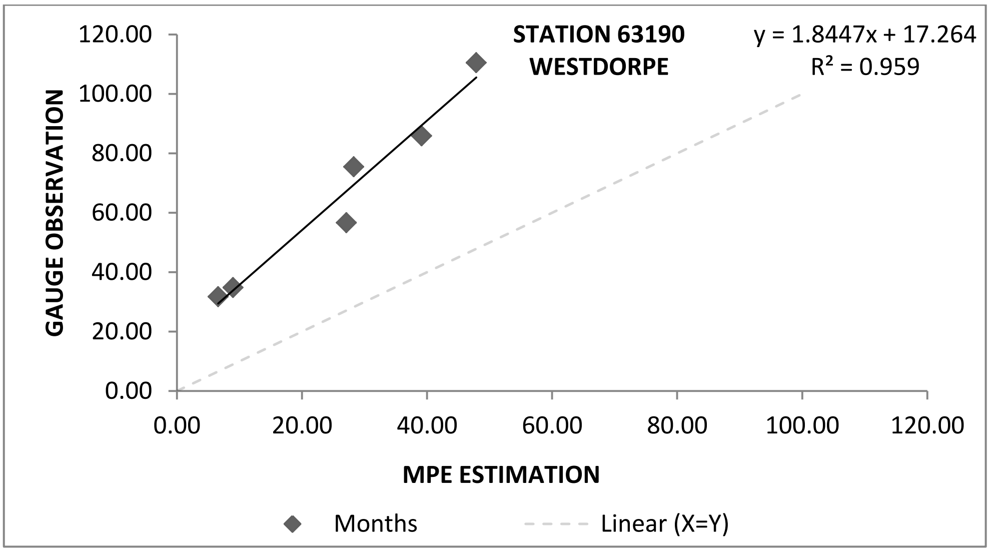
STATION 63190
WESTDORPE
y = 1.8447x + 17.264
R² = 0.959
GAUGE OBSERVATION
MPE ESTIMATION
Months
Linear (X=Y)

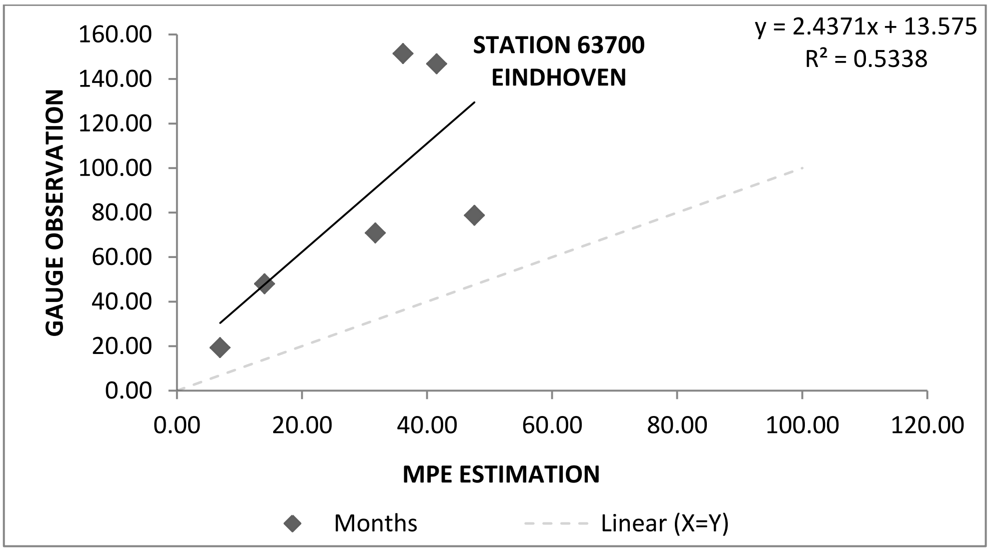
STATION 63700
EINDHOVEN
y = 2.4371x + 13.575
R² = 0.5338
GAUGE OBSERVATION
MPE ESTIMATION
Months
Linear (X=Y)

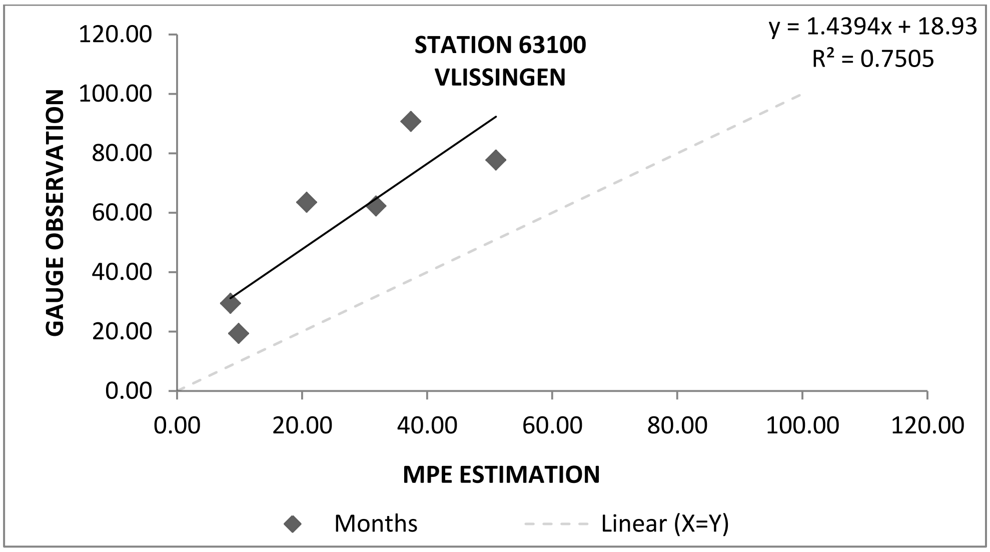
STATION 63100
VLISSINGEN
y = 1.4394x + 18.93
R² = 0.7505
GAUGE OBSERVATION
MPE ESTIMATION
0.00
20.00
40.00
60.00
80.00
100.00
120.00
Months
Linear (X=Y)

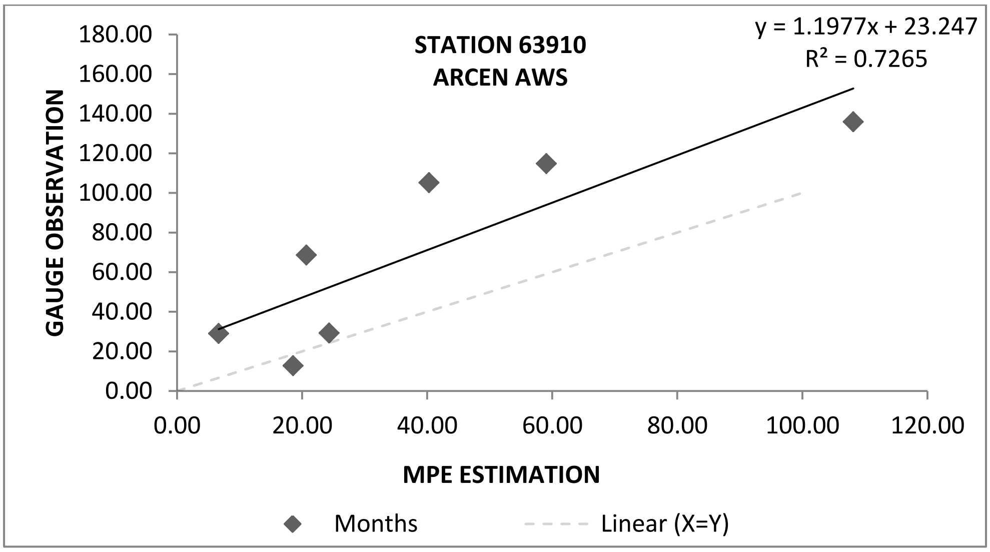
STATION 63910
ARCEN AWS
y = 1.1977x + 23.247
R² = 0.7265
GAUGE OBSERVATION
MPE ESTIMATION
0.00
20.00
40.00
60.00
80.00
100.00
120.00
140.00
160.00
180.00
Months
Linear (X=Y)

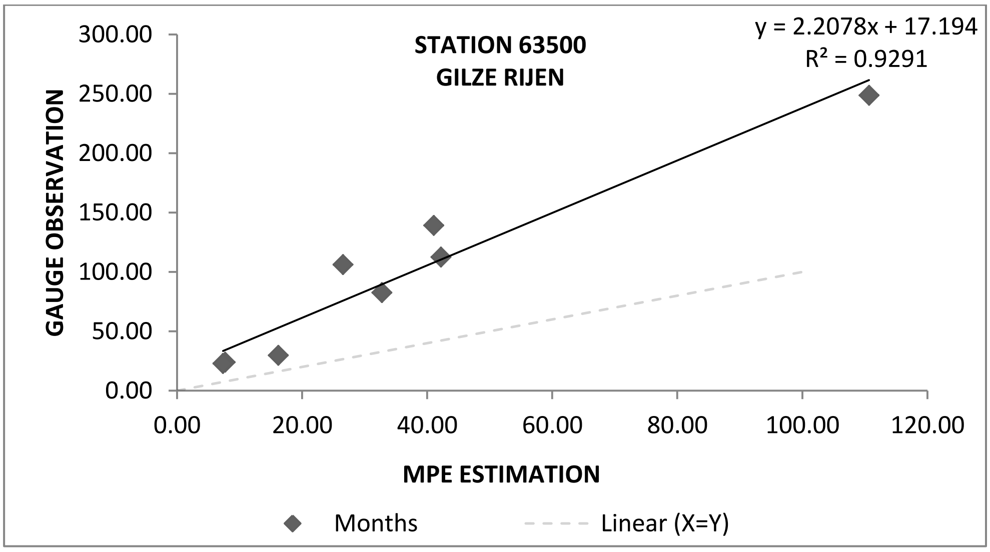
STATION 63500
GILZE RIJEN
y = 2.2078x + 17.194
R² = 0.9291
GAUGE OBSERVATION
MPE ESTIMATION
0.00
50.00
100.00
150.00
200.00
250.00
300.00
20.00
40.00
60.00
80.00
120.00
Months
Linear (X=Y)

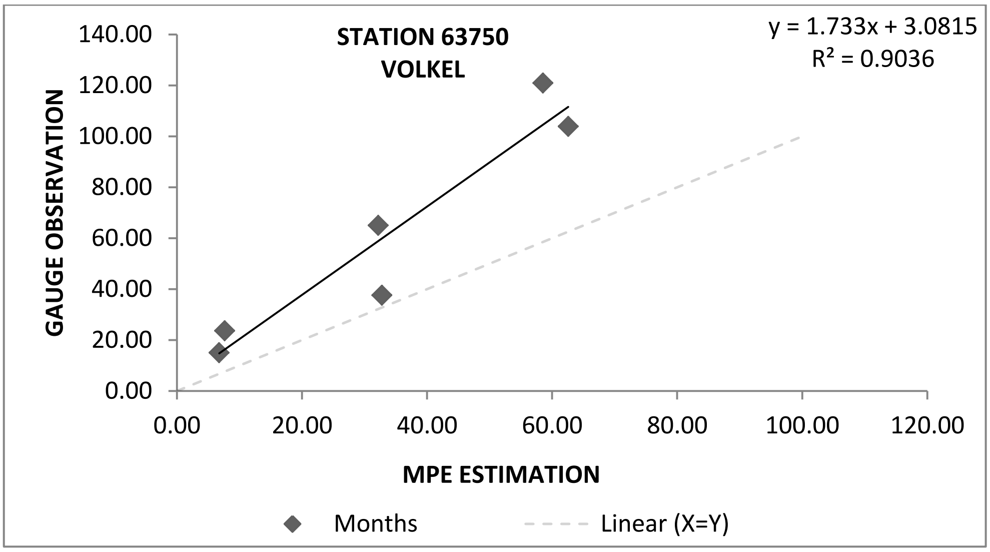
STATION 63750
VOLKEL
y = 1.733x + 3.0815
R² = 0.9036
GAUGE OBSERVATION
MPE ESTIMATION
0.00
20.00
40.00
60.00
80.00
100.00
120.00
140.00
Months
Linear (X=Y)

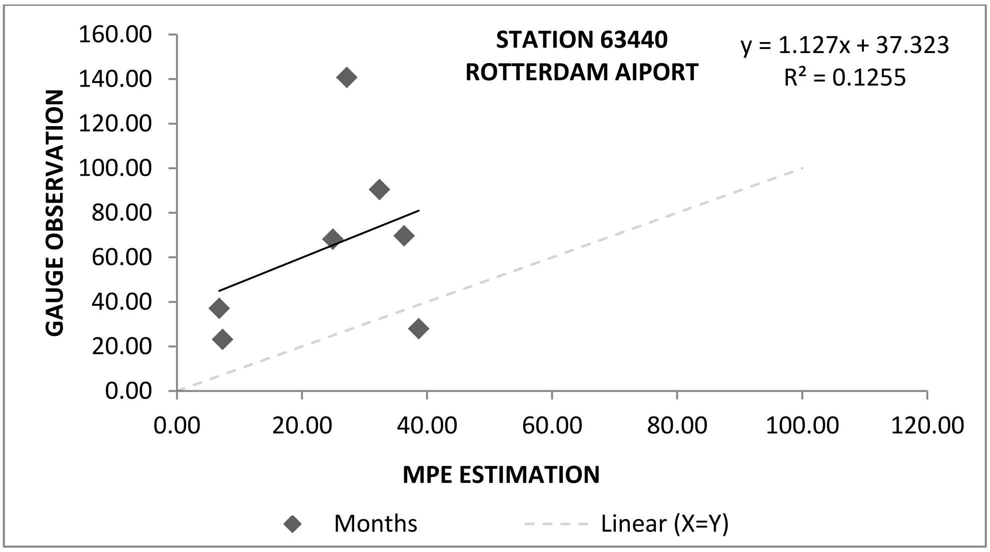
STATION 63440
ROTTERDAM AIPORT
y = 1.127x + 37.323
R² = 0.1255
GAUGE OBSERVATION
MPE ESTIMATION
0.00
20.00
40.00
60.00
80.00
100.00
120.00
140.00
160.00
Months
Linear (X=Y)

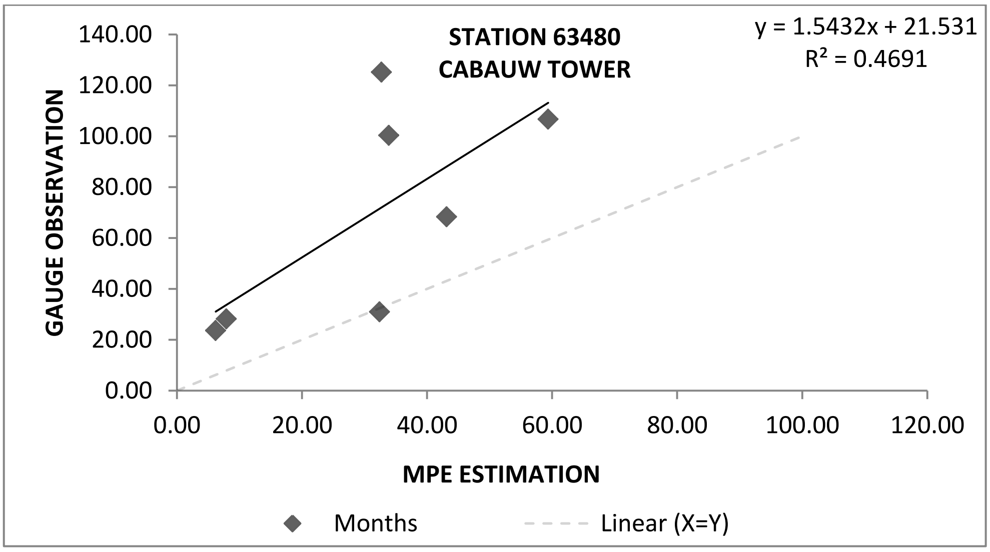
STATION 63480
CABAUW TOWER
y = 1.5432x + 21.531
R² = 0.4691
GAUGE OBSERVATION
MPE ESTIMATION
0.00
20.00
40.00
60.00
80.00
100.00
120.00
140.00
Months
Linear (X=Y)

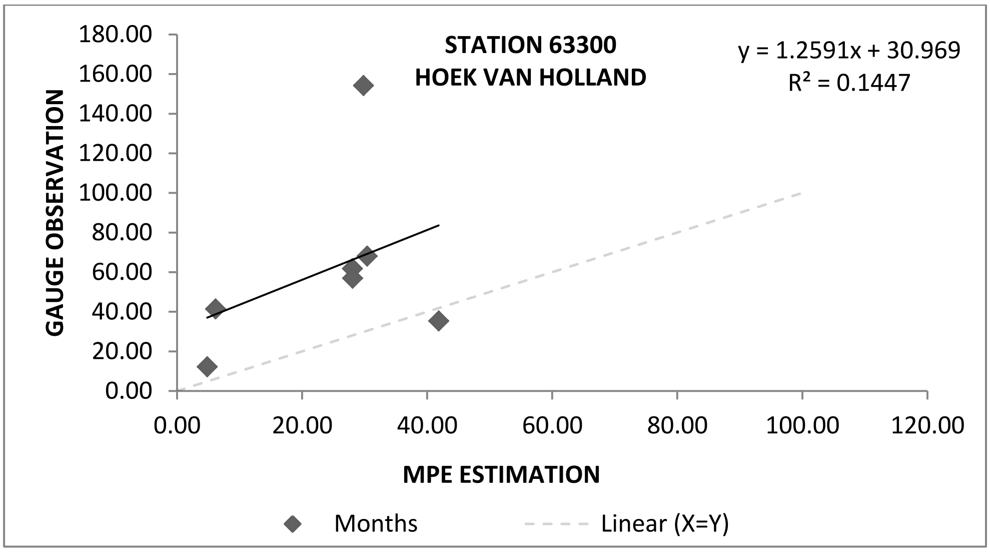
STATION 63300
HOEK VAN HOLLAND
y = 1.2591x + 30.969
R² = 0.1447
GAUGE OBSERVATION
MPE ESTIMATION
Months
Linear (X=Y)

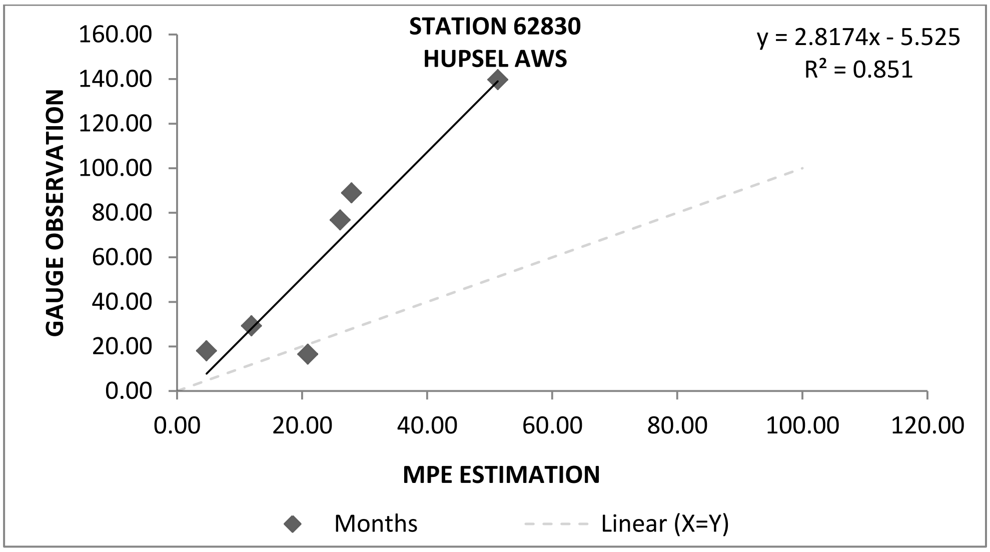
STATION 62830
HUPSEL AWS
y = 2.8174x - 5.525
R² = 0.851
GAUGE OBSERVATION
MPE ESTIMATION
Months
Linear (X=Y)

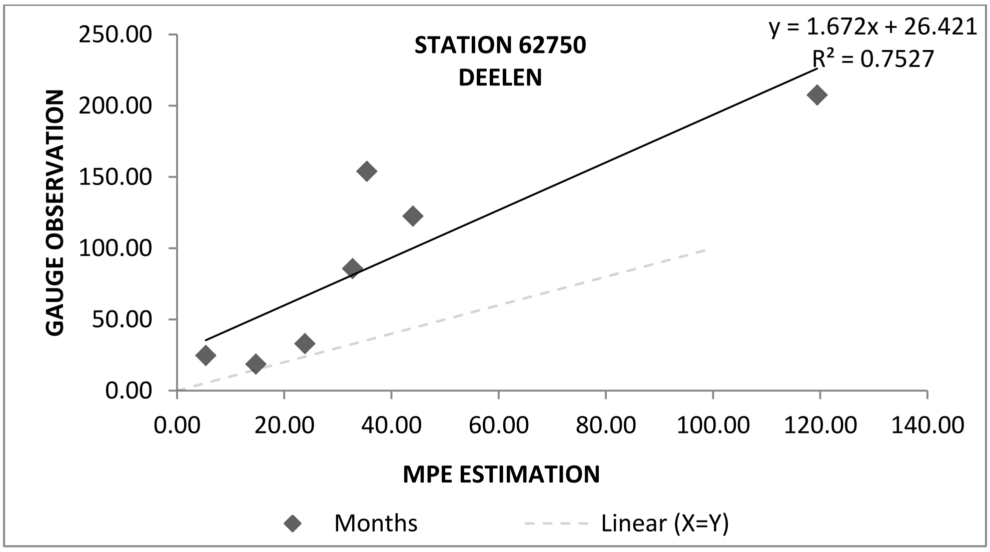
STATION 62750
DEELEN
y = 1.672x + 26.421
R² = 0.7527
GAUGE OBSERVATION
MPE ESTIMATION
Months
Linear (X=Y)

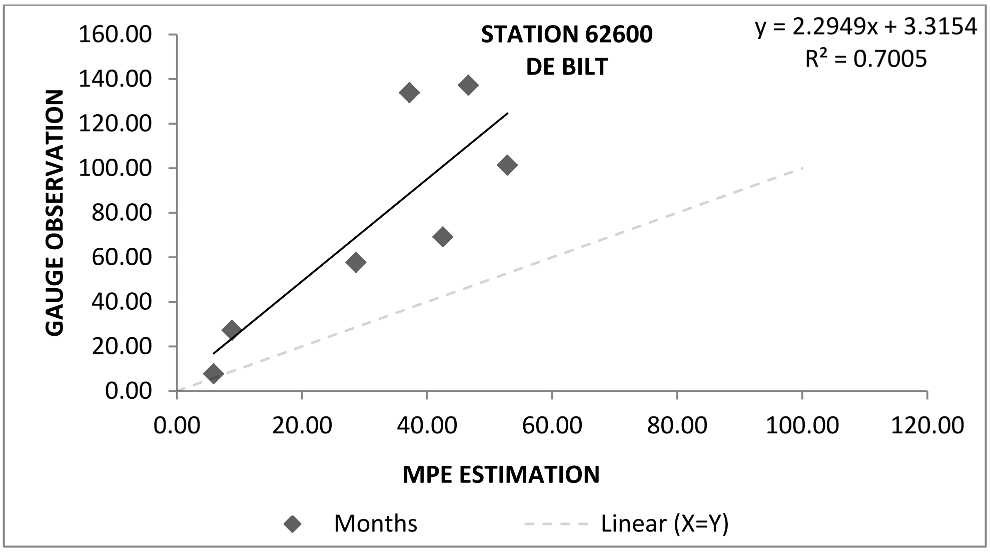
STATION 62600
DE BILT
y = 2.2949x + 3.3154
R² = 0.7005
GAUGE OBSERVATION
MPE ESTIMATION
Months
Linear (X=Y)

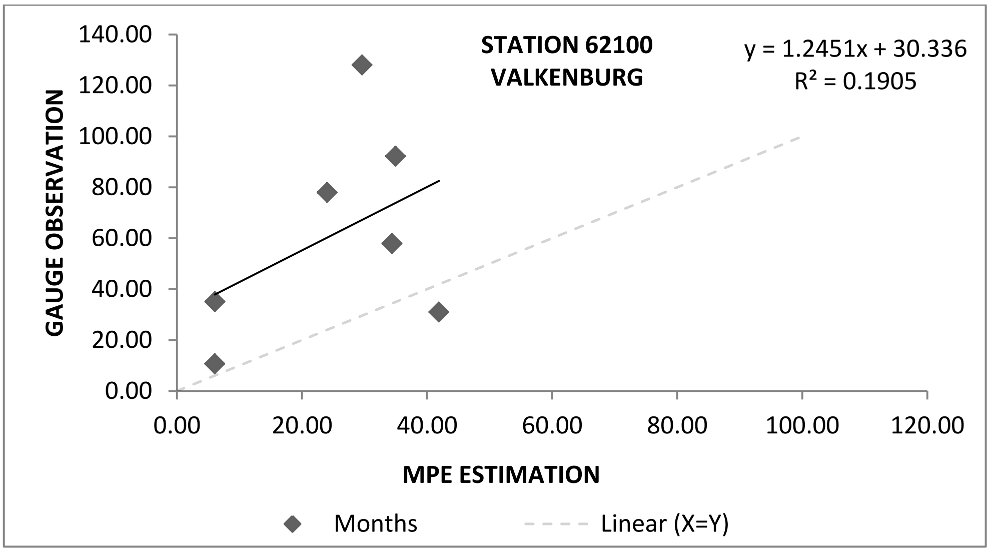
STATION 62100
VALKENBURG
y = 1.2451x + 30.336
R² = 0.1905
GAUGE OBSERVATION
MPE ESTIMATION
Months
Linear (X=Y)

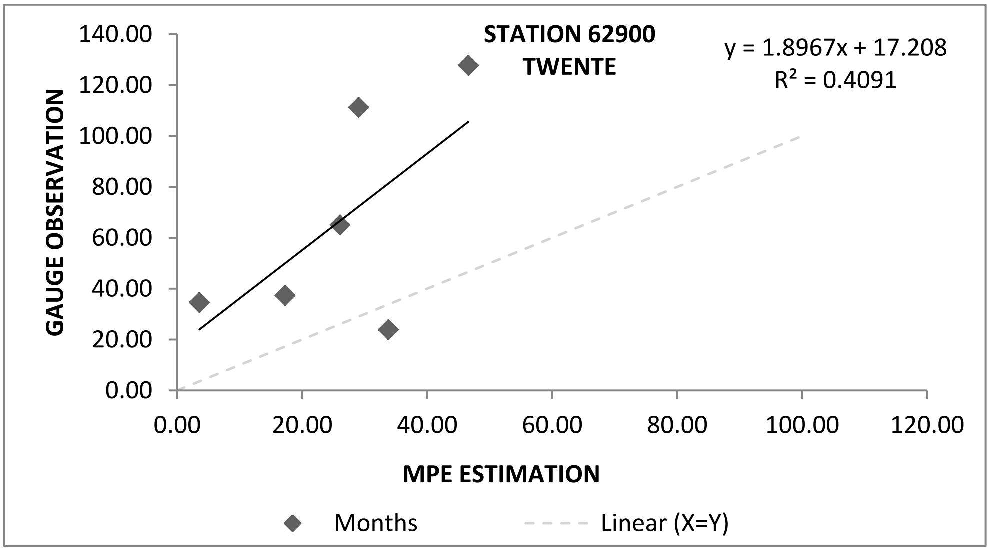
STATION 62900
TWENTE
y = 1.8967x + 17.208
R² = 0.4091
GAUGE OBSERVATION
MPE ESTIMATION
Months
Linear (X=Y)

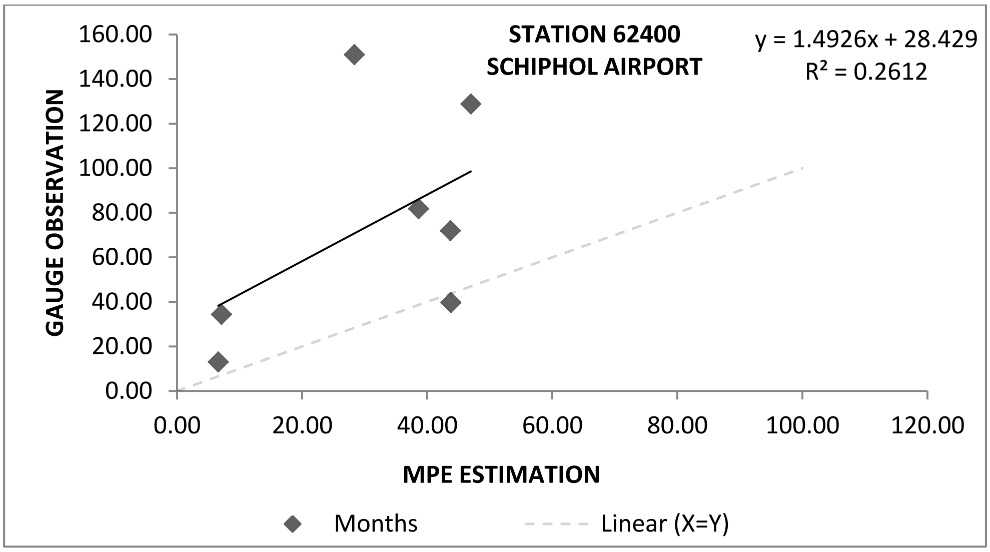
STATION 62400
SCHIPHOL AIRPORT
y = 1.4926x + 28.429
R² = 0.2612
GAUGE OBSERVATION
MPE ESTIMATION
Months
Linear (X=Y)

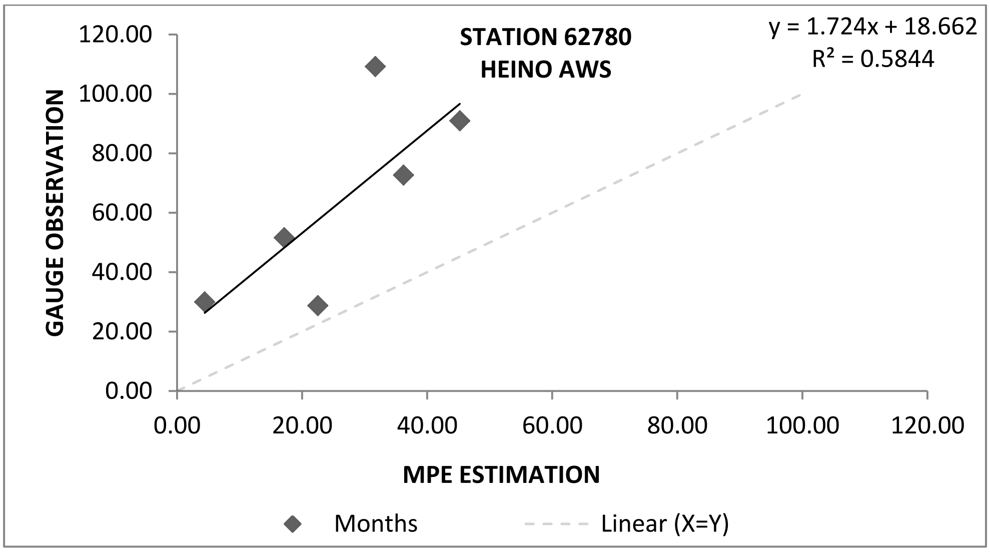
STATION 62780
HEINO AWS
y = 1.724x + 18.662
R² = 0.5844
GAUGE OBSERVATION
MPE ESTIMATION
Months
Linear (X=Y)

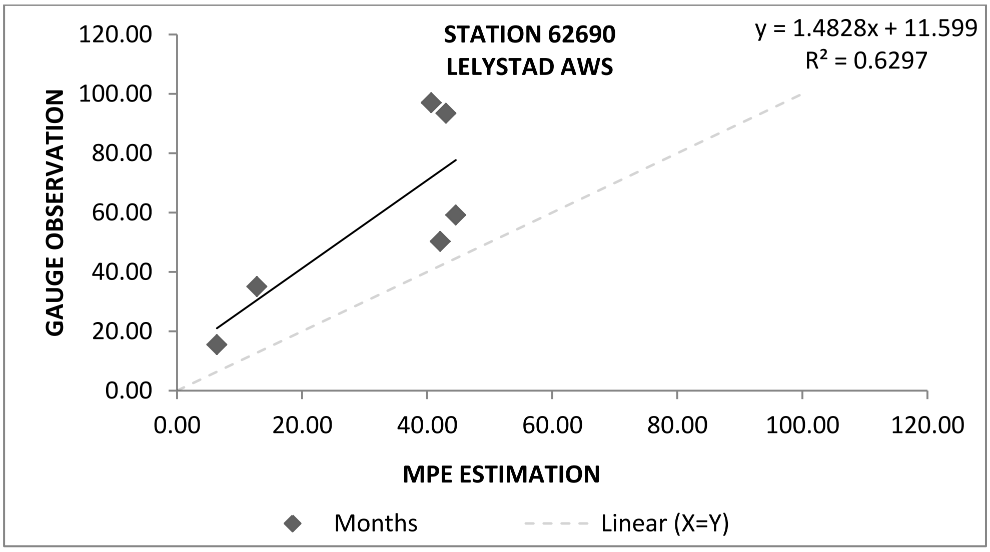
STATION 62690
LELYSTAD AWS
y = 1.4828x + 11.599
R² = 0.6297
GAUGE OBSERVATION
MPE ESTIMATION
Months
Linear (X=Y)

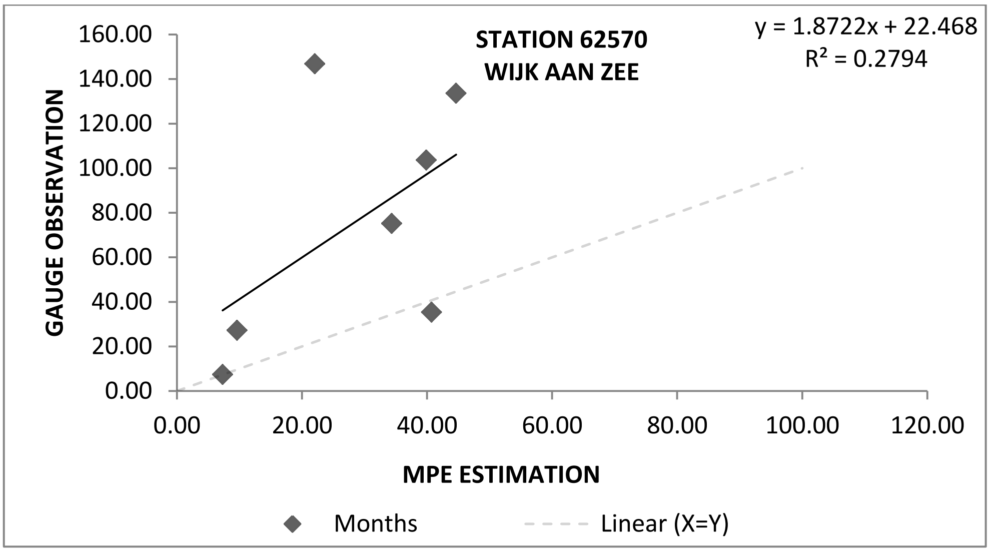
STATION 62570
WIJK AAN ZEE
y = 1.8722x + 22.468
R² = 0.2794
GAUGE OBSERVATION
MPE ESTIMATION
Months
Linear (X=Y)

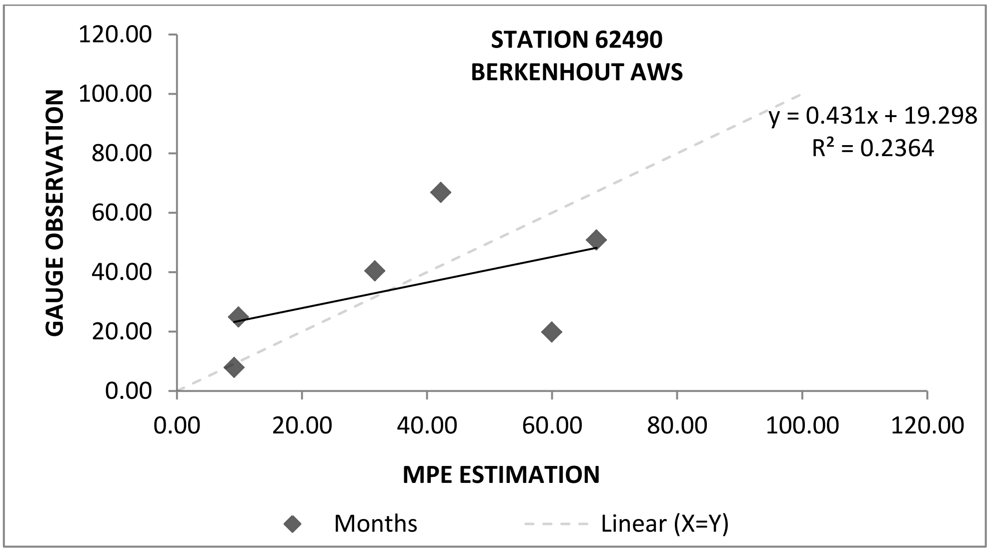
STATION 62490
BERKENHOUT AWS
y = 0.431x + 19.298
R² = 0.2364
GAUGE OBSERVATION
MPE ESTIMATION
Months
Linear (X=Y)

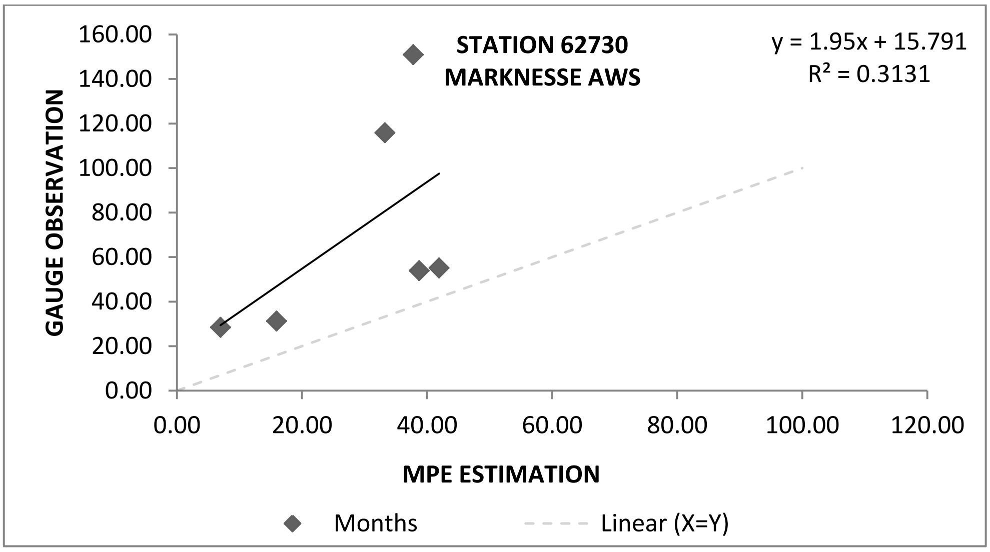
STATION 62730
MARKNESSE AWS
y = 1.95x + 15.791
R² = 0.3131
GAUGE OBSERVATION
MPE ESTIMATION
Months
Linear (X=Y)

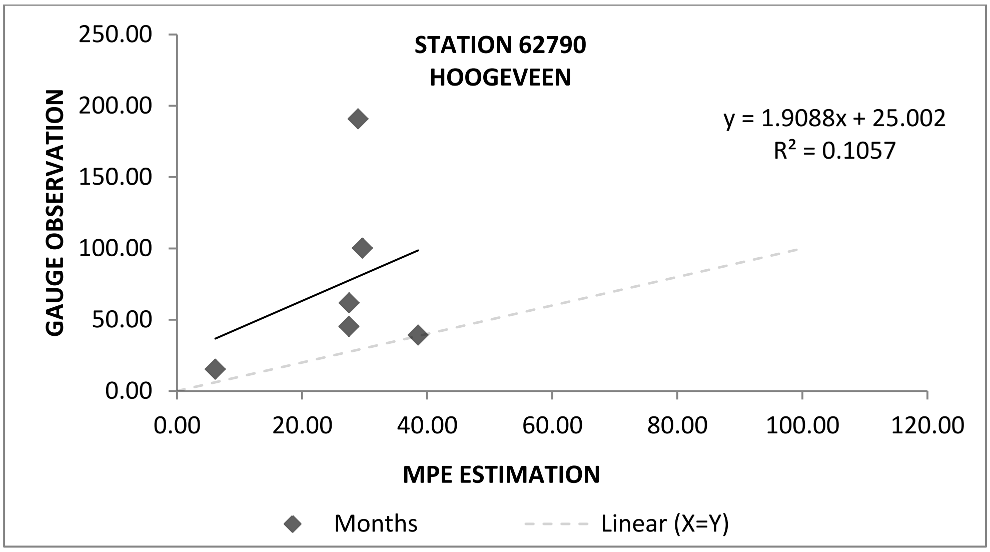
STATION 62790
HOOGEVEEN
y = 1.9088x + 25.002
R² = 0.1057
GAUGE OBSERVATION
250.00
200.00
150.00
100.00
50.00
0.00
0.00
20.00
40.00
60.00
80.00
100.00
120.00
MPE ESTIMATION
Months
Linear (X=Y)

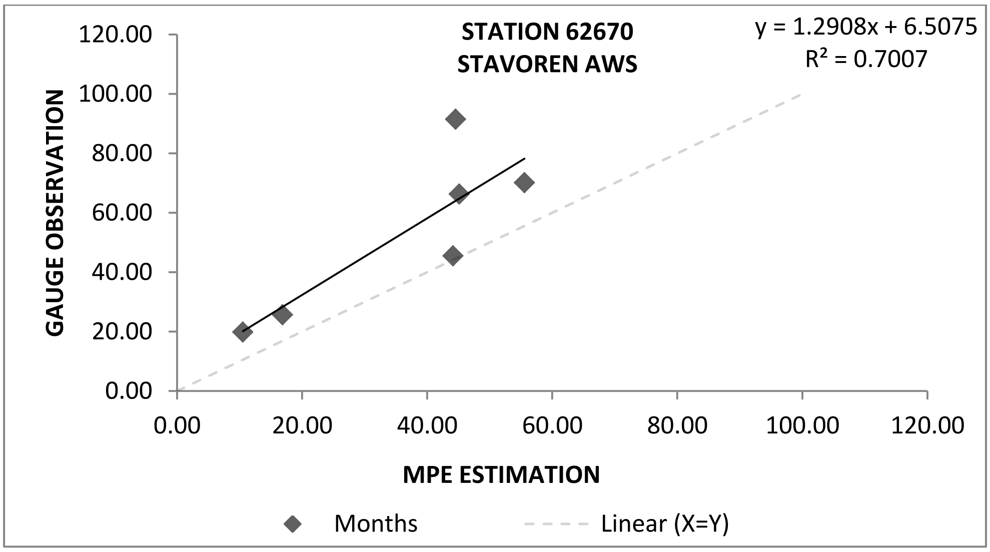
STATION 62670
STAVOREN AWS
y = 1.2908x + 6.5075
R² = 0.7007
GAUGE OBSERVATION
120.00
100.00
80.00
60.00
40.00
20.00
0.00
0.00
20.00
40.00
60.00
80.00
100.00
120.00
MPE ESTIMATION
Months
Linear (X=Y)

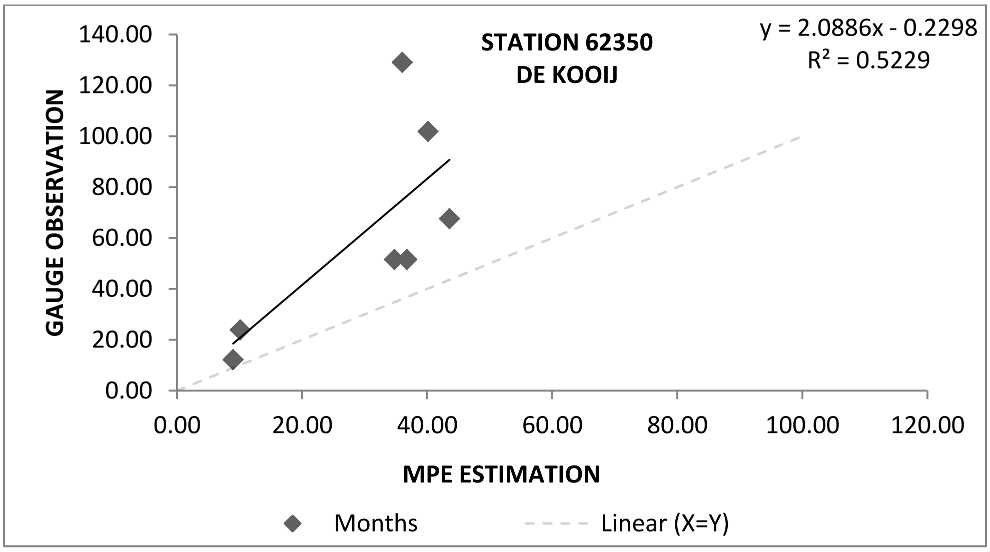
STATION 62350
DE KOOIJ
y = 2.0886x - 0.2298
R² = 0.5229
GAUGE OBSERVATION
140.00
120.00
100.00
80.00
60.00
40.00
20.00
0.00
0.00
20.00
40.00
60.00
80.00
100.00
120.00
MPE ESTIMATION
Months
Linear (X=Y)

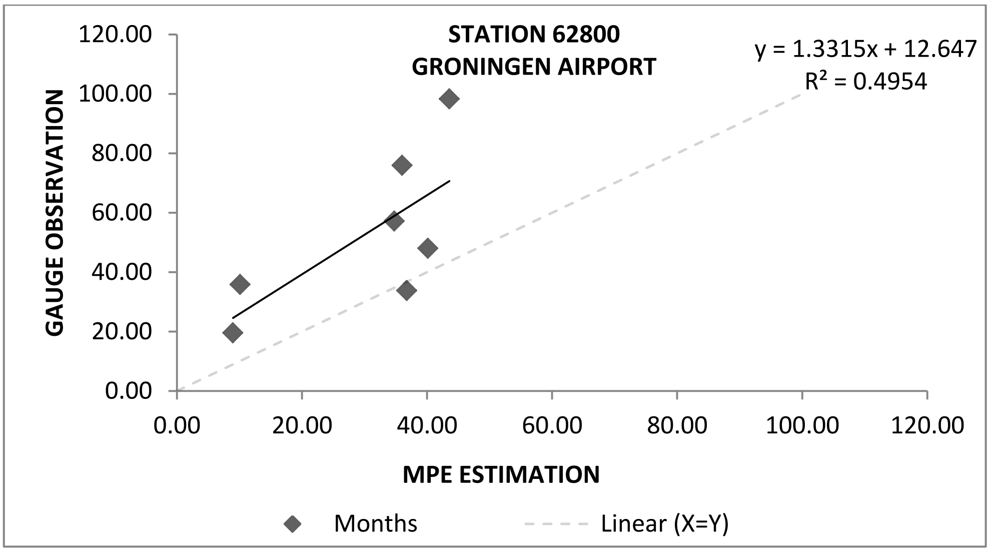
STATION 62800
GRONINGEN AIRPORT
y = 1.3315x + 12.647
R² = 0.4954
GAUGE OBSERVATION
MPE ESTIMATION
Months
Linear (X=Y)

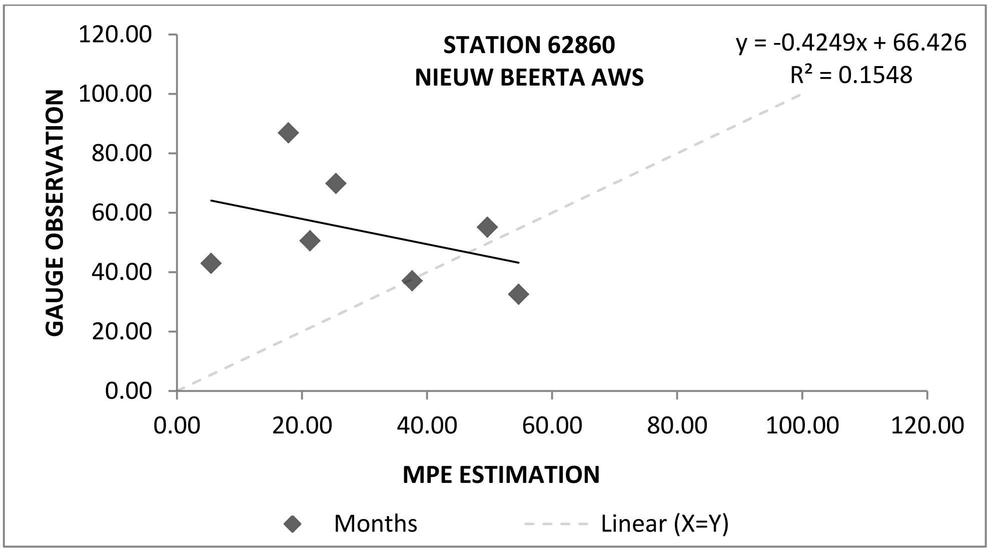
STATION 62860
NIEUW BEERTA AWS
y = -0.4249x + 66.426
R² = 0.1548
GAUGE OBSERVATION
MPE ESTIMATION
Months
Linear (X=Y)

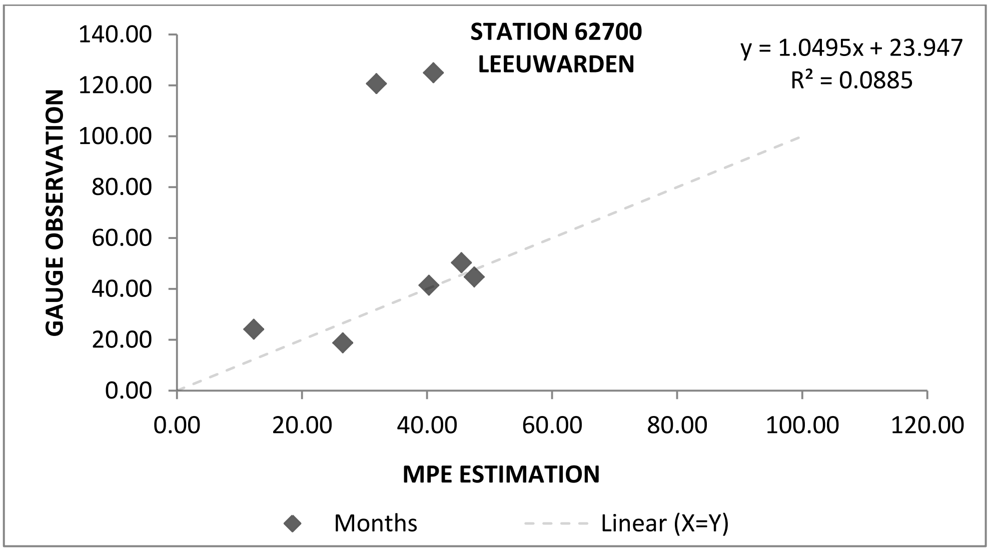
STATION 62700
LEEUWARDEN
y = 1.0495x + 23.947
R² = 0.0885
GAUGE OBSERVATION
MPE ESTIMATION
Months
Linear (X=Y)

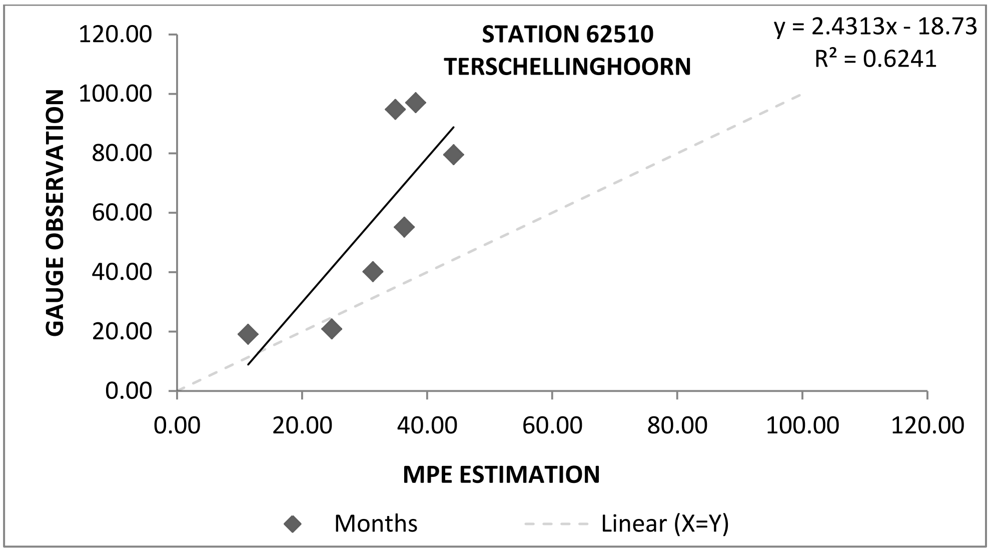
STATION 62510
TERSCHELLINGHOORN
y = 2.4313x - 18.73
R² = 0.6241
GAUGE OBSERVATION
MPE ESTIMATION
0.00
20.00
40.00
60.00
80.00
100.00
120.00
Months
Linear (X=Y)

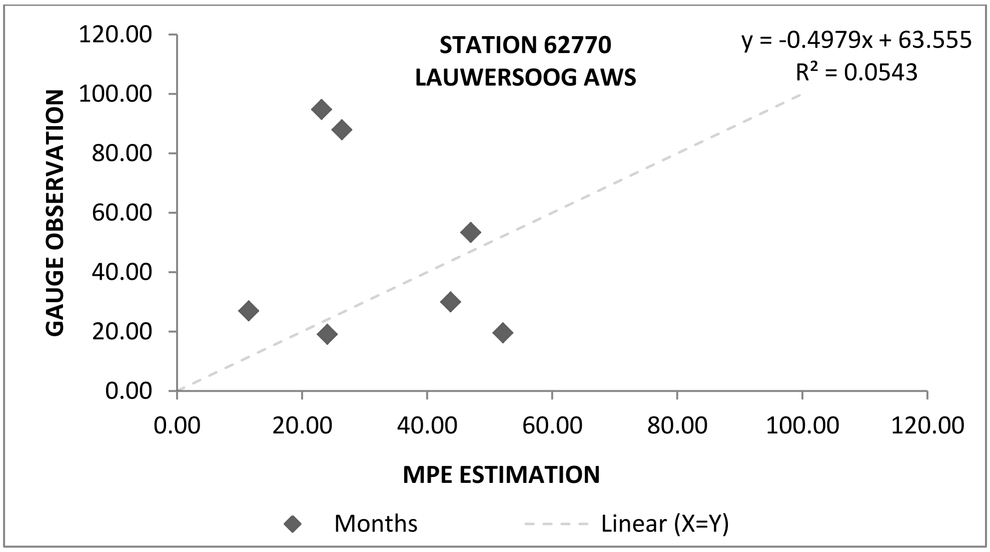
STATION 62770
LAUWERSOOG AWS
y = -0.4979x + 63.555
R² = 0.0543
GAUGE OBSERVATION
MPE ESTIMATION
0.00
20.00
40.00
60.00
80.00
100.00
120.00
Months
Linear (X=Y)

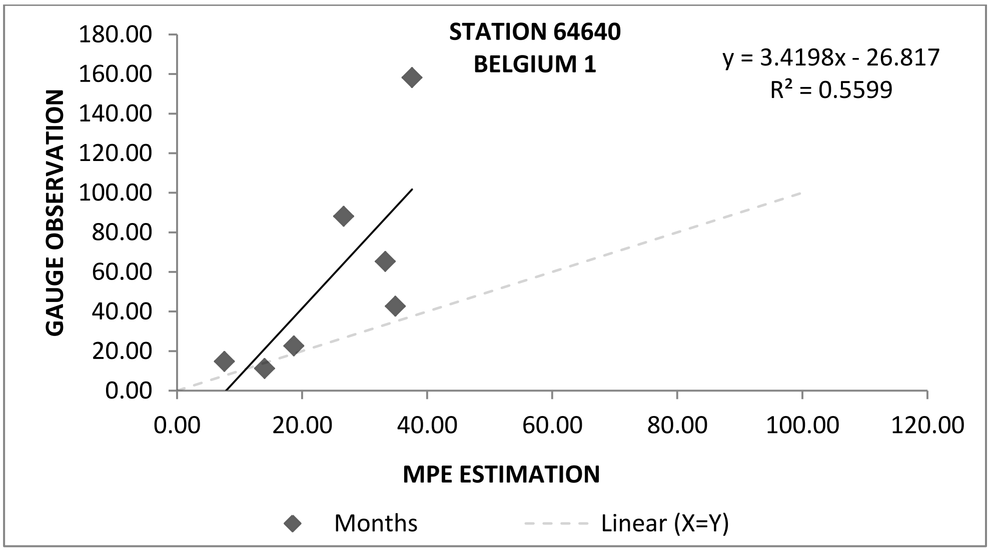
STATION 64640
BELGIUM 1
y = 3.4198x - 26.817
R² = 0.5599
GAUGE OBSERVATION
MPE ESTIMATION
0.00
20.00
40.00
60.00
80.00
100.00
120.00
140.00
160.00
180.00
Months
Linear (X=Y)

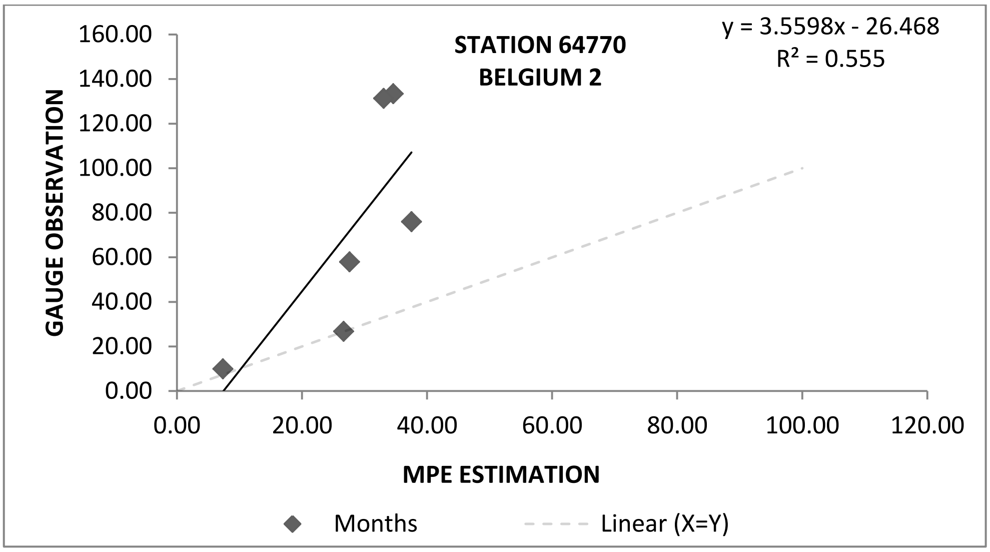
STATION 64770
BELGIUM 2
y = 3.5598x - 26.468
R² = 0.555
GAUGE OBSERVATION
MPE ESTIMATION
160.00
140.00
120.00
100.00
80.00
60.00
40.00
20.00
0.00
0.00
20.00
40.00
60.00
80.00
100.00
120.00
Months
Linear (X=Y)

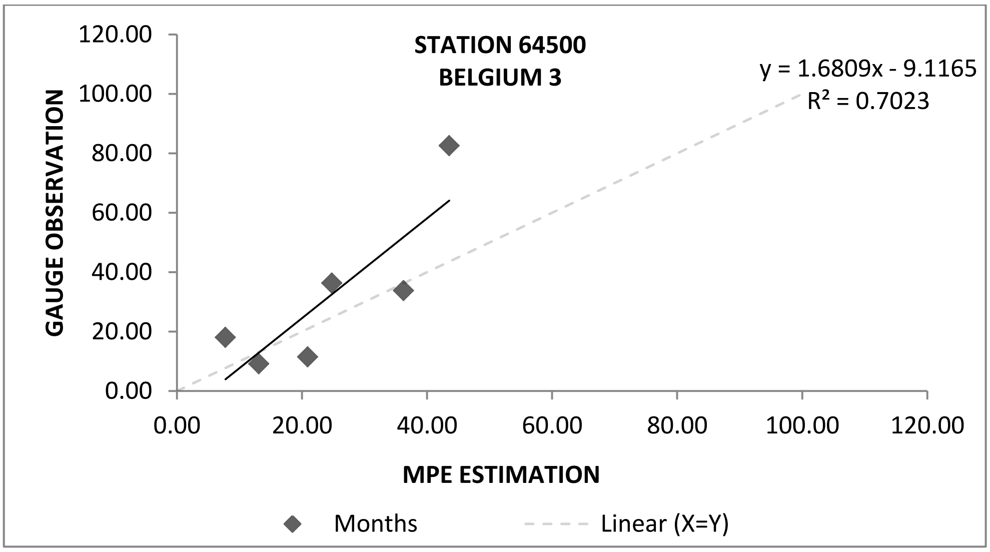
STATION 64500
BELGIUM 3
y = 1.6809x - 9.1165
R² = 0.7023
GAUGE OBSERVATION
MPE ESTIMATION
120.00
100.00
80.00
60.00
40.00
20.00
0.00
0.00
20.00
40.00
60.00
80.00
100.00
120.00
Months
Linear (X=Y)

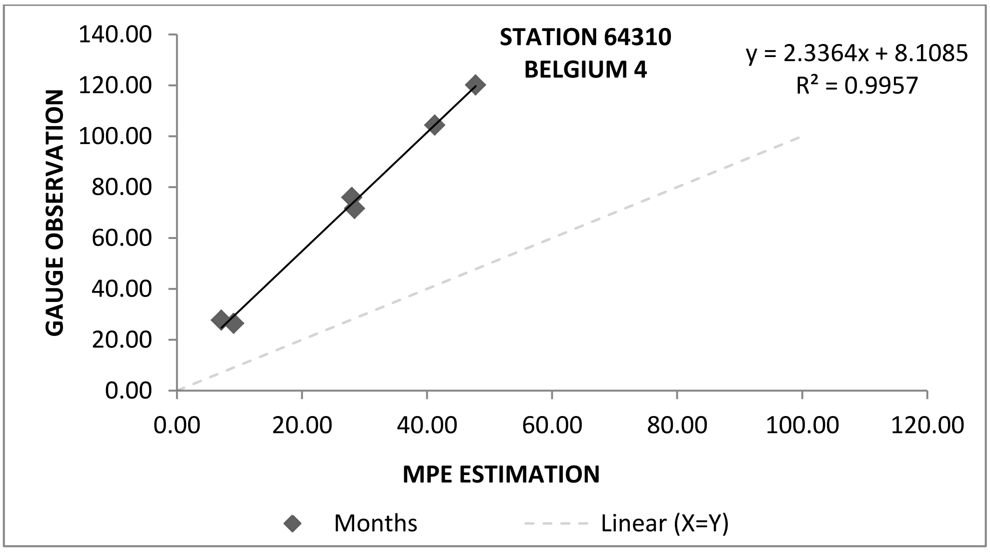
STATION 64310
BELGIUM 4
y = 2.3364x + 8.1085
R² = 0.9957
GAUGE OBSERVATION
MPE ESTIMATION
140.00
120.00
100.00
80.00
60.00
40.00
20.00
0.00
0.00
20.00
40.00
60.00
80.00
100.00
120.00
Months
Linear (X=Y)

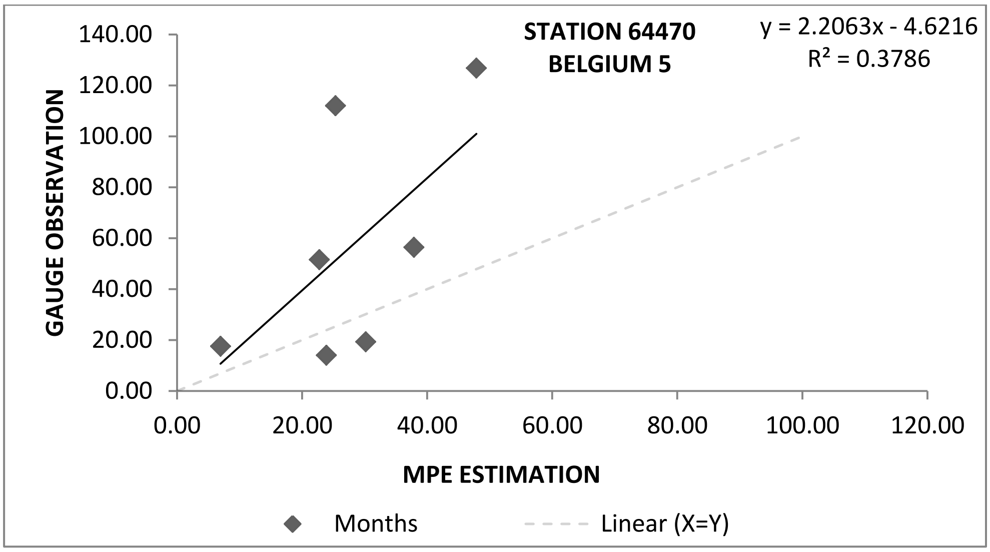
STATION 64470
BELGIUM 5
y = 2.2063x - 4.6216
R² = 0.3786
GAUGE OBSERVATION
MPE ESTIMATION
0.00
20.00
40.00
60.00
80.00
100.00
120.00
140.00
Months
Linear (X=Y)

Appendix E.

Rainfall fields in raster to raster comparisons

MARCH		Estimated values of GPM		TOTAL
		Yes	No	
Estimated values of TRMM	Yes	88843	154924	243767
	NO	20814	311419	332233
TOTAL		109657	466343	576000

APRIL		Estimated values of GPM		TOTAL
		Yes	No	
Estimated values of TRMM	Yes	110566	145971	256537
	NO	23537	295926	319463
TOTAL		134103	441897	576000

MAY		Estimated values of GPM		TOTAL
		Yes	No	
Estimated values of TRMM	Yes	109487	152496	261983
	NO	21080	292937	314017
TOTAL		130567	445433	576000

JUNE		Estimated values of GPM		TOTAL
		Yes	No	
Estimated values of TRMM	Yes			TOTAL
	NO			TOTAL
TOTAL		TOTAL	TOTAL	Number of all pixels

JULY		Estimated values of GPM		TOTAL
		Yes	No	
Estimated values of TRMM	Yes	54922	170560	225482
	NO	25191	325327	350518
TOTAL		80113	495887	576000

AUGUST		Estimated values of GPM		TOTAL
		Yes	No	

Estimated values of TRMM	Yes	67263	175743	243006
	NO	22962	310032	332994
TOTAL		90225	485775	576000

SEPTEMBER		Estimated values of GPM		TOTAL
		Yes	No	
Estimated values of TRMM	Yes	77052	163678	240730
	NO	31135	304135	335270
TOTAL		108187	467813	576000

OCTOBER		Estimated values of GPM		TOTAL
		Yes	No	
Estimated values of TRMM	Yes	97333	156633	253966
	NO	25790	296244	322034
TOTAL		123123	452877	576000

MARCH		Estimated values of GPM		TOTAL
		Yes	No	
Estimated values of MPE	Yes	8235	26166	34401
	NO	44427	141492	185919
TOTAL		52662	167658	220320

APRIL		Estimated values of GPM		TOTAL
		Yes	No	
Estimated values of MPE	Yes	15387	22470	37857
	NO	39635	142828	182463
TOTAL		55022	165298	220320

MAY		Estimated values of GPM		TOTAL
		Yes	No	
Estimated values of MPE	Yes	14158	21029	35187
	NO	35289	149844	185133
TOTAL		49447	170873	220320

JULY		Estimated values of GPM		TOTAL
		Yes	No	
Estimated values of MPE	Yes	9282	18004	27286
	NO	19135	173899	193034
TOTAL		28417	191903	220320

AUGUST		Estimated values of GPM		TOTAL
		Yes	No	
Estimated values of MPE	Yes	10641	15951	26592
	NO	31083	162645	193728
TOTAL		41724	178596	220320

SEPTEMBER		Estimated values of GPM		TOTAL
		Yes	No	
Estimated values of MPE	Yes	12102	17859	29961
	NO	33145	157214	190359
TOTAL		45247	175073	220320

OCTOBER		Estimated values of GPM		TOTAL
		Yes	No	
Estimated values of MPE	Yes	14627	22093	36720
	NO	45963	137637	183600
TOTAL		60590	159730	220320

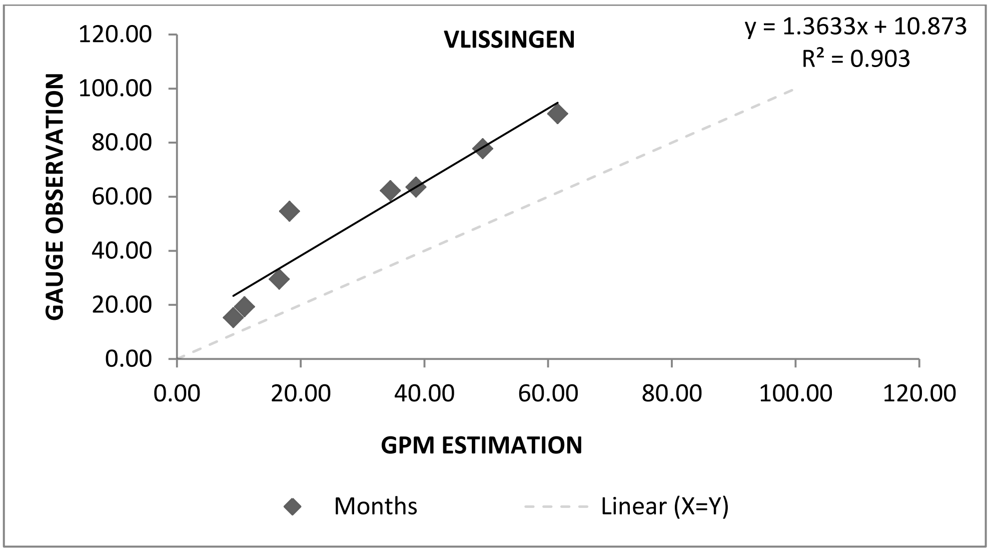
VLISSINGEN
y = 1.3633x + 10.873
R² = 0.903
GAUGE OBSERVATION
GPM ESTIMATION
0.00
20.00
40.00
60.00
80.00
100.00
120.00
Months
Linear (X=Y)